Rectal Cancer –

Functional Molecular Profiling and Targeting of Tumor Hypoxia in Radiation Response and Metastasis

Marie Grøn Sælen

Department of Tumor Biology
Institute for Cancer Research
Division of Cancer Medicine, Surgery and Transplantation
The Norwegian Radium Hospital
Oslo University Hospital

Institute of Clinical Medicine
Faculty of Medicine
University of Oslo

Series of dissertations submitted to the
Faculty of Medicine, University of Oslo
No. 1797

ISBN 978-82-8264-823-3

Cover: Inger Sandved Anfinsen.
Printed in Norway: AIT Oslo AS.

Produced in co-operation with Akademika Publishing.
The thesis is produced by Akademika Publishing merely in connection with the thesis defence. Kindly direct all inquiries regarding the thesis to the copyright holder or the unit which grants the doctorate.

Table of Contents

1 Preface

1.1 Acknowledgements

The work presented in this thesis was carried out at the Department of Tumor Biology, Institute for Cancer Research, The Norwegian Radium Hospital, Oslo University Hospital from 2009-2013 including a one-year maternity leave in 2012. The financial support from the European Union 7th Framework Programme - METOXIA (Grant No. HEALTH-F2-2009-222741) and the PhD grant from South-Eastern Norway Regional Health Authority (Helse Sør-Øst; Grant No. 2010-014) is gratefully acknowledged.

First of all, my sincere gratitude goes to my excellent supervisors, Anne Hansen Ree and Kjersti Flatmark, who introduced me to cancer research and have contributed substantially to this work. Despite your busy schedules, you always find the time to give advice on all aspects of research. We have had many inspiring meetings with rewarding discussions. You complement each other in many ways; while Anne tends to be extremely enthusiastic, Kjersti usually offers a more pragmatic perspective. You are both thorough researchers and constitute a strong team. I admire your broad knowledge on experimental and clinical cancer research along with extensive clinical experience.

I would like to thank Gunhild Mælandsmo as head of The Department of Tumor Biology and all my colleagues at the department for creating a stimulating research environment. I missed you while finishing the thesis from Tromsø, but enjoyed the regular visits to the Radium Hospital.

I am grateful to my coauthors and I want to thank you for your contributions to this work. I want to thank Sigurd Folkvord for welcoming me at the department and introducing me to the research area and Øystein Fodstad for including me in his research group when I first started. I wish to thank Torveig Weum Abrahamsen for guidance and cooperation in the laboratory. I would like to thank Karianne Giller Fleten and Alexandr Kristian for help with animal experiments, and to Torbjørn Furre for assisting with the *in vivo* radiation. Thanks to Rik de Wijn for help with statistical analysis, to Ingrid H. G. Østensen and Erta Kalanxhi for biostatistical help, to everyone involved with the LARC-RRP study: Svein Dueland, Kathrine Røe, Marianne Johansen, Therese Seiersted and Knut Håkon Hole; and to Helga H. Hektoen and Kristina Schee for helping with laboratory experiments in my maternity leave.

I want to thank my family and friends for their invaluable support. Thanks to my husband Anders for believing in me and helping with smaller and larger challenges. A special thanks to my father Bjørn for being the best babysitter. Finally I want to thank my sons Jakob (5) and Edvard (1.5) for reminding me that other aspects of life are more important than work.

Marie J Sølen

January 2014

1.2 Abbreviations

Frequently used abbreviations are listed below. Other abbreviations are indicated in the text when appropriate

5-FU	5-fluorouracil
CEA	Carcinoembryonic antigen
CTC	Circulating tumor cells
CRC	Colorectal cancer
CRM	Circumferential resection margin
CRT	Chemoradiotherapy
CT	Computer tomography
DFS	Disease-free survival
DLT	Dose-limiting toxicity
DTC	Disseminated tumor cells
HAT	Histone acetyl transferase
HIF-1α	Hypoxia-inducible factor type 1α
HDAC	Histone deacetylase
IR	Irradiation
LARC	Locally advanced rectal cancer
LARC-RRP	Locally advanced rectal cancer – radiation response prediction
MFS	Metastasis-free survival
MRI	Magnetic resonance imaging
MRF	Mesorectal fascia
MTD	Maximum-tolerated dose
NACT	Neoadjuvant chemotherapy
pCR	Pathological complete response
OS	Overall survival
OXA	Oxaliplatin
PBMC	Peripheral blood mononuclear cells
PDGFRB	PDGF receptor type β
PRAVO	Pelvic radiation and vorinostat
RT-qPCR	Realtime quantitative polymerase chain reaction
TGD	Tumor growth delay
TNM	Tumor Node Metastasis
TRG	Tumor regression grade
VEGF	Vascular endothelial growth factor A

1.3 List of papers

Paper I: **Saelen MG**, Flatmark K, Folkvord S, de Wijn R, Rasmussen H, Fodstad O, Ree AH:
Tumor kinase activity in locally advanced rectal cancer: angiogenic signaling and early systemic dissemination.
Angiogenesis 2011, 14:481-489.

Paper II: **Saelen MG**, Ree AH, Kristian A, Fleten KG, Furre T, Hektoen HH, Flatmark K:
Radiosensitization by the histone deacetylase inhibitor vorinostat under hypoxia and with capecitabine in experimental colorectal carcinoma**.**
Radiat Oncol 2012, 7:165.

Paper III: Ree AH, **Saelen MG**, Kalanxhi E, Østensen IHG, Schee K, Røe K, Abrahamsen TW, Dueland S, Flatmark K:
Biomarkers of histone deacetylase inhibitor activity in a phase 1 combined-modality study with radiotherapy
PLoS One 2014, in press.

Paper IV: Flatmark K, **Saelen MG**, Seierstad T, Hole KH, Abrahamsen TW, Fleten KG, Røe K, Dueland S, Ree AH:
Is oxaliplatin-containing neoadjuvant chemotherapy an alternative to radiation in T3 rectal cancer?
Manuscript

2 Introduction

Rectal cancer is common in both genders and among all adult age groups, with the highest incidence in elderly people. In Europe it has been estimated that nearly 447,000 were diagnosed with colorectal cancer (CRC) in 2012; of these cases, about 30% were in the rectal anatomic site[1]. The management of rectal cancer is multidisciplinary, involving precision diagnostics within pathology and radiology, along with highly specialized knowledge within oncology and surgery (**Figure 2.1**). The therapy is multimodal; while surgery remains the principal treatment modality in achieving tumor clearance, the introduction of neoadjuvant radiotherapy administered with radiosensitizing chemotherapeutics has significantly reduced local recurrences in patients with locally advanced rectal cancer (LARC) [2,3]. The response to neoadjuvant chemoradiotherapy (CRT) is nevertheless variable, and even with successful local treatment a substantial number of patients develops metastatic disease. Tumor hypoxia is recognized as common determinant of resistance to radiotherapy and metastatic disease progression; hence, targeting tumor hypoxia in radiation response and metastasis is an appealing strategy to improve overall outcome of rectal cancer patients.

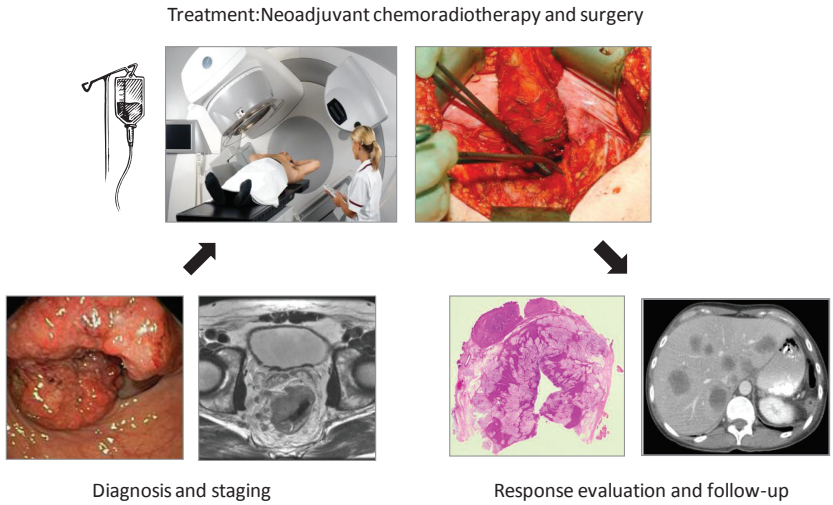

Figure 2.1 Multimodal treatment in locally advanced rectal cancer. Following diagnostic procedures and staging, chemoradiotherapy is given prior to surgery. Treatment response is evaluated and patients are followed for 5 years to detect local or distant recurrences. Pictures adapted from www.gastrolab.net, www.danisfoundation.org, Oslo University Hospital, and AH Ree; printed with permission.

3 Background

3.1 Rectal cancer

3.1.1 Epidemiology

The annual incidence of rectal cancer in the Norwegian population of 5.0 million adds up to more than 1,300. The age-adjusted incidence rates per 100 000 persons-years is 17.0 for men and 11.5 for women, leading to a male:female ratio of 1.5 [4*]. Most patients have regional disease at the time of diagnosis (**Table 3.1**). The age-specific incidence rates show that rectal cancer is mainly a disease of the elderly, with a significant rise in incidence from the age of 60. The incidence rates have been stable for more than 30 years but are expected to increase due to an aging population [5]. Worldwide, CRC incidence rates are highest in the more developed regions (Australia, New Zealand, USA and Europe), and Norway has one of the highest incidence rates in Europe [1,6].

Five-year relative survival for rectal cancer was 64.8 % for men and 67.9 % for women in Norway in 2007-11 and was considerably higher in patients with localized and regional disease than in patients with systemic disease (**Table 3.1**)[4]. The survival rates (of all stages) of rectal cancer have increased over the last 40 years in Norway (**Figure 3.1**) and are among the highest in the world [2,7,8].

	Men		Women	
Stage	Rate per 100 000	5-year survival (%)	Rate per 100 000	5-year survival (%)
Total	17.0 (100%)	65	11.5 (100%)	68
Localized	4.2 (24%)	82	3.3 (29%)	90
Regional	9.0 (53%)	76	5.7 (50%)	74
Distant	3.2 (18%)	16	2.1 (17%)	16
Unknown	0.6 (6%)	56	0	66

Table 3.1 Age-adjusted incidence rates and 5-year relative survival (%) from rectal cancer according to stage for tumors diagnosed 2007-11. Data from the Cancer Registry of Norway.

[*] Numbers from the Cancer Registry of Norway include tumors of the rectum, rectosigmoid large bowel, and anal canal.

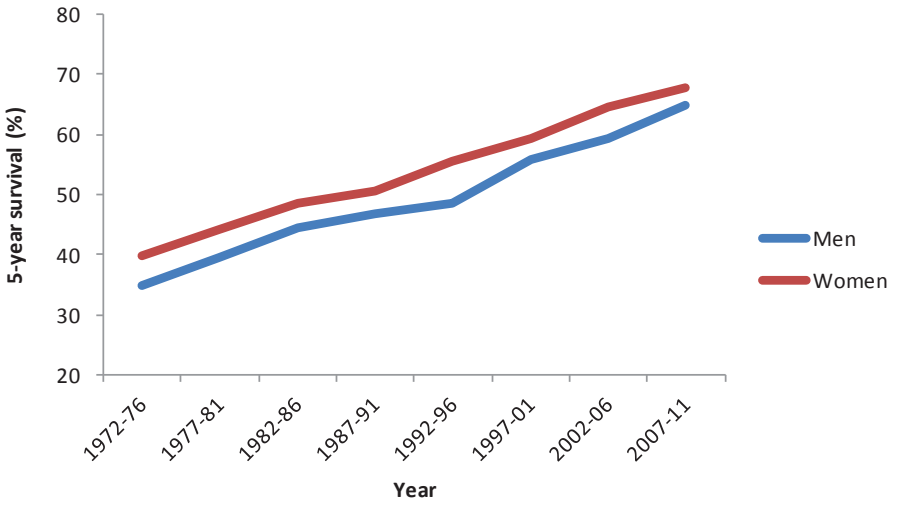

Figure 3.1 5-year relative survival from rectal cancer by period and gender in 1972-2011. Data from the Cancer Registry of Norway.

3.1.2 Diagnosis and staging

When a rectal tumor is suspected, typically in a patient presenting with rectal bleeding or altered stool habits, diagnostic procedures include digital rectal investigation and endoscopy with tumor biopsies, to determine the precise site and histopathological characteristics of the tumor. The disease site(s) within the pelvic cavity is confirmed by magnetic resonance (MRI) imaging. There is no clear anatomical border between the sigmoid colon and the rectum. A rectal tumor is by definition located up to 15 cm from the anal verge as determined by rigid endoscopy (corresponding to 12 cm when determined by MRI) [9]. Rectal cancers are commonly categorized into low/mid/high cancers according to their distal edge measured from the anal verge. Most rectal cancers are adenocarcinomas, but a small fraction (1-2%) are neuroendocrine tumors with different prognosis and treatment [10]. A histological subtype of rectal adenocarcinoma (5-15%) is the mucinous carcinoma, in which large amounts of mucin are produced. This subtype is associated with poorer response to CRT and a poorer prognosis than non-mucinous rectal tumors [11,12].

Prognosis of rectal cancer is highly heterogeneous, and staging of the disease at diagnosis is essential to stratify patients into subgroups and accordingly, determine the treatment strategy [13,14]. Among patients with potentially curative disease, some are at high risk of local recurrence from surgery alone and will benefit from CRT prior to surgery. If the disease is extensively disseminated at diagnosis, symptom palliation and prolonged survival are the aim of treatment; in contrast, if metastasis is limited to a single organ, curative treatment is increasingly considered possible with multimodal approaches[9]. Treatment decisions should be made in multi-disciplinary teams of specialist surgeons, oncologists, pathologists and radiologists, and be based on patient history and examination, and diagnostic and staging procedures [9, 15,16].

Tumor Node Metastasis (TNM) staging

The TNM system of classification of malignant tumors is also the standard staging system for rectal cancer. It categorizes cancers based on the anatomic extent of disease; size and extent of the primary tumor (T-stage), involvement of regional lymph nodes (N-stage) and presence or absence of distant metastasis (M-stage)[13] (**Table 3.2).** The prefix "c" denotes clinical staging, while histopathologic staging is designated "p". Clinical or histopathologic staging after neoadjuvant therapy is designated by the prefix "yc" or "yp".

T	T1	Tumor invades submucosa
	T2	Tumor invades muscularis propria
	T3	Tumor invades through the muscularis propria into the mesorectum
	T4	Tumor grows through the mesorectal fascia and invades or is adherent to a) the visceral peritoneum b) other organs or structures
N	N0	No regional lymph node metastasis
	N1	Metastasis in 1-3 regional lymph nodes
	N2	Metastasis in 4 or more regional lymph nodes
M	M0	No distant metastasis
	M1	Distant metastasis

Table 3.2 TNM staging of rectal cancer, from the American Joint Committee on Cancer's Cancer Staging Manual 7th Edition. Subclassification of T4 was introduced in the 6th Edition, and the order changed in the 7th Edition.

TNM stage at diagnosis is determined by imaging (cTNM). MR imaging is the recommended modality for the evaluation of tumor extent in the pelvic cavity (extramural T3-4 tumors), while endoscopic rectal ultrasound is commonly more accurate for assessing tumor growth into the

bowel wall (T1-2 tumors)[9]. Both modalities allow detection of regional lymph node metastases, while CT (computed tomography) is used to examine thoracic and abdominal organs for any distant metastases[17]. The most common sites for rectal cancer metastases are the liver, peritoneum, and lungs, or more infrequently, the skeleton or the brain.

Mesorectal fascia (MRF) involvement

The rectum is surrounded by the mesorectum, a fatty layer containing lymph nodes and vessels delineated by the mesorectal fascia. The standard surgical technique in rectal cancer, total mesorectal excision (TME), involves removal of the rectum and the entire mesorectum to the MRF, keeping the tumor and all locally draining lymph nodes intact **(Figure 3.2).** The surgeon dissects in the plane of the MRF, establishing the lateral or circumferential resection margin (CRM). The goal of curative surgery is to obtain resection margins with no tumor cells, as involvement of resection margins, in particular the CRM, is associated with disease recurrence and poor survival [18-21].

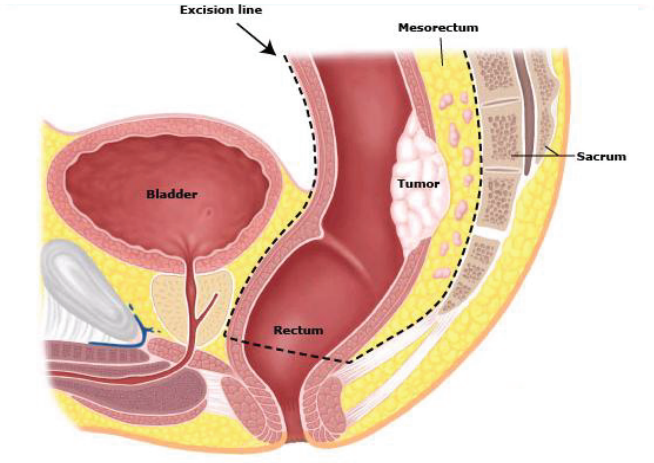

Figure 3.2 Total mesorectal excision: Sagittal picture of a male pelvis depicting the boundaries for mesorectal excision of a rectal adenocarcinoma. Adapted from Bleday R, Shibata D. Surgical oncologic principles for resection of primary rectal adenocarcinoma. UpToDate, Basow DS (Ed), UpToDate, Waltham, MA, 2013. Copyright © 2013. Printed with permission.

Preoperative MR evaluation can predict if it is possible to achieve a free CRM after surgery [22,23] If the MRF is involved or positive, defined as proximity (≤1 mm) [24] or actual infiltration by

tumor, pathologic lymph nodes or infiltrated vessels into the MRF (**Figure 3.3**), the risk of an involved CRM after surgery is high [9,19]. In T4 rectal tumors, the MRF is infiltrated per definition; while in T3 tumors the MRF is not infiltrated, but may be classified as positive if the tumor is closer than 1 mm.

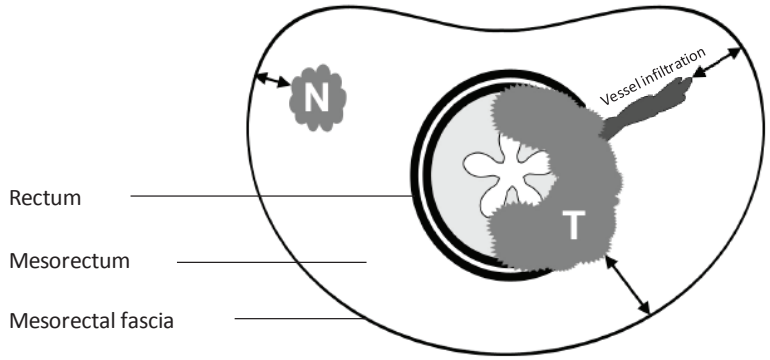

Figure 3.3 Positive mesorectal fascia (MRF). The MRF is positive if the distance to the MRF from the primary T3 tumor (T), lymph node metastasis (N) or vessel infiltration is shorter than 1 mm. Adapted from Knut Håkon Hole, Oslo University Hospital, printed with permission.

Currently, TNM stage and predicted distance to MRF are the parameters evaluated in staging at diagnosis of rectal cancer in Norway[17]. Other prognostic factors suggested for inclusion in diagnostic staging are tumor location (low tumors spread more easily via venous and lymphatic vessels), extent of extramural spread of T3-tumors (> 5mm extramural spread indicates poor prognosis), extramural venous invasion and pelvic sidewall lymph node involvement [14,25,26].

3.1.3 Radiotherapy in locally advanced rectal cancer

While surgery is the principal treatment in rectal cancer, additional cancer therapy is administered to patients with locally advanced rectal cancer (LARC) to improve outcome [27]. The classic definition of LARC is a rectal tumor that grows beyond the rectal wall or has lymph node spread to an extent that precludes complete removal by surgery alone, warranting additional treatment [3]. The definition of LARC has changed with increasing knowledge of risk factors and

with improved staging. In this thesis, the term LARC comprises rectal cancer patients for whom neoadjuvant radiotherapy with curative intent is recommended in the Norwegian guidelines: T4 tumors, T3 tumors within 3 mm from the MRF and tumors of any T stage with pathological lymph nodes or vessel infiltration within 3 mm from to the MRF, as assessed by diagnostic MRI [17] **(Figure 3.4).** In the national guidelines, the 3 mm margin was recently changed to less than 2mm.

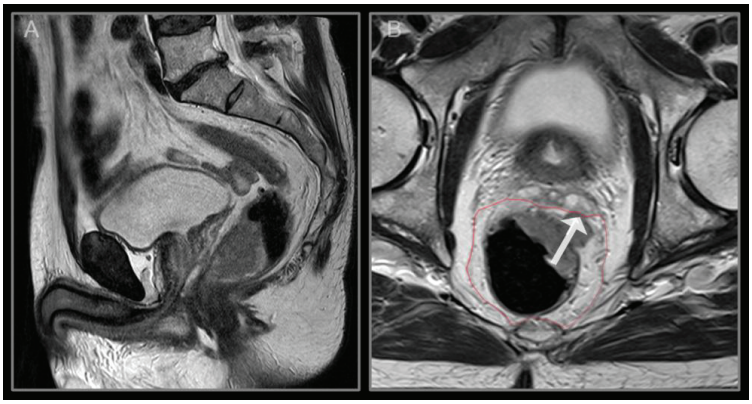

Figure 3.4 Sagittal (A) and transversal (B) magnetic resonance images of middle/low anterior T3 rectal cancer with tumor extension within 1 mm from the left seminal vesicle, indicated by arrow. The red line indicates the mesorectal fascia. Images provided by Knut Håkon Hole, Oslo University Hospital, printed with permission.

In LARC, neoadjuvant CRT, consisting of fractionated radiotherapy in combination with chemotherapy, is the standard treatment. While LARC traditionally has been associated with high risk of local recurrence and poor patient survival, the introduction of the TME surgical technique along with neoadjuvant CRT has reduced the rate of local recurrences from up to 40 % to about 5% [28-30].

Radiotherapy

Radiotherapy is given prior to surgery in LARC patients to achieve macroscopic tumor downsizing and control of subclinical tumor extension within the pelvic cavity, to enable complete tumor removal with sufficient microscopic margins by surgical resection. Preoperative radiotherapy as part of LARC treatment was introduced in randomized trials in European

countries in the 1980-90's [31,32]. In 2001 a large randomized trial reported reduced risk of local recurrence in patients receiving preoperative radiotherapy and surgery compared to surgery alone [32]. Compared to adjuvant treatment, advantages of preoperative radiotherapy include potential downsizing of the tumor, less toxicity and higher compliance [33,34]. While adjuvant radiotherapy was the standard for years in *e.g.* the USA, the current international standard treatment is preoperative radiotherapy combined with chemotherapy.

One of two preoperative radiotherapy regimens are generally applied in rectal cancer; the conventional long-course regimen (2 Gy × 25 or 1.8 Gy × 28) with concomitant 5-fluorouracil (FU)/capecitabine or a short-course regimen (5 Gy × 5, in one week) [9]. Downsizing and downstaging effects are more pronounced with the first approach [35,36], and this is the standard treatment regimen in LARC in most countries. In Norway the standard neoadjuvant therapy is the long-course regimen combined with capecitabine: 23 daily fractions of 2 Gy to macroscopic tumor volume and area of risk, followed by 2 daily boost fractions of 2 Gy to macroscopic tumor volume, as determined by CT-based planning. Surgery is usually scheduled 6-8 weeks after the last radiation dose to allow tumor shrinkage.

Neoadjuvant chemoradiotherapy

Not long after the introduction of preoperative radiotherapy, chemotherapeutic agents that sensitize tumor cells to ionizing radiation (*i.e.* radiosensitizing agents) were integrated into the combined modality treatment to improve the efficacy of the radiotherapy [37,38]. Three randomized phase III studies established preoperative 5FU-based CRT as standard therapy in LARC[33,39,40]. The trials showed a significant reduction in local recurrence rates by preoperative 5-FU-based CRT compared to postoperative 5-FU based CRT[33] and compared to preoperative radiotherapy alone [39,40]. The oral fluoropyrimidine capecitabine is a more convenient alternative, and early results from trials comparing the two regimens indicate that capecitabine is equivalent to 5-FU [41,42].

Adding fluoropyrimidine-based chemotherapy to preoperative radiotherapy may increase acute and late toxicity in some degree [39,43,44], but the main contributor to the toxicity seen after CRT is

the radiotherapy. The standard CRT regimen in rectal cancer is reported to confer considerable postoperative morbidity and toxicity in clinical studies [33, 45]. Radiotherapy for rectal cancer is associated with considerable long-term adverse effects on bowel and anorectal function, especially in terms of bowel frequency, urgency and fecal incontinence [43,46].

3.1.4 Response evaluation

Re-staging of rectal tumors after neoadjuvant therapy is performed to evaluate tumor response and potentially modify the subsequent therapy. Parameters of tumor response are often used as early surrogate end points for outcome in clinical trials.

Histopathologic tumor response is regarded as the primary outcome of preoperative treatment in rectal cancer. The surgical resection margins are evaluated for residual disease, and especially the positive CRM status (*i.e.,* residual tumor in the resection margin) is correlated to poor prognosis [47] (R0 = no residual tumor, R1 = microscopic residual tumor, R2 = macroscopic residual tumor)[13]. Histopathologic TN stage ('pTN' or 'ypTN' if neoadjuvant therapy is administered) is determined by examination of the surgical specimen. Pathological complete response (pCR), defined as absence of viable tumor cells in the primary tumor (ypT0), is associated with a favorable long-term outcome. The validity of pCR as a prognostic marker have been debated, but a recent pooled analysis of more than 3.000 patients found that patients with pCR after standard CRT has better long-term outcome than those without pCR [48]. While the TNM system considers viable tumor cells and not the degree of tumor tissue regression, an alternative method to evaluate histopathologic response is tumor regression grade (TRG) [49,50]. Based on the presence of residual tumor cells and the extent of fibrosis as proposed tumor regression in surgically excised rectal tumors can be graded on a scale from 1-5 [51] , or more simplified, a scale of TRG 1-3.

MR-based radiological methods to evaluate tumor response are currently under investigation[52]. Conventional MR can be used to determine anatomical tumor regression [53] (yTN stage[54], TRG [55], tumor volume [56-58]), while functional MR may determine biological parameters as markers of treatment response [59].

The ultimate evaluation of response to treatment in clinical trials is 5-year overall survival (OS)[51], while other survival endpoints, *e.g.,* disease-free survival (DFS) or metastases-free survival (MFS), may also be used depending on the setting[60].

3.1.5 Strategies to improve rectal cancer treatment

Although the local control with standard CRT treatment is good for the majority of LARC patients, some patients experience poor response to the treatment. These patients could benefit from further improvement of the neoadjuvant treatment. Intensification of treatment by integration of combination chemotherapy into the standard single-agent (fluoropyrimidine-based) CRT has been investigated in clinical trials. Addition of oxaliplatin (OXA) is being investigated in clinical phase III trials. Results of the early endpoints (*i.e*. pCR and toxicity) are disappointing, although results of long-term endpoints are awaited [42,61-65]. Integration of molecularly targeted agents as radiosensitizers in LARC is currently being investigated in early clinical trials.

The potentially improved local control of intensified treatment must be balanced with the increased risk of toxicity. While acute toxicities may cause interruption in the CRT delivery and delay definitive surgical treatment, surgical complications and long-term sequelae may strongly impede patients' quality of life [2,28].

Despite reduced rates of local recurrence, distant recurrences remain a significant problem in rectal cancer. Local control seems insufficient to reduce the rate of distant recurrences. 20-40% of radically treated rectal cancer patients develop metastases [66]. Distant metastases are now the predominant reason for reduced life expectancy in rectal cancer, and new strategies must include focus on distant control. The introduction of systemic chemotherapy in rectal cancer treatment has been suggested to target micrometastatic disease. *Adjuvant* chemotherapy is administered to LARC patients in the USA and at many European centers [9]. The evidence for a survival benefit from adjuvant chemotherapy is debated, and in Norway it is currently not recommended [17,67-69] [70]. Systemic *neoadjuvant* chemotherapy (NACT) as a supplement to CRT in LARC is under investigation in clinical trials [71-75].

3.2 Tumor hypoxia

Hypoxia, oxygenation deficiency, is a hallmark of solid tumors associated with an aggressive tumor phenotype, resistance to cytotoxic treatment, and metastatic behavior [76]. Tumor hypoxia is a result of imbalance between supply and consumption of oxygen [77]. As the tumor vasculature cannot meet the demands of the cancer cells, solid tumors are invariably less well oxygenated compared to the normal tissue of origin [78]. In an attempt to improve oxygenation, tumors induce the expression of proangiogenic factors activating angiogenesis, the formation of new blood vessels. However, tumor vasculature formed by angiogenesis is dysfunctional and unable to supply sufficient oxygen to the tumor tissue [79,80] (**Figure 3.5).** The resulting tumor hypoxia stimulates further angiogenesis; establishing a viscous circle of hypoxia and angiogenesis [81].

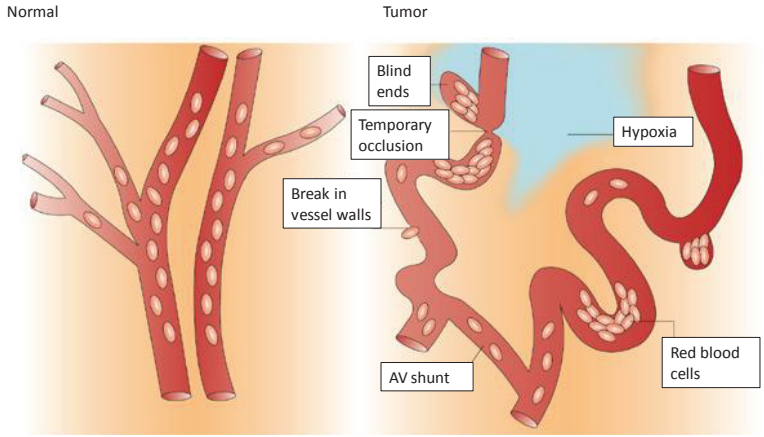

Figure 3.5 The vascular network of normal tissue versus tumor tissue. The tumor vessels are malformed and in a state of continuous reconfiguration. The vessels are tortuous with blind ends and arterio-venous (AV) shunts. The blood flow is poor and erratic, due to the malformations and unpredictable dilatation and constriction of the vessels [79,80]. Adapted from Brown and Wilson 2004, printed with permission.

Tumor hypoxia is a combination of 'chronic' (diffusion-limited) and 'acute' (perfusion-limited) hypoxia. Chronic hypoxia is a result of tumor angiogenesis lagging behind tumor growth and is found distal to blood vessels, beyond the diffusion distance of oxygen. Acute hypoxia is located in the proximity of poorly functioning tumor vasculature that is temporarily occluded [77,82]. Hypoxic areas are heterogeneously distributed within tumor volumes, but the tumor-to-tumor variability of oxygenation is greater than intra-tumor variability [77].

There is no exact threshold discriminating hypoxia from normoxia, and the term can refer to different cell populations in different contexts. Genomic and proteomic responses to hypoxia occur at different levels of the hypoxic scale [76,83]. Methods to measure hypoxia in human tumors are based on three different principles. Firstly, the physical amount of oxygen may be measured in tumors accessible for electrode measurement. Secondly, presence of hypoxic metabolic active cells can be detected by their ability to reduce specific compounds, *i.e.* exogenous markers (*e.g.* pimonidazole, **Figure 3.6**). Lastly, products of biological processes activated by hypoxia can be studied as a measure of hypoxia, *i.e.* endogenous markers (*e.g.* the hypoxia-inducible factor (HIF) type 1α, carbonic anhydrase-IX (CA9), vascular endothelial factor (VEGF)) [76,84]. Suggested imaging techniques to assess hypoxia are PET (positron emission tomography) scanning and functional MRI techniques [85,86].

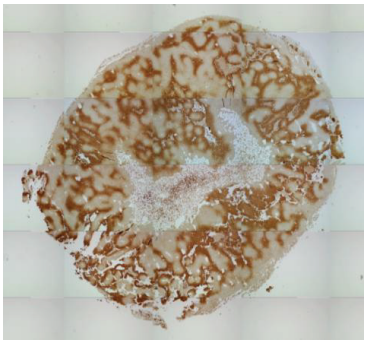

Figure 3.6 A section of a colorectal xenograft that is immunohistochemically stained with the exogenous hypoxia marker pimonidazole (brown; pimonidazole).

3.2.1 Cellular adaptive responses to hypoxia

Severe or prolonged hypoxia is detrimental to the cell, but tumor cells undergo a variety of adaptive changes enabling them to survive in a hypoxic environment. The adaptive hypoxic cellular processes involve alterations in gene expression, collectively contributing to a more clinically aggressive phenotype [77,84,87]. By exerting a selective pressure on tumor cells, hypoxia results in the emergence of tumor cells that favor tumor progression [88,89].

The HIF-1α-pathway is the core cellular hypoxic response pathway. The stability and functional activity of the transcription factor HIF-1α is oxygen-regulated. In normoxic conditions, HIF-1α is inactivated by posttranslational modifications and subsequent proteosomal degradation. In contrast, under hypoxia, it is stabilized and interacts with the constitutively expressed HIF β subunit to form the heterodimeric HIF complex which binds to the hypoxia response element of a number of target genes to regulate their transcription [83,90] (**Figure 3.7**). Activation of the HIF-1α-pathway affects numerous target genes. This has implications for a range of cellular processes *e.g.* angiogenesis, glucose metabolism, pH regulation, oxygen transport, DNA repair, apoptosis, cell proliferation and cell migration [77,82]. Angiogenesis is stimulated under hypoxia by the HIF-1α-directed upregulation of VEGF and several other angiogenic factors[88].

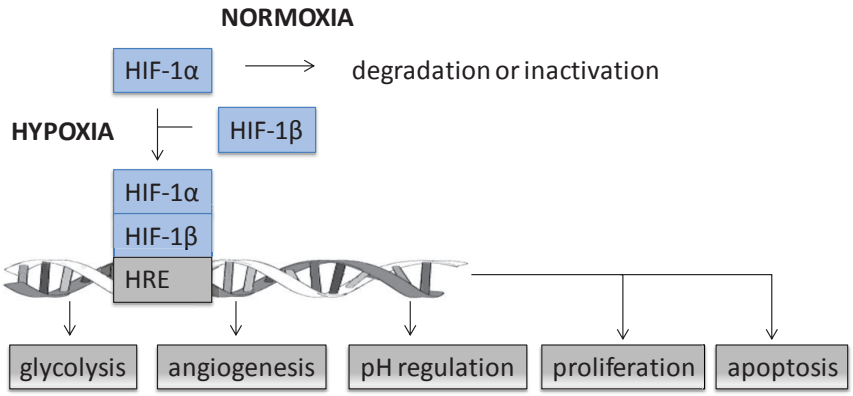

Figure 3.7 In hypoxic conditions, HIF-1α interacts with HIF-1β, binds to the HRE (hypoxia response element) and regulates genes involved in many cellular processes.

3.2.3 Hypoxia and radiation response

The 'oxygen effect', the phenomenon that molecular oxygen influences the biological effect of ionizing radiation (IR), was first recognized at the beginning of the 19th century when it was observed that skin reactions decreased if the radiation source was pressed tightly to the skin, indicating that blood flow could modify radiation response[91]. In the 1950s, Gray *et al* [92,93]

presented the 'oxygen fixation hypothesis' stating that oxygen molecules react with free radicals produced by IR to yield stable changes in the chemical composition of DNA (oxygen "fixates" the DNA damage) [27,94-96].

Tumor hypoxia also influences cellular radiation response through HIF-1α-induced alterations in gene expression. HIF-1α may increase radioresistance of solid tumors, independently of the tumor oxygenation status [97,98]. HIF-1α-regulated cellular processes that may influence tumor radiosensitivity are *e.g.* DNA repair, apoptosis, metabolism, proliferation and angiogenesis [96,99,100]. The ratio of doses administered under hypoxic versus normoxic conditions, needed to achieve the same biological effect, is called the 'oxygen enhancement ratio' and is characteristically in the order of 2.7-3.0 [76].

3.2.2 Hypoxia and metastasis

While hypoxia has been recognized as a main mechanism involved in tumor resistance to radiotherapy for many years, more recent research supports the hypothesis that tumor hypoxia is one of the major driving forces of the metastatic process. Experimental and clinical studies have shown that hypoxic tumors have increased propensity to develop metastatic disease. Hypoxic tumor signaling can affect nearly every step of the metastatic process [81,88]. For example, hypoxia promotes the processes of endothelial mesenchymal transition (EMT) and intravasation. HIF1α-signaling in tumor cells may render the tumor vasculature leaky by affecting the cell layers tumor cells must cross to reach the circulation [88] **(Figure 3.8).** The endothelial cells of functional vessels are supported by a pericyte coating promoting stability and permeability control. During hypoxia-mediated angiogenesis the pericytes detach[101]. Although the role of pericytes in metastasis is still unclear, experimental and clinical studies suggest that poor pericyte coverage is associated with development of metastasis [102,103].

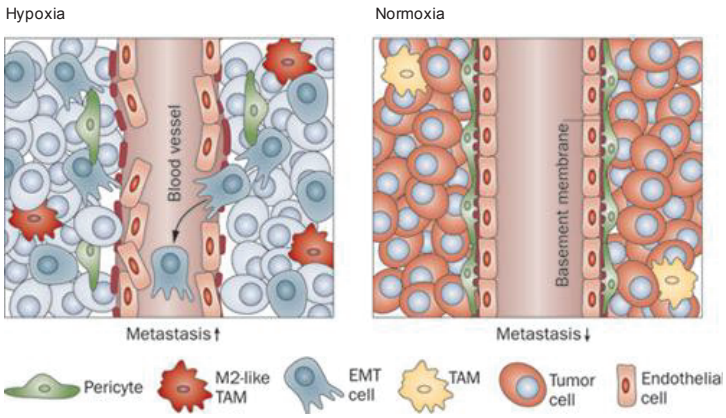

Figure 3.8 Tumor hypoxia and intravasation. Hypoxia stimulates the development of abnormal tumor vessels, characterized by loosely connected endothelial cells, a disrupted basement membrane and detached pericytes facilitating intravasation. Tumor-associated macrophages (TAM) stimulate growth of abnormal vessels in hypoxic tumors. Hypoxia promotes the biological process termed endothelial mesenchymal transition (EMT). Adapted from De Bock et al 2011, printed with permission.

3.2.3 Strategies to target tumor hypoxia

A number of strategies have been explored to target tumor hypoxia in radiation response. The first strategies aimed to overcome the hypoxic radioresistance by improving tumor oxygenation during radiotherapy, *e.g.* hyperbaric oxygenation, carbogen breathing (95% O_2), red blood cell transfusions and erythropoietin injections [85]. Oxygen-mimicking drugs that specifically radiosensitize hypoxic cells (*e.g.* nitroimidazole derivates)[76] , hypoxia-activated prodrugs (*e.g.* tirapazamine)[104] have been evaluated in clinical trials. With the discovery of HIF-1α, a molecular target of the hypoxic response was identified. The approach of targeting hypoxic radioresistance by suppression of the radioresistant phenotype of hypoxic tumor cells, is being investigated in clinical trials [104,105]. This strategy includes targeting HIF-1α itself [106] and targeting proteins in HIF-1α-mediated cellular processes influencing radiosensitization (*i.e.* targeting VEGF [88,97] in angiogenesis and CA9 [96] in glycolysis). Several therapeutic agents not originally intended to target HIF-1α, are shown to exert effects on this factor [107].

Strategies to target tumor hypoxia in metastatic disease progression has not been widely explored yet, although some experimental studies have reported encouraging results by inhibitors of HIF-1α [108] and of the HIF-1α-regulated CA9 [109] and VEGF [88].

3.3 The metastatic process

The main cause of cancer deaths is metastatic disease; the spread of cancer from one organ to another non-adjacent organ. The formation of a metastasis is a multistep process involving dissemination of cancer cells to distant organ sites and subsequent adaption to the microenvironment [110]. The cascade includes establishment of a vascular network in the primary tumor, invasion of the host stroma, intravasation, survival in the circulation and arrest in a new organ where the reverse processes of extravasastion and invasion take place [111] (**Figure 3.9**).

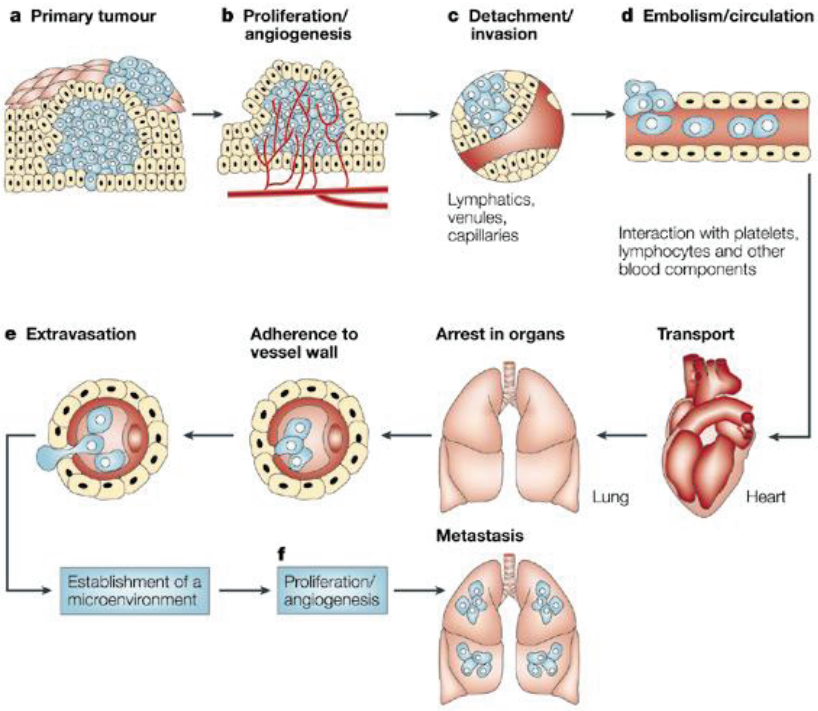

Figure 3.9 The main steps in the metastasis development. Adapted from Fidler 2003, printed with permission.

Primary tumor proliferation and angiogenesis

When tumors grow beyond a few millimeters in diameter, new blood vessels must be formed to support further tumor growth. Hypoxia and nutrient deprivation triggers an 'angiogenic switch'; a change in the balance between angiogenic activators and inhibitors promoting angiogenesis,

the formation of new blood vessels [112]. The pro-angiogenic factor VEGF which binds to its receptors on endothelial cell membranes, is the main regulator of angiogenesis[113]. In contrast to vasculogenesis, the creation of tumor vessels seen during embryogenesis, angiogenesis involves sprouting of new vessels from existing vessels [113].

Capillary vessels are supported by perivascular cells, pericytes [114], that wrap around the endothelial tubing to provide stability and permeability control (**Figure 3.10**). During the process of angiogenesis, the pericytes detach from mature blood vessels to permit remodeling of the vessels and establishment of a tumor capillary network [112]. PDGF, which signals through the PDGFRB (PDGF receptor type β) on pericytes, stimulates recruitment of pericytes along the advancing endothelial sprout, pericyte attachment and proliferation [115]. The pericyte layer of tumor vessels is often non-functional, and the neovasculature is commonly prone to leakiness and in a state of continuous reconfiguration, facilitating tumor cell intravasation [101,102].

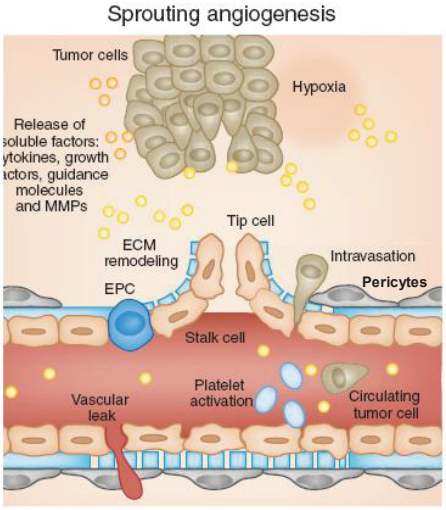

Figure 3.10 Tumor angiogenesis
During angiogenesis, stimulatory signals within the microenvironment induce pericyte detachment from mature blood vessels to allow sprouting of new vessels.

ECM: extracellular matrix; EPC: endothelial progenitor cell; MMP: matrix metalloproteinases

Adapted from Weis & Cheresh 2011, printed with permission.

Local invasion and intravasation

To reach the circulation, tumor cells must invade the surrounding extracellular matrix (ECM) and stromal cell layers and intravasate into the lumina of lymph or blood vessels. To invade the ECM, cellular adhesion molecules and ECM components must be degraded through proteolytic

activity, *e.g.* by matrix metallopreoteases. Cellular migration through the ECM also requires tumor cell motility. Altered adhesive properties of tumor cells are necessary to both to promote detachment of cells from the primary tumor, and to allow adhesion to ECM proteins and endothelial cells. Various cell adhesion molecules, *e.g.* integrins and cadherins regulate the process of adhesion[116]. During the process of EMT, tumor cells within epithelial sheets lose their adherent properties and dissociate into individual motile cells[110]. To reach the systemic circulation after moving through the ECM, cancer cells must cross the layers of pericytes and endothelial cells [110, 117].

Survival in the circulation and arrest at a distant organ

After entering the blood or lymphatic vessels, tumor cells can disseminate widely through the systemic circulation. Single tumor cells or small cell clusters may be detected in the blood (*i.e.* circulating tumor cells) and bone marrow (*i.e.* disseminating tumor cells) as they enter circulation. The bone marrow seems to be a common homing organ for blood-borne disseminated cells from various epithelial tumors [118]. Individual carcinoma types form metastases in a limited subset of target organs. According to the hypothesis of Stephan Paget, certain tumor cells (the 'seeds') have specific affinity for the microenvironment of certain organs (the 'soil') [111,119]. Consistent with this hypothesis, the formation of overt metastasis may reflect the adaptability of tumor cells to a particular foreign microenvironment [110].

Extravasation and metastatic colonization

To enter the tissue parenchyma of a new tissue, cancer cells must adhere to and penetrate the vessel wall [110]. The establishment of a metastatic foci involve the same processes as in the primary tumor (*i.e.* adhesion, proteolysis and migration). The extravasated carcinoma cells must survive in the foreign microenvironment to form micrometastasis. To become overt metastases, the tumor cells must proliferate and form macroscopic metastases; the process of metastatic colonization [111].

3.4 Cancer treatment

The three traditional modalities of cancer treatment, surgery, radiotherapy and chemotherapy, are increasingly combined, as focus on individualized cancer therapy has shifted treatment strategies towards multimodal treatment. The aim of combined modality treatment is to tailor each of the modalities so their antitumor effect is maximized with minimal toxicity to normal tissues [120]. Rectal cancer was probably the first cancer form to exploit the multidisciplinary approach systematically, combining all treatment modalities.

3.4.1 Surgery

Surgery is the oldest cancer treatment modality and the primary treatment strategy of most solid malignancies. For some cancer forms, the extent of the surgical procedure has been reduced in the modern era, while it has been extended in the case of rectal cancer. The current standard surgical technique in rectal cancer, TME, was developed in the 1980s [121] and was established as a standard technique in most European countries in the 1990s[30].

While surgery is effective as curative treatment in locally resectable tumors, combination with radiotherapy or chemotherapy is often warranted in patients with locally advanced cancers at high risk of local recurrences following surgery alone [27]. Radiotherapy and/or chemotherapy may be administered before or after surgery, as *neoadjuvant* or *adjuvant* therapy, respectively [122].

3.4.2 Radiotherapy

The use of IR for the treatment of cancer dates back to the late 19th century after the discovery of x-rays by Wilhelm Röntgen in 1895 and radium by Marie and Pierre Curie in 1898 [91,123]. Today around 50% of cancer patients will receive radiotherapy during the course of their illnesses, either as part of curative or palliative therapy [124]. Radiotherapy has a place in local treatment of most types of cancers, either as an alternative to surgery in early-stage cancers, or more often as an element of multimodal treatment [125]. With recent technological advances, it is expected that the role and use of radiotherapy will increase. Curative radiotherapy can be classified as *radical*, given as a definitive treatment; or *adjuvant*, given before or after definitive management of the

primary tumor, usually surgery. Administered prior to surgery, the main aim of radiotherapy is to decrease the tumor size and render the tumor resectable, while the aim of postoperative radiotherapy is to eradicate any residual, microscopic disease [124].

The rationale of radiotherapy is to produce DNA damage that will induce tumor cell death. Radiotherapy exploits high-energy IR, to induce DNA damage, particularly DNA double-strand-breaks [27]. The DNA damage is created either directly through the ionization within the DNA molecule or indirectly through formation of free radicals; highly reactive molecules which initiate a chain of events that result in DNA damage. Upon DNA damage, the cell activates DNA damage response mechanisms. A variety of cellular responses are initiated in order to repair the DNA damage or alternatively kill the cells if the DNA cannot be repaired. Compared to normal cells, rapidly proliferating tumor cells have reduced capacity to repair radiation-induced DNA damage and are therefore more sensitive to IR than normal cells [126-127].

Fractionation, the delivery of several fractions of IR, with each fraction consisting of a relatively small dose, typically 2 Gy, is an important principle in radiotherapy. The '5Rs of radiobiology' is a model that explains how fractionated radiation exploits differences between tumor cells and normal cells to target tumor cells [127-129]. Normal tissues proliferate relatively slowly and have time to **repair** damage before replication, while in rapidly proliferating tumor tissue unrepaired damage can be lethal. The rate of **repopulation** between fractions is lower in the tumor than in the normal tissue, allowing the normal tissue to tolerate a larger fractionated dose. After a dose of radiation, most surviving cells will be in the radioresistant cell cycle S phase. In contrast to normal tissues, tumor cells are allowed to **redistribute** throughout the cell cycle before the next dose of IR into more radiosensitive phases. The process of **reoxygenation** limits the negative effect of hypoxic cells in fractionated therapy [87]. Immediately after a dose of radiation the proportion of hypoxic cells in a tumor will be increased, but due to reoxygenation the proportion of hypoxic cells is reduced if sufficient time is allowed [94]. Cellular **radiosensitivity**, may differ in tumor and normal cells as it is influenced by intrinsic factors, *e.g.* genetic aberrations, as well as extrinsic factors, *e.g.* oxygenation.

Fractionation aims to protect the normal tissue as radiotherapy exerts normal tissue toxicity. Early (acute) side effects in rapidly proliferating tissues are usually transient, while late (chronic) side effects in tissues with a slower turnover are often irreversible and progressive[46,130].

3.4.3 Systemic therapeutics

Chemotherapy

Surgery and radiotherapy dominated the field of cancer therapy into the 1960s, when chemotherapy was increasingly incorporated into cancer treatment [120]. Traditional chemotherapeutic agents target tumor cells, mainly by initiating massive DNA damage in rapidly diving cells inducing cell death. The aim of chemotherapy applied in systemic doses is to target tumor cells in the primary tumor as well as disseminated tumor cells. Like radiotherapy, chemotherapy may be applied as curative therapy, alone or as supplement to the definitive treatment; or as palliative treatment. Applied as neoadjuvant therapy, micrometastatic disease can be targeted early [122].

Concomitant chemoradiation refers to the administration of chemotherapeutic agents in combination with radiotherapy. Combined with radiotherapy, chemotherapeutic agents may be applied to increase tumor control and to eradicate distant micrometastases outside the radiation field [131, 132]. Some chemotherapeutic agents exhibit radiosensitizing effects and may be administered concomitantly with radiotherapy to enhance the local treatment effect of radiation (*i.e .radiosensitizers*) [97 37,38]. Strictly speaking, radiosensitizing agents need not necessarily have inherent cytotoxic activity; however most radiosensitizers do and may thereby contribute to normal tissues toxicity. Radiosensitizers are generally administered in lower doses than when the drug is given as monotherapy to protect the normal tissues, limiting the systemic effects. Concurrent use of multiple radiosensitizing agents is challenging, for example, the added toxicity may necessitate dose reductions and interruptions in treatment [133,134].

Preoperative fluoropyrimidine-based CRT is well-established as standard treatment regimen in rectal cancer. The potential role of OXA as radiosensitizer in rectal cancer and the administration

of OXA-based chemotherapy as systemic therapy, is currently being investigated in clinical trials.

5-FU

The pyrimidine analogue 5-FU exerts its cytotoxic effect by inhibiting the thymidylate synthase enzyme, leading to reduced production of the nucleotide base thymidine and impaired DNA synthesis. Leucovorin/folinic acid may be given together with 5-FU to enhance its the cytotoxic activity [34]. Administered in sublethal concentrations in combination with radiotherapy, 5-FU exerts radiosensitizing effects, due to altered DNA repair and cell cycle regulation [34,37,135].

5-FU based chemotherapy is applied as adjuvant treatment in colon cancer and in metastatic CRC [9]. 5-FU is used concurrently with radiotherapy in several cancer forms including rectal cancer [132]. The most frequent mode of 5-FU administration in combination with radiotherapy is continuous intravenous infusion, which compared to bolus infusions confers better effects [, 34, 136]. The oral fluoropyrimidine capecitabine is a more convenient alternative. Capecitabine is a prodrug of 5-FU with the convenience of oral administration. Capecitabine-based regimens are compared to 5-FU based regimens in phase III trials in rectal cancer, and early results indicate that capecitabine is equivalent to 5-FU in CRT regimens [41,42].

OXA

The platinum analog OXA exerts cytotoxic effects by induction of DNA lesions and inhibition of DNA synthesis [137]. Clinical trials have established OXA in combination with fluoropyrimidines as adjuvant treatment in curative treatment of colon cancer [138] and as treatment of metastatic CRC [139]. Further, in CRC patients with resectable liver metastases, perioperative chemotherapy, *i.e.* before and after surgery, with 5FU/leucovorin and OXA is recommended [140]. After the success of OXA in treatment of metastatic CRC and in the adjuvant setting in colon cancer, expectations were high for OXA as additional component of CRT in LARC, although there was a scarcity of preclinical evidence regarding radiosensitizing effects of OXA in CRC [141,142].

OXA as part of the preoperative CRT regimen in rectal cancer is being investigated in five ongoing phase III trials. In three of the trials addition of OXA to 5-FU-based CRT did not

improve pCR rates, while toxicity was increased compared to 5-FU alone [42,61-63]. In contrast, in a fourth trial [64], pCR rates were improved; although the increase was small, without increased toxicity. A fifth study has recently been completed [65]. Although final data on local control and long-term survival are awaited, the available data indicate increased toxicity without added benefit from OXA, and do not support the use of OXA in standard neoadjuvant CRT regiments in LARC. The role of OXA in rectal cancer is not clear, *e.g.* OXA-based NACT is under investigation in early clinical trials [143], both in combination with CRT [71-75] and as an alternative to CRT in patients with intermediate risk.

Molecularly targeted therapeutics

Ideally molecularly targeted therapeutics would be agents designed specifically against well-defined targets critical for tumor survival not compromising for normal tissues. The target should be measurable in the clinic, and levels should correlate with clinical outcome when the targeted drug is administered [144,145] .

Most targeted therapeutics interfere with aberrant cell signaling pathways that drive malignant transformation in tumors. Activation of cell signaling pathways are typically initiated by the binding of a ligand to the extracellular domain of a transmembrane receptor, thereby activating its tyrosine kinase intracellular domain, initiating a cascade of intracellular reactions [146]. The main therapeutic strategies to target cell signaling are monoclonal antibodies and small-molecule tyrosine kinase inhibitors. The antibodies may be directed against the ligand or against the extracellular part of the receptor, while tyrosine kinase inhibitors diffuse into cells to reach their target at the intracellular part of the receptor or in downstream pathways [147].

There is growing interest in the potential value of combining targeted drugs with radiotherapy[132]. A number of currently available targeted agents may be expected to modulate one or more of the phenomena described by 'the 5Rs' of classic radiobiology and thereby have the potential to enhance tumor radiosensitivity. As targeted agents confer other types of toxicity than conventional chemotherapy, overlapping toxicity with radiotherapy may be less pronounced [148,149] . In rectal cancer several drugs targeting cell proliferation and angiogenesis have shown

promising results evaluated in combination with standard CRT in preclinical and clinical trials. Recently, a new class of targeted agents, histone deacetylase inhibitors, has been implemented as radiosensitizers in preclinical and early clinical trials in rectal cancer.

Inhibitors of the EGFR pathway

The transmembrane EGFR regulates signaling pathways of cell proliferation and survival, and is overexpressed in many tumor types [150]. *Cetuximab* and *panitumumab* are monoclonal antibodies that bind to EGFR with high specificity and prevent downstream EGFR-mediated signaling. In metastatic CRC, the antibodies have shown to improve survival in patients with wild-type KRAS tumors [150,151]. The potential role of cetuximab as a radiosensitizer was assessed in a landmark randomized phase III study in patients with locally advanced head and neck cancer, which showed that cetuximab in combination with radiotherapy significantly improved OS compared to radiation alone [152]. Cetuximab and panitumumab have been evaluated as part of preoperative CRT in rectal cancer in several phase I/II trials. Longer follow-up and finally randomized trials are needed, but early surrogate endpoints (pCR, TRG) have not showed significantly improved response to treatment, while toxicity is relatively frequent [28,151,153]. Nevertheless, it remains possible that a subset of patients will benefit from cetuximab- or panitumumab-based CRT in rectal cancer [154].

The small-molecule tyrosine kinase inhibitors *gefitinib* and *erlotinib* specifically target the kinase activity of the EGFR. They are implemented in the treatment of lung cancer patients with EGFR-mutations, and have shown promising results as a radiosensitizer in preclinical [155] and in early clinical trials in rectal cancers [156]. High-grade toxicity have necessitated dose-reductions in the clinical trials and further studies are ongoing to evaluate tolerability and efficacy [151].

Angiogenesis inhibitors

As angiogenesis is important for tumor growth and malignant progression, it is an attractive target for anticancer treatment. Most antiangiogenic strategies target the VEGF pathway by inhibiting the functions of the key proangiogenic growth factor VEGF or its corresponding receptors [97,157]. These agents probably exhibit their antiangiogenic effects by paradoxically normalizing tumor vessels, transiently reducing tumor hypoxia. Vessel normalization confers a

more efficient delivery of drugs and oxygen to the cancer cells, with the potential of enhancing efficacy of chemotherapeutic drugs and radiotherapy [151,158]. This hypothesis of mechanism behind the effects of antiangiogenic agents could explain why angiogenesis inhibitors have showed limited success as single agents in clinical trials, but seem to be more effective in combination with chemotherapy or radiation [38,97,158].

Bevacizumab is a monoclonal antibody directed against the VEGF ligand preventing it from binding to its receptor on endothelial cells. For metastatic CRC, bevacizumab improves survival when combined with chemotherapy [159,160], while in the adjuvant setting in colon cancer addition of bevacizumab have failed to improve survival in phase III trials [161,162]. Bevacizumab have shown radiosensitizing effects in experimental models [163] and have been evaluated in phase I-II trials in combination with CRT in rectal cancer. The pCR rates are not impressive in most trials, and increased toxicity and postoperative complications are worrying [151,164,165] .

Histone deacetylase (HDAC) inhibitors

HDAC inhibitors were originally designed as epigenetic therapeutics. While cancer traditionally has been considered to originate from genetic defects[166], growing evidence suggests that epigenetic modulation also plays a crucial role in cancer development[167]. Epigenetic changes refer to regulation of gene expression via posttranslational modification of protein complexes associated with DNA, without alterations in the DNA sequence [168]. Unlike genetic alterations, epigenetic alterations are reversible, and therefore an intriguing potential target for therapy [169].

The DNA strand is wound around cores of histone proteins, composing nucleosome units that comprise the chromatin. Altered chromatin structure by posttranslational modifications of histone tails regulate gene expression [169] . Acetylation of lysine residues on histone tails is regulated by two enzymes; while acetylation is mediated by histone acetyl transferase, it is prevented by HDAC [170]. HDAC also affect acetylation status of numerous non-histone proteins [171] and it has been suggested that HDAC should be redefined as *lysine* deacetylases, to reflect that its substrate is acetylated lysyl residues, not exclusive for histones [107].

HDAC inhibition as a potential form of epigenetic therapy has been suggested for a range of diseases, including cancer [167] as aberrant HDAC activity is a common feature of malignant cells [170,172]. HDAC inhibitors promote acetylation of histones; a process generally associated with activated gene transcription[173]. The regulation of transcription by histone acetylation is probably more complex[174] and HDAC inhibitors may also result in downregulation of genes[172]. Further, HDAC inhibitors induce acetylation of a large number of non-histone proteins, thereby influencing their function; *e.g.* transcription factors and multiple proteins involved in cellular processes [172](**Figure 3.11**). Hence, gene expression is affected by HDAC inhibitors by direct transcriptional effects by acetylation of histones and indirectly by acetylation of *e.g.* transcription factors. It is presumed that 5-10% of genes are influenced by HDAC inhibitors [171]. Acetylation of histone and non-histone proteins by HDAC inhibitors affects a variety of cellular processes closely connected with tumor progression.

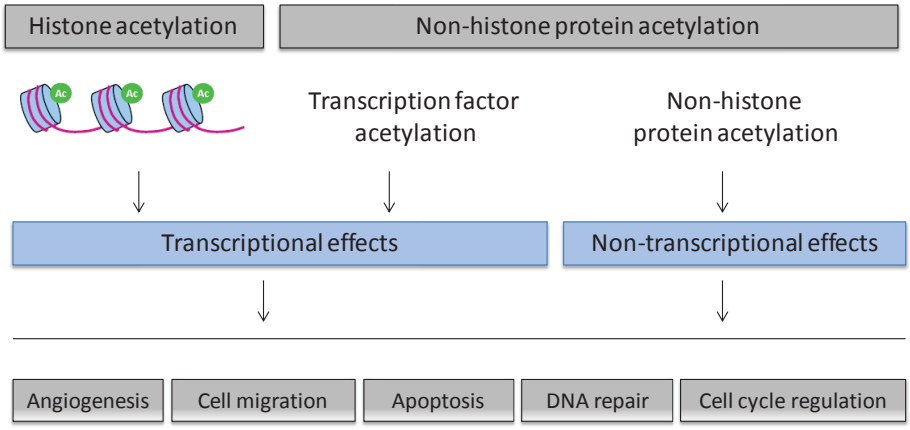

Figure 3.11 HDAC inhibitors induce acetylation of histone and non-histone proteins with resultant changes in key cellular functions.

The molecular effects of the HDAC inhibitors are not fully revealed. HDAC inhibition may affect the DNA damage response by downregulation of DNA repair genes and altered activity of DNA repair proteins[171]. Cell motility and proliferation are also inhibited, while apoptosis and cell cycle arrest are induced[173]. Several types of HDAC inhibitors are found to repress

angiogenesis, and accumulating evidence supports that this repression is mediated by disrupting the functions of HIF-1α, the master regulator of the cellular hypoxic response[171]. Recently some HDAC inhibitors have been shown to repress HIF-1α function, and it has gradually been realized that the tumor growth inhibiting effects of HDAC inhibitors are partially mediated by this mechanism [107,175]. The precise biochemical mechanisms for the HDAC inhibitor-initiated repression of HIF1α-functions remain unclear [107,176].

After identification of the first HDAC in 1996, more than twenty HDAC inhibitors have been investigated in clinical trials as single agents or in combination therapies [177]. In 2006, the first HDAC inhibitor, also the first agent to target the epigenome, *vorinostat*, was approved as single-agent treatment in refractory cutaneous T-cell lymphoma (CTCL) [178]. Clinical trials on HDAC inhibitors as single-agent therapy for various solid malignancies have reported tolerable, reversible side effects (fatigue, nausea, diarrhea, hematological effects). Despite promising result in CTCL, clinical benefit of HDAC inhibitors as single agent for various cancer forms has been variable [171]. Early clinical trials evaluating HDAC inhibitors in combination with cytotoxic therapies, *i.e.* conventional chemotherapeutic agents[179-181] and IR[182] are more encouraging. In preclinical studies, HDAC inhibitors have shown radiosensitizing effects in several tumor types [169 170]. HDAC inhibitor-induced suppression of DNA damage repair is shown in experimental studies [170,173,183]. A number of ongoing clinical trials are examining the combination of HDAC inhibitors and radiotherapy for various malignancies [169].

3.5 Biomarkers

A biological marker or biomarker can be defined as a characteristic that is objectively measured as an indicator of normal biological processes, pathological processes, or a response to a therapeutic intervention [184,185]. Biomarkers may be used as diagnostic tools, as tools for staging of disease or to predict and monitor clinical treatment response [184] and as early surrogate endpoints in clinical trials. *Prognostic* biomarkers give information on expected patient outcome independent of treatment or after standard treatment [186]. *Predictive* biomarkers aim to determine response to a specific therapy[187]. *Pharmacodynamic* biomarkers measure treatment effects in the target tissue [146].

The clinicopathological TNM staging system is the gold standard for evaluating prognosis in rectal cancer, but there are numerous other prognostic markers. One of the first biomarkers introduced in CRC was serum carcinoembryonic antigen (CEA), a normal cell product that is overexpressed in many adenocarcinomas and in a variety of inflammatory diseases [188,189]. In CRC, elevated serum CEA level at diagnosis (≥ 5 ng/mL) have been shown to have an adverse impact on prognosis, independent of tumor stage [47]. CEA-levels are followed in CRC patients as an indicator of disease progression, although 30 % of recurrences do not produce CEA [26]. A more recently proposed biomarker in CRC is the presence of tumor cells in blood or bone marrow (*i.e.* circulating tumor cells (CTC) or disseminated tumor cells (DTC), respectively) [190-192]. When entering the circulation as part of the metastatic process, single tumor cells or small cell clusters can be detected in the blood or in the bone marrow, hence detection of CRC or DTC may be a useful marker of early systemic dissemination.

Increasing numbers of predictive biomarkers have been implemented into clinical routine to guide treatment decisions with the introduction of molecularly targeted agents. Presence of gene aberrations in the patient's tumor [193] has been the main method to identify subpopulations of patients that may benefit from specific agents [194] (**Table 3.3**). However, as many targeted agents inhibit kinases at the hub of cell signaling cascades, the activity of several downstream kinases is influenced and aberrations of several genes affect response to therapy. For example, the mutational status of several other proteins downstream to the EGFR has been shown to predict outcome of anti-EGFR therapies in metastatic CRC, but currently KRAS, BRAF, and NRAS

mutational status is the only predictive biomarkers incorporated into clinical practice. Mutations in different codons of a gene may influence the response to treatment, exemplified by the individual mutations within the KRAS gene [193]. Pathway signaling activity conducted by the drug target may reflect mutation status of several genes and can potentially be used as a biomarker of drug response [195]. For many targeted drugs, *e.g.* antiangiogenic agents, there are currently no validated predictive biomarkers [151,196,197].

Drug	Tumor	Target(s)	Biomarker
Cetuximab	CRC	EGFR	*KRAS/BRAF/NRAS* wildtype
Panitumumab	CRC	EGFR	*KRAS/BRAF/NRAS* wildtype
Gefitinib	NSCLC	EGFR	*EGFR* mutations
Erlotinib	NSCLC	EGFR	*EGFR* mutations
Crizotinib	NSCLC	ALK, MET	*ALK* rearrangement, *MET* amplification
Trastuzumab	Breast cancer (gastric cancer)	HER-2	HER-2 expression, *ERBB2* amplification
Lapatinib	Breast cancer (gastric cancer)	HER-2	HER-2 expression, *ERBB2* amplification
Imatinib	CML, ALL, GIST	KIT, BCR/ABL, PDGFR	*KIT* mutations (exon 9 and 11), *PDGFRA* mutations, *BCR/ABL* translocation
Dasatinib	CML, ALL	BCR/ABL, SRC	*BCR/ABL* translocation
Nilotinib	CML	BCR/ABL	*BCR/ABL* translocation
Vemurafenib	Melanoma	RAF	*BRAF* mutation (V600)
Everolimus	Renal cell carcinoma	mTOR	*TSC1* or *TSC2* mutation/deletion
Temsirolimus	Renal cell carcinoma	mTOR	*TSC1* or *TSC2* mutation/deletion
Sunitinib	Renal cell carcinoma, GIST	PDGFR, VEGFR, KIT	*KIT* mutations (exon 9)
Ruxolitinib	Myelofibrosis	JAK2	*JAK2* mutations
Vandetanib	Medullary thyroid cancer	RET	*RET* mutations

Table 3.3 Targeted therapeutics with established predictive biomarkers.
CRC, colorectal cancer; NSCLC, non-small-cell lung cancer; CML, chronic myelogenous leukemia; ALL, acute lymphatic leukemia, GIST, gastrointestinal stromal tumor; ALL, acute lymphatic lymphoma.

The concept of integrating tumor biological parameters in treatment decisions by the use of predictive biomarkers may also be applied for multimodal treatment combining radiotherapy and chemotherapy. There are several potential predictive biomarkers of radiation response *e.g.* markers of tumor hypoxia, but these are currently not sufficiently validated to be integrated in the clinical decision process [187] . In rectal cancer predictive biomarkers of response to the standard CRT have been proposed [198-200].

In drug development, the identification of biomarkers is necessary to measure drug delivery and activity as well as to assess which patients that are likely to benefit from the therapy [201]. While predictive biomarker are useful to aim to the patient response, *pharmacodynamic* biomarkers

measure drug effect on its target, *i.e.* biological activity [146]. The biological activity of a drug is not necessarily the mechanism of drug action and may not be linked to tumor response. For example, in clinical trials combining HDAC inhibitors and radiotherapy, tumor histone acetylation has been proposed as a pharmacodynacmic biomarker. While useful as a marker for HDAC inhibition at the target, tumor histone hyperacetylation does not appear to reflect tumor response [202,203].

With the introduction of targeted agents, pharmacodynamic biomarkers may be used to determine the optimum dose of a new drug. Traditionally phase I trials have been used to determine the maximum tolerated dose (MTD), by escalating the treatment dose until predefined dose-limiting toxicity (DLT) is reached [204]. For molecularly targeted agents, the dose that results in clinically relevant levels of target modulation may differ from MTD, and the optimum dose may be the dose as the dose that is associated with a pharmacodynamic biomarker reflecting the mechanism of drug action in the tumor [149,205,206].

Recently, search for new biomarkers have focused on imaging and molecular biomarkers [9]. With the development of the microarray technique during, molecular profiling as a novel approach to the discovery of biomarkers has emerged. Gene and protein expression profiling is among the most widely recognized and extensively studied methods to identify molecular biomarkers. Another promising strategy to identify new biomarkers is the utilization of emerging imaging technologies [207].

A biomarker test should be simple to perform, easy and fast to evaluate, accurate (high sensitivity and specificity), cost-effective and reproducible [186,208]. Most biomarkers described to date have been identified in retrospective studies, to be used in the clinic biomarkers should be validated in prospective, randomized clinical trials [207].

4 Aims

Rectal cancer is a heterogeneous disease in terms of response to treatment, frequently multimodal, and the ability to metastasize. Recognizing that tumor hypoxia is a common determinant of resistance to cytotoxic therapies and metastatic behavior, the principal aim of the present work was to characterize this particular phenotype by applying a number of translational approaches in experimental and clinical cancer research, with the ultimate goal of improving radiation response and inhibiting metastasis in rectal cancer.

This ambition was endeavored through the following study objectives:

1 The characterization of hypoxic tumor kinase activities associated with early systemic disease dissemination in LARC patients scheduled to receive neoadjuvant CRT.
2 The evaluation of radiosensitizing effects of the HDAC inhibitor vorinostat under hypoxia and in combination with capecitabine in experimental CRC models.
3 The identification of biomarkers of HDAC inhibitor activity within the context of a phase I study undertaken in patients receiving pelvic radiotherapy in combination with vorinostat.
4 The examination of chemotherapy effects on tumor radiation sensitivity in the clinical setting of neoadjuvant treatment of LARC and in experimental CRC models.

5 Summary of papers

Paper I: Tumor kinase activity in locally advanced rectal cancer: angiogenic signaling and early systemic dissemination

Even with successful local treatment, a substantial number of patients with LARC develop metastatic disease as a result of systemic dissemination of non-eradicated tumor cells. Tumor hypoxia initiates adaptive cellular responses which involve activation of a range of kinase signaling pathways that contribute in driving the metastatic process. The prospective phase II CRT trial, the LARC-RRP study: Locally Advanced Rectal Cancer – Radiation Response Prediction (ClinicalTrials NCT00278694) enrolled 113 patients from October 2005 to March 2010. Patients received NACT and CRT followed by surgery and no further treatment. The aim of the Paper I study was to assess how kinase activities of the primary tumor from the LARC-RRP study patients may be associated with early systemic disease dissemination, defined as the presence of DTC in bone marrow. A high-throughput peptide microarray technology [209,210] was used to study the effect on *ex vivo* tyrosine kinase activity of the kinase-inhibitor sunitinib, an anti-angiogenic agent, in baseline tumor biopsies of 55 patients. The absence or presence of DTC in patient bone marrow sampled at the time of diagnosis was determined by immunomagnetic selection, and association between tumor kinase activity profiles and DTC status was studied.

Sixty percent of cases were DTC-positive and these patients had a significantly poorer metastasis-free survival than patients without DTC in the bone marrow. Sunitinib inhibition of overall tyrosine kinase activity was stronger in the DTC-negative patients. Phosphorylation of 31 of 102 array kinase substrates was significantly more strongly inhibited by sunitinib in tumor samples from the DTC-negative patients compared to the tumor samples from patients with positive DTC status. Among kinase substrates that were differentially inhibited, a significant portion was involved in angiogenesis-related pathways, mainly peptides representing receptors of PDGF, VEGF, and erythropoietin.

In summary, hypoxic tumor kinome signaling was different in rectal cancer patients with and without early systemic dissemination. Low signaling mediated by PDGFR in patients with DTC in the bone marrow may represent a poorly functioning pericyte layer, enabling metastatic progression.

Paper II: Radiosensitization by the histone deacetylase inhibitor vorinostat under hypoxia and with capecitabine in experimental colorectal carcinoma

Responses to established neoadjuvant CRT in LARC may vary considerably. Strategies to improve radiation response, i.e., by novel radiosensitizing agents, are warranted. The HDAC inhibitor vorinostat has been shown to sensitize experimental tumor models to radiation. In this study we wanted to expand the preclinical investigation [203] of vorinostat as a radiosensitizing agent in rectal cancer.

Since solid tumor, including rectal carcinomas, often contain a substantial fraction of hypoxic radioresistant cells, novel radiosensitizers should be evaluated both under normoxic and hypoxic conditions in preclinical models. Furthermore, before introduction in clinical trials, potential interactions between a new drug and the established treatment regimen should be investigated in experimental models. We therefore aimed to study radiosensitizing effects of vorinostat under hypoxia and in combination with fluroropyrimidine-based chemotherapy that is currently used in LARC treatment.

In four CRC cell lines and one CRC xenograft model, radiosensitizing effects of vorinostat under hypoxic conditions were evaluated by measuring *in vitro* clonogenic cell survival and *in vivo* tumor growth delay, respectively. In two CRC xenograft models, radiosensitizing effect of vorinostat when combined with capecitabine was evaluated by tumor growth delay assessment.

Vorinostat caused radiosensitization under hypoxic conditions both *in vitro,* in terms of significantly lowering clonogenicity of irradiated cells, and *in vivo* by enhancing radiation-

induced tumor growth delay. In addition, vorinostat synergized with the sensitizing effect of capecitabine in radiation-induced tumor growth delay.

Taken together, our results from the expanded preclinical investigation of vorinostat as radiosensitizer in CRC models support the introduction of vorinostat as an additional component of CRT in LARC trials.

Paper III: The identification of potential biomarkers of histone deacetylase inhibitor activity in a phase I combined-modality study with radiotherapy

Following promising result of the histone deacetylase inhibitor vorinostat as radiosensitizer in experimental CRC models, the PRAVO trial was conducted [182,211]. This phase I trial was designed to evaluate both clinical and novel biomarker endpoints in patients with advanced gastrointestinal malignancies receiving pelvic palliative radiotherapy combined with vorinostat.

Potential pharmacodynamic biomarkers of vorinostat activity reflecting timing of vorinostat administration relative to the fractionated radiotherapy were explored by gene expression profiling of peripheral blood mononuclear cells (PBMC) sampled from 14 study patients at baseline (T0) and two and 24 hours (T2 and T24) after the patients had received vorinostat. Gene expression was compared for T2 *versus* T0, for T24 *versus* T2, and for T24 *versus* T0.

Functional annotation analyses of the approximately 2100 differentially expressed genes for the comparisons T2 *versus* T0 and T24 *versus* T2 identified several enriched biological processes, with the Gene Ontology (GO) term transcription (GO:0006350) as the most significant in both comparisons. The top-three biological pathways were common for both comparisons and included signaling factors of the cell cycle. 1602 transcripts revealed a biphasic pattern of regulation from T0 through T2 and T24, as they were found to be differentially expressed both at two hours of vorinostat exposure (T2 *versus* T0) and on the T24 *versus* T2 comparison, while no differential expression was observed comparing the T24 and T0 groups. With a stricter p-value cutoff and by introducing a $\log_2$-fold change cutoff of 1.0, the list of differentially expressed

probes with biphasic pattern was reduced to 38 genes. Five of these genes were recognized both as players in the DNA damage response and targets for regulation by HDAC inhibitors and were therefore selected for verification by Realtime-quantitative polymerase chain reaction (RT-qPCR) which confirmed significant time-dependent changes for all genes. The expression of the same five genes was assessed further by RT-qPCR analysis of two colorectal xenografts after exposure of vorinostat, revealing significant and transient MYC repression.

The confirmation of MYC as the only one of the selected genes with rapid and transient change in expression in all tested conditions may point to a particular importance of myc in the therapeutic setting of vorinostat in combination with fractionated radiation.

Paper IV: Is oxaliplatin-containing neoadjuvant chemotherapy an alternative to radiation in T3 rectal cancer?

In LARC, neoadjuvant therapy is generally given as long-term CRT or short-term radiotherapy, which may cause significant toxicity. Recent data from randomized studies indicate no additional benefit from OXA in CRT [42,61-64,212]. Still, OXA is well established in adjuvant and palliative regimens in CRC and in NACT in liver metastasis surgery, which suggests potential neoadjuvant benefit also in LARC.

In a non-randomized study of LARC patients (LARC-RRP ClinicalTrials NCT00278694 [212]), two NACT cycles with the Nordic FLOX regimen were administered prior to long-term CRT. Tumor volumes were calculated from MRI examinations at baseline, after NACT and after NACT + CRT for 72 patients. Additionally, the impact of previous OXA exposure on experimental radiosensitivity was examined in CRC cell lines.

All tumors except one responded to NACT, and in all but three patients, additional tumor volume reduction resulted from the subsequent CRT (median volume reduction of 63% and 68%, respectively). The NACT volume responses were significantly larger in T3 than in T4 cases (70.5% and 47.9%, respectively; $p < 0.001$). Only 11% of patients required FLOX dose

adjustment because of toxicity. OXA-resistant CRC cells were significantly more radiosensitive than the OXA-sensitive counterparts.

In LARC, OXA-containing NACT led to substantial tumor volume reduction, as assessed by MRI volumetry, with particularly good responses in T3 cases. Additional tumor volume reduction was observed after subsequent CRT in almost all cases, suggesting that pretreatment with OXA-containing NACT did not impede tumor response to CRT. Experimental results rather suggested enhanced radiosensitivity of OXA-resistant CRC cells. Individualization of neoadjuvant therapy, omitting CRT for more favorable toxicity profiles in LARC T3 cases, is worth investigating.

.

6 Methodological considerations

	Model system	Methods
Paper I	Clinical trial LARC-RRP	Immunomagnetic selection of disseminated tumor cells
		Tumor kinase activity profiling
Paper II	Cell cultures	Clonogenic survival (under normoxia and hypoxia)
	Xenografts	Tumor growth delay (under normoxia and hypoxia)
Paper III	Clinical trial PRAVO	Gene expression profiling, RT-qPCR
	Xenografts	RT-qPCR
Paper IV	Clinical trial LARC-RRP	Tumor MR volumetry
	Cell cultures	Clonogenic survival

Table 6.1 Model system and main assays. RT-qPCR, real-time qualitative polymerase chain reaction; MR: magnetic resonance.

6.1 Experimental CRC models

6.1.1 Cell cultures

Tumor cells grown in culture are valuable as models of cancer, as continuous growth permits performance of standardized experiments. One of the main limitations of this model is the lack of a tumor microenvironment, and cells grown *in vitro* lack the architectural and cellular complexity of *in vivo* tumors [213]. Unwanted selection pressure during prolonged culture may modify the genotype and phenotype of the cells, and as a result the cell line may not be representative of the original tumor *in situ* [214]. Furthermore, there is a risk of cross contamination between different cell lines used in the laboratory. To ensure that the cells are not modified or contaminated, cell line identity should be verified prior to experiments. Identities of the cell lines used in this thesis were validated by short tandem repeat profiling (genetic fingerprinting) [215 216].

Cell line	Derived from	Patient (gender/age)	Origin	Reference
HCT116	Primary colon carcinoma	Male /-	ATCC	[217]
SW620	Lymph-node metastasis from colon cancer	Male /51	ATCC	[218]
HT29	Primary colon carcinoma	Female/44	ATCC	[219]
KM20L2	Primary colon carcinoma	-	NCI	[220]

Table 6.2 Characterization of colorectal carcinoma cell lines used in this thesis. ATCC, American Type Culture Collection; NCI, National Cancer Institute (of the United States of America).

6.1.2 Xenografts

In the animal experiments described in this thesis, ectopic xenografts were established by subcutaneous injections of cells in culture on athymic nude mice (T-cell deficient). Xenografts are created by transplanting human tumor cells into mice or rats; either by injection of cells in suspension or by implantation of human tumor tissue (from the original tumor or from a xenograft established from cells in suspension) [221]. The xenografts may be established subcutaneously (ectopic xenografts) or in the organ system of the original tumor (orthotopic xenografts)[214]. The microenvironment of orthotopic xenografts is more similar to the *in situ* tumor. However, disadvantages of the orthotopic model include difficult establishment, commonly the need for imaging to monitor tumor response, and possibility that the tumor or the treatment may disrupt vital organ functions [131]. Ectopic models are usually preferred to study radiation response as radiation can be delivered without exposing critical organs [214]. To avoid rejection of the human tumor cells, immunocompromised mice are commonly used. Although mice share 99% of their genes with humans [222], the predictive value of xenograft models for performance in clinical trials have been questioned and there are several limitations to this model. For xenografts established from cell lines grown *in vitro*, selection pressure might have altered the cells [221]. The microenvironment is different from an *in situ* tumor; and radiation response may be influenced by abnormal immune responses and presence of mouse rather than human stroma [131,214].

6.1.3 Experimental treatments

Systemic therapeutics

For *in vitro* experiments involving the HDAC inhibitor vorinostat, the drug was diluted in culture medium from frozen stock solutions immediately before addition to cell cultures. Vorinostat (1or 2μM) was added to the cell cultures for an incubation period of 18 hours. In animal experiments, vorinostat (100 mg/kg) was diluted in dimethyl sulfoxide (DMSO) and given by intraperitoneal injections three hours before IR; capecitabine (359 mg/kg) was suspended in Arabic gum and given orally to mice by gavage.

Radiation

IR was delivered to cell lines in culture by an x-ray unit (dose rate of 1.0 Gy/min) 24 hours after cell seeding. Control cells were simultaneously placed in room temperature. To irradiate tumor xenograft, a linear accelerator was used (dose rate of 2.6 Gy/min). Control mice were also anaesthetized, by subcutaneous injections of the zoletil mixture (tiletamine, zolazepam, xylazine and butorphanol), and brought to the radiation room. The xenografts were irradiated with a schedule of four or five fractions of 2 Gy with 24 hours between each fraction.

Hypoxic radiation

Hypoxia chamber

An unequivocal *in vitro* model of a cellular hypoxic environment has not been established [223]. Chambers, in which a desired oxygenation level is established by flushing with 5% CO_2 and N_2, are often used to establish hypoxia [223-225]. Mimicking hypoxia by pharmacological means is not recommended. Although HIF1-α may be activated pharmacologically, other consequences of hypoxia will not be reproduced [224,226].

A hypoxia chamber was used to establish hypoxic conditions (1% O_2) of cell cultures in order to study radiation response under hypoxia *in vitro*. While the oxygen tension in the chamber is controlled, the actual oxygenation level at the cellular level might be different [224, 227]. The oxygenation level at the time of radiation is critical for induction of DNA damage; hence the cells must be kept hypoxic during IR to study hypoxic radiation response. The cells were kept in sealable plastic flasks and transferred to the x-ray unit for immediate IR after removal from the hypoxia chamber [228]. Alternatively, transportable preincubated chambers could have been used to keep cells hypoxic during IR [225,229].

The technique of western blot immunostaining [230] was used to evaluate the HIF1α-level, to assess if cells responded to hypoxia upon treatment in the chamber. Proteins were separated by gel electrophoresis and transferred to a membrane for detection by antibodies specific to the target protein, and presence of immunoreactive proteins were detected by chemiluminescence.

Radiobiologically, hypoxia is often defined as oxygen concentrations below those causing maximum resistance to radiation, by the oxygen effect; about 0.02 per cent. Radioresistance may already occur at oxygen levels of 4-5% and from a clinical standpoint it has been proposed that intermediate hypoxic cells are the most important for prognosis, as they are resistant to therapy and still have the ability to proliferate [83,231]. The fact that we observed increased HIF1α-levels in cells treated with hypoxia and increased radioresistance of cells irradiated under hypoxia, indicate that the cells did experience hypoxia.

Figure 6.1 Hypoxia chamber
A Ruskinn INVIVO$_2$ 200 Hypoxic Workstation was used to establish oxygen level of 1%.

Cells were incubated for 18 hours and simultaneously exposed to vorinostat or control before sealing the flasks and transferring them to a nearby x-ray unit for immediate irradiation.

Clamping

The technique of clamping was used to study radiation response under hypoxia *in vivo*, [232-235]. Xenografts were established distally on the thigh of the mice to allow a clamp to be placed over the proximal thigh of anesthetized mice during IR **(Figure 6.2)**. Unilateral xenografts were used in the treatment-experiments as only one leg can be clamped at the time and differential treatment of tumors on the same mouse is not recommended. To confirm that tumor blood supply to clamped xenografts was minimal, radioactive iodine was injected intravenously to the mice; and radioactivity in excised xenografts were compared for clamped and unclamped tumors of the same mice, revealing significantly reduced radioactivity in clamped tumors (3% of radioactivity in unclamped tumors). Blood pressure and tumor blood flow may be influenced by *e.g.*

anesthesia and stress [236], underlining the importance of keeping non-treatment related conditions as similar as possible across treatment groups. An alternative method described to establish hypoxia *in vivo* involves exposing mice to cycles of oxygen-reduced air [237], but this method would not allow IR under hypoxic conditions.

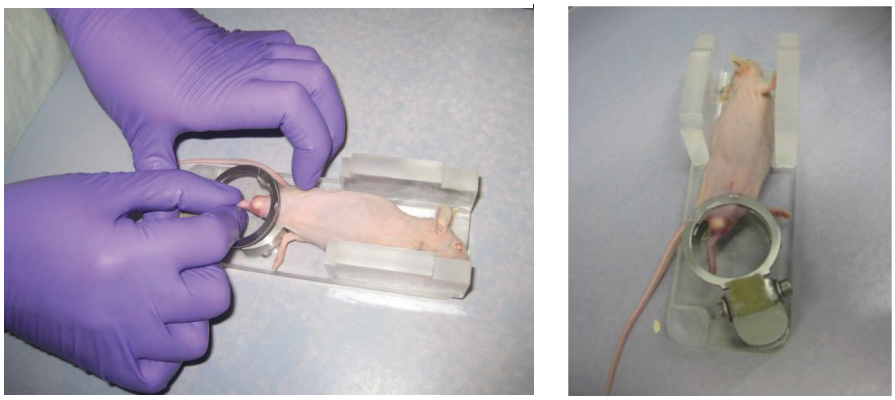

Figure 6.2 The clamping procedure. Before clamping, the mice were anesthetized and vaseline was applied to protect the skin. The clamp (with a step to protect the femoral bone), were placed over the proximal thigh of the mice. After 3.5 minutes of clamping, the tumors were irradiated. The mice were clamped for a total period of 5 minutes.

Immunohistochemical stains of the exogenous hypoxia marker pimonidazole were made from seven mice with bilateral xenografts (data not included in paper). The same fraction of pimonidazole stained cells was detected in unclamped and clamped xenografts (31%). Pimonidazole needs a hypoxic period of 30 min to form complexes and its expression is mostly seen at a certain distance from the blood vessels, hence this marker is thought to identify mainly chronically hypoxic cells [238]. As the tumors were exposed to hypoxia for only five minutes in our experiments, a clamping-induced increased fraction of pimonidazole-stained cells could not be expected.

Establishment of OXA-resistant cell lines

The human colorectal carcinoma cell lines HT29 and KM20L2 were repeatedly exposed to increasing concentrations of OXA for 7 and 9 months, respectively, using two exposure regimens. To establish the 4OXA variants, the cells were exposed to OXA for 4 h, starting at an initial OXA concentration of 2 μM; increasing by 2-μM increments (terminating at 46 μM and

28 μM for HT29 and KM20L2, respectively). The 72OXA variants were generated by exposure to OXA for 72 h, with an initial OXA concentration of 0.2 μM, increasing by 0.2-μM increments (terminating at 4.0 μM and 3.0 μM for HT29 and KM20L2, respectively). Resistance was maintained by exposing the cells to the final concentrations every 4-6 weeks.

OXA resistance of the variant cell lines was confirmed by the *MTS cell proliferation assay*. The MTS assay is based on the fact that living cells can reduce the MTS compound (3-(4,5-dimethylthiazol-2-yl)-5-(3-carboxymethoxyphenyl)-2-(4-sulfophenyl)-2H-tetrazolium) into a colored product that can be measured spectrophotometrically [239]. By measuring the cellular metabolic activity, the fraction of proliferating cells is determined and can be used to study short-term (usually 72 hours) cell culture drug resistance.

6.1.4 Experimental radiosensitivity

Clonogenic cell survival assay

The clonogenic cell survival assay is the *in vitro* gold standard for the measurement of cell kill following IR exposure. The assay measures the proliferative or clonogenic capacity of individual cells [214,226,240]. Cell death after IR is primarily caused by mitotic catastrophe, which may require several cell divisions, reflected in this long term assay. Radiation induces transient growth arrest, which can be misinterpreted as cytotoxicity in short term assays based on cell number [214]. In the most common form of the clonogenic assay, single cell suspensions are seeded into tissue culture plates or flasks, and after attachment of the cells to the plates (>6 hours) the cells are treated [240]. In our experiments, cells were irradiated 24 hours after seeding, before replication. Colonies (> 50 cells) were counted after 7-14 days depending on the specific cell line, and surviving fractions relative to the relevant control were calculated.

Tumor growth delay (TGD) assay

In the TGD assay, the most common assay to assess *in vivo* radioresponse, xenografts are allowed to grow to a certain size or volume, then the mice are randomized and experimental therapy is given. The smallest and largest tumor diameter are measured typically 2-3 times a week to calculate the tumor volume [241] relative to the tumor volume at the start of treatment.

Commonly, time to doubling or five-doubling (T2x and T5x) of tumor volume is calculated for all tumors and TGD is calculated as the difference between T2x/T5x for each tumor compared to the average of the control tumors. The average TGD for the control group and each treatment group is reported [214].

6.2 Clinical trials

6.2.1 Phase I and II study design

Careful design of study protocols and rigorous control of study conduct are necessary to enable evaluation of relevant clinical and biomarker endpoints in clinical trials [242].

The main aim of a phase I study is to determine safety and tolerability, typically in terms of establishing MTD and DLT, of a novel therapeutic agent [205]. The 3 + 3 expansion cohort design is traditionally used; the occurrence of an acute DLT in one of three patients on the same dose level triggers recruitment of further three patients to the same dose level. The dose escalation continues until at least two patients in a cohort of three to six patients experience a DLT [206]. Phase I studies evaluating the combination of systemic drugs with presumed radiosensitizing activity and radiation or standard chemoradiation, confer additional challenges compared to conventional studies of systemic cytotoxic chemotherapy [131]. For example, it may be difficult to decide whether a toxic event is greater than could be expected from radiotherapy alone.

The aim of a phase II trial is to assess activity, safety and feasibility of a new treatment. Traditionally phase II trials have been designed as single-arm studies with no control group, but randomized phase II designs are increasingly chosen to allow direct comparison of a new treatment to standard treatment [204]. Predictive biomarker are increasingly incorporated into study design to select eligible patients based on treatment tolerability and response [243].

6.2.1 The LARC-RRP trial

In the non-randomized phase II trial LARC-RRP (Locally Advanced Rectal Cancer – Radiation Response Prediction; ClinicalTrial NCT00278694 [212]), OXA-based NACT and CRT were given to patients with LARC scheduled for CRT and subsequent surgery. The study was approved by the Regional Committee for Medical and Health Research Ethics South-East Norway and was performed in accordance with the Declaration of Helsinki. Written informed consent was required for participation. The primary inclusion criterion was histologically confirmed rectal adenocarcinoma from LARC tumors as defined by the Norwegian guidelines at the time of the conduct of the study: T4 tumors, T3 tumors within 3 mm from the MRF and tumors of any T stage with pathological lymph nodes within 3 mm from the MRF, as assessed by diagnostic MRI [17]. A total of 113 patients were enrolled between October 2005 and March 2010. Patients with systemic disease at diagnosis were included if the metastases were potentially resectable and curative treatment was planned (n = 10). Diagnostic investigations included clinical assessment, rigid rectoscopy, pelvic MRI and CT of the chest and abdomen. The rectoscopy was performed under heavy sedation, and in this setting the primary tumor was biopsied and for a subgroup of patients, bone marrow was collected from the anterior iliac crests, As described in paper I, the presence of DTC in bone marrow and kinase activity profiling in study-specific tumor biopsies were evaluated for a subgroup of patients (n = 55) **(Figure 6.3)**.

The treatment protocol included two 2-weekly cycles of NACT, the Nordic FLOX regimen: OXA 85 mg/m^2 on day 1, 5-FU 500 mg/m^2 and folinic acid 60 mg/m^2 daily on days 1 and 2. Following NACT, CRT was delivered over five weeks. Radiotherapy was given according to the Norwegian guidelines (25 x 2 Gy to target volumes as detailed previously). During the radiotherapy course, concomitant chemotherapy was given as OXA 50 mg/m^2 once weekly and capecitabine 825 mg/m^2 twice daily on days of radiotherapy. Surgery was planned 6-8 weeks after completion of the preoperative treatment. The resected primary tumor specimens were subjected to routine histological evaluation according to standard criteria (ypTN stage and CRM) and TRG, using the five-point scale proposed by Bouzourene *et al* [50]. Further, radiological response to neoadjuvant chemotherapy and CRT was evaluated by MRI (ycTN stage). As described in paper IV, a study-specific MRI was performed after the administration of NACT and the first three radiotherapy fractions in a subgroup of patients (n = 72).

Seventy-two LARC-RRP patients had MRI examinations both at baseline, after NACT and after completed CRT. To calculate tumor volumes, the tumors were manually contoured in the tumor-containing axial MR images by the study radiologist, and whole-tumor volumes were obtained by multiplying the cross-sectional tumor area in individual slices by the sum of the slice thickness and slice gap. Recent advances in MRI technology has improved the accuracy in tumor size measurement, and MR volumetry after preoperative CRT has been investigated as a parameter of treatment response in rectal cancer and is reported to correlate well with downstaging, TRG and disease-free survival DFS [53,56,244]. Tumor volume changes after NACT, after CRT and after the total preoperative treatment were calculated **(Figure 6.3)**.

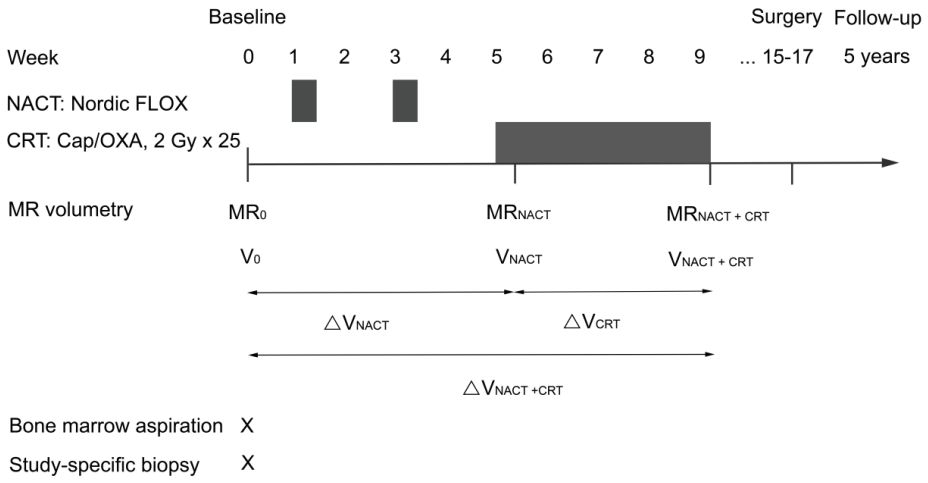

Figure 6.3 LARC-RRP Timeline

Patients were scheduled for follow-up consultations for five years postoperatively, at three- and six-month intervals for the first and second year, respectively, and every twelve months thereafter. Review procedures included clinical examination, blood tests, and CT scanning of the chest, abdomen, and pelvis. Locally recurrent or metastatic disease and death of any cause were recorded. Valid observations of the presence or absence of distant metastases or local recurrence

required designated radiological examination and/or bioptic verification. A flow chart describing the two subgroups evaluated in paper I and IV is given in **Figure 6.4**.

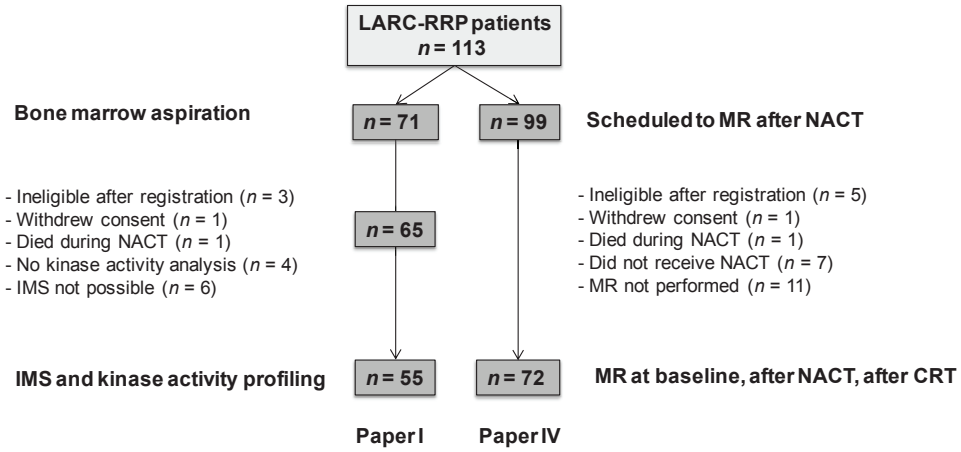

Figure 6.4 Patient cohorts analyzed in papers I and IV. LARC-RRP, locally advanced rectal cancer – radiation response prediction; NACT, neoadjuvant chemotherapy; IMS, immunomagnetic selection, MR, magnetic resonance; CRT, chemoradiotherapy.

6.2.2 The PRAVO trial

In the Pelvic Radiation and Vorinostat (PRAVO) phase I study (ClinicalTrials NCT0045351)[212] the HDAC inhibitor vorinostat was administered in combination with fractionated radiation to pelvic target volumes in patients with advanced gastrointestinal carcinoma. The study was approved by the Regional Committee for Medical and Health Research Ethics South-East Norway and was performed in accordance with the Declaration of Helsinki. Written informed consent was required for participation. The principal eligibility criterion was histologically confirmed carcinoma scheduled to receive pelvic palliative radiation. The primary objective of the PRAVO trial was to determine tolerability of vorinostat when administered concomitantly with palliative radiation to pelvic target volumes [182]. The trial was the first clinical trial to report on the combination of a HDAC inhibitor and radiotherapy when published in 2010, and showed that vorinostat could be safely combined with short-term pelvic radiotherapy. This study further aimed to assess the biological activity of vorinostat, in terms of tumor histone acetylation [182], and

to identify possible biomarkers reflecting timing of HDAC inhibitor administration with regard to radiotherapy.

Seventeen patients were enrolled between Feb 2007 and May 2009. One patient withdrew consent after the first treatment day. Ten patients had rectal cancer, whereas the rest had primary tumors in the colon (n=6) or stomach (n=1). Radiotherapy was delivered to target volumes in 3 Gy-fractions to a total dose of 30 Gy over two consecutive weeks. Vorinostat was administered orally once daily, 3 hours before each radiotherapy fraction. The study adopted the standard 3+3 design [206], where patients were enrolled onto four sequential dose levels of vorinostat, starting at 100 mg daily with dose escalation (in 100 mg increments) for every third evaluable patient, provided no dose-limiting toxicity had been observed at the preceding dose. Tumor biopsies were sampled at baseline and on the third treatment day to assess histone deacetylation. Peripheral blood for was drawn from patients at baseline (before commencement of study treatment; termed T0) and on the third treatment day (two and 24 hours after the patients had received the daily dose of vorinostat; termed T2 and T24 respectively) (**Figure 6.5**).

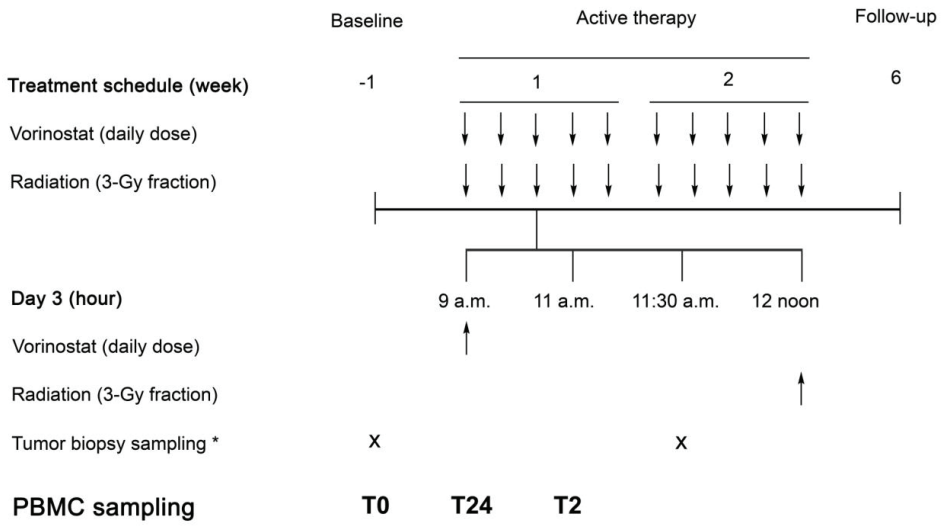

Figure 6.5 PRAVO study timeline. PBMC, peripheral blood mononuclear cells. Figure adapted from Ree et al 2014 (paper III)

6.3 Functional assays

6.3.1 Detection of disseminated tumor cells

An immunocytological technique of immunomagnetic selection (IMS) was used to detect DTC in bone marrow from 71 patients (**Figure 6.5**) [245,246]. Mononuclear cells were isolated from the bone marrow aspirate and incubated with magnetic beads coated with the MOC31 antibody which recognizes the Ep-CAM antigen, a membrane protein that is highly expressed in CRC cells but not in normal bone marrow cells [247]. The cells were subsequently exposed to a magnetic field to separate bead-rosetting cells from unbound cells. A patient sample was classified as positive for DTC if a minimum of two rosetted cells were identified by microscopy. The immunomagnetic method has demonstrated high sensitivity for detection of DTC in CRC patients and allows a rapid enrichment of tumor cells from a high number of mononuclear cells [245]. Limitations are related to antibody specificity and sensitivity. Other methods for detection of DTC in bone marrow are immunocytochemistry and RT-qPCR [248].

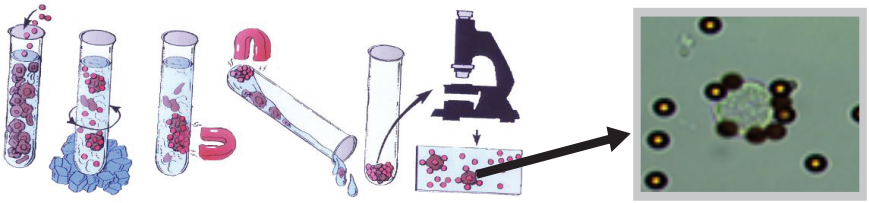

Figure 6.5 Immunomagnetic selection of tumor cells from bone mallow sample. Picture from the Department of Tumor Biology, the Radium hospital, Oslo University Hospital. Printed with permission.

6.3.2 Tumor tyrosine kinase activity profiling

The cell phenotype is determined not only by gene and protein expression levels, but also by posttranslational modifications of proteins, *e.g.* phosphorylation catalyzed by protein kinases[249]. The protein kinase component of the human genome, the kinome, was identified by Manning and colleagues in 2002 [250]. Of 518 protein kinases, 90 are tyrosine kinases *i.e.* protein kinases that catalyze phosphorylation of protein tyrosine residues [210]. Tyrosine kinases are involved in cell signaling as part of transmembrane receptors and as enzymes located inside the cell [251]. Protein

kinase activity may be assessed by protein phosphorylation levels representing end products of kinase activity rather than the enzymatic activity resulting in it, *e.g.* by mass spectrometry. Kinase activity assays measure the actual enzymatic activity leading to a specific signal transduction [249,252]. In paper I, a high-throughput kinase substrate microarray technology (Tyrosine Kinase PamChip® Arrays) was used to determine tyrosine kinase activity in tumor samples from LARC patients. A chip containing peptide substrates with sites for phosphorylation generates an individual phophosubstate signature from each sample lysate, allowing functional comparison of active signaling pathways in different biological samples.

Baseline tumor biopsies (snap-frozen in liquid nitrogen and stored at -80C) were sectioned by a cryostat microtome. Hematoxylin-eosin stained slides were evaluated for tumor content and normal tissue present was roughly removed by dissection guided by the stains. ~ 5 mm^3 tumor tissue was cut in 10 μm sections by the microtome (the required number of sections was calculated after measuring the samples' width and length). As kinase activity is sensitive to small variations, all samples were lysed simultaneously. The Pam Chip 96-well array were used: 144 peptides representing 100 different proteins are spotted to a porous membrane. Each peptide represents a sequence corresponding to a specific tyrosine kinase substrate. The sample lysates are pumped through interconnected pores to allow enzymatic reaction with the peptide substrates. Adenosine triphosphate (ATP) is added to initiate phosphorylation reaction. Upon addition of a fluorescent-labeled antiphosphotyrosine antibody, phosphorylation levels are determined by recording spot fluorescent signal intensities [253] (**Figure 6.6**).

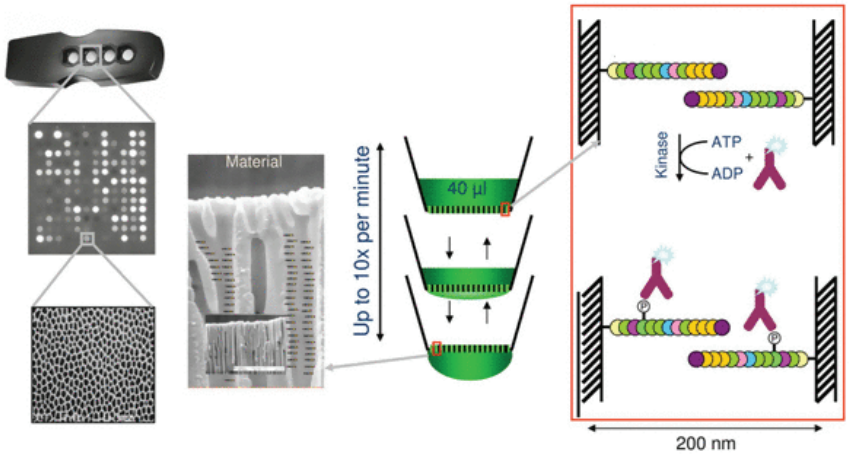

Figure 6.6 Peptide microarrays for profiling of kinase activity. Adapted from Hilhorst *et al*, printed with permission. The chips on the picture is a 4-well chip, while we used 96-well plates. ATP, adenosine triphosphate; ADP, adenosine diphosphate.

In addition to four technical replicates from each patient tumor, three replicates were incubated with the tyrosine kinase inhibitor sunitinib, to diminish the problem of inter-unit variation between array plates; as peptide phosphorylation levels in presence of sunitinib could be normalized against the corresponding baseline levels, measured on the same unit (**Figure 6.7**).

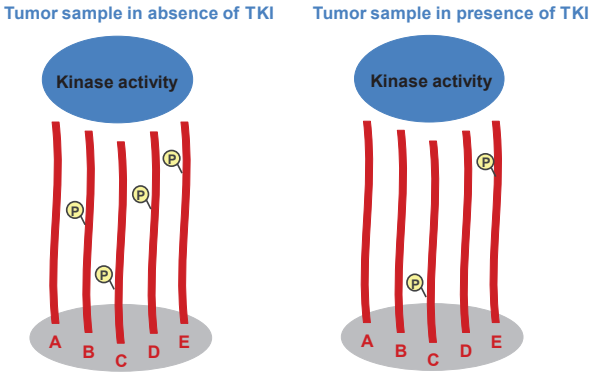

Figure 6.7 Tyrosine kinase activity array – the principle of analysis. The level of individual array peptide substrate phosphorylation (P) generated by the patient's tumor sample was measured in the absence and presence of the specific tyrosine kinase inhibitor (TKI; *e.g.*, sunitinib). The inhibition ratio (signal intensities with/without tyrosine kinase inhibitor) was calculated. Five (of the total number of 144) array peptides (A-E) are drawn for simplicity. TKI; tyrosine kinase inhibitor.

Signal intensities for each spot, *i.e.* for each kinase peptide substrate per array were calculated by using the software BioNavigator (PamGene International B.V.) and subsequently log_2-transformed. For each peptide, the sunitinib-induced log_2-fold change was calculated by subtracting the log_2-transformed signal in the absence of sunitinib from that in the presence of sunitinib. Peptides with sample-averaged signal less than 2^{10} in the control condition were excluded, leaving 102 of the 144 array peptides for further analysis.

Levels of sunitinib inhibition in DTC-positive and DTC-negative patients were compared by a two-sample t-test. Principal component analysis was performed using the 55 samples as observations and the 102 peptide substrates as variables. The sunitinib inhibition profiles were determined by sorting the data according to the value of the first principal component (peptides) and the value of the scores on the first principal component (samples). Distribution of value of the score on the first principal component was compared to clinical parameters using correlation coeffecients for continuous variables and one-way ANOVA tests for categorical data. Data processing was performed in Matlab R2010A.

Kinase activity profiling by the PamGene Platform has been used in functional characterization of cancer biology, particularly for therapy prediction [198,252,254-256]. Advantages of kinase peptide substrate arrays include quick, parallel readout of many peptides requiring small quantities of protein (5-15 µg) [210]. A detailed annotation of potential upstream kinases of specific peptide substrates is essential for this analysis and has gained reliability over the last years [252]. Peptide sensitivity to kinases will however not necessarily be the same *ex vivo* as *in vivo,* as the tertiary structure and spatiotemporal regulatory mechanisms which normally control enzyme specificity are largely lost, hence the upstream kinases for a given peptide substrate could be different in the *ex vivo* setting [249,252]. The technology is relatively new and computational tools for data analysis/methods for analyzing results from kinase activity microarrays and data validation are not standardized. A potential method to validate results is to assess levels of phosphorylated array peptide substrates or downstream proteins by western immunoblot, but in our study scarcity of patient material did not enable it. To account for intra-tumor heterogeneity, several tumor biopsies from each tumor should ideally be analyzed [257] but will also be hampered by limited availability and quantity of relevant tissue in a clinical study setting.

6.3.4 Gene expression profiling

As described in paper III, gene expression profiling of PBMC was performed to identify possible pharmacodynamic biomarkers of vorinostat activity when combined with fractionated radiotherapy. To identify biomarkers that reflect mechanisms of action of a systemic agent with proposed radiosensitizing effects, tumor biopsies sampled after the patient has started radiation treatment cannot be analyzed as any regulatory activity would reflect the combined treatment of radiation and the systemic drug, and the accumulated radiation dose would probably be the main contributor[149]. Tumor biopsy sampling is too invasive to consistently use tumor tissue for determining drug activity in the clinical setting [205]. Non-irradiated PBMC is an easy accessible surrogate tissue, which allows performance of analysis at several time points. Several studies have demonstrated biological activity of HDAC inhibitor in PBMCs in terms of histone acetylation [181,258].

By microarray technology, transcriptional activity in term of messenger RNA, *i.e.* gene expression, of thousands of genes can be assessed simultaneously. The subsequent data analysis is called gene expression profiling. In paper III a standard DNA microarray analysis was performed by the Norwegian Microarray Consortium on RNA from PBMC samples of the 14 study patients for whom a full set of three PBMC samples was obtained. Following RNA isolation, the purified RNA was copied into labeled complementary RNA (cRNA). The cRNA was amplified and then hybridized against the Illumina Human WG-6 v3 BeadChip DNA microarray platform, consisting of 48 000 probes. Spot intensities from all probes, reflecting bound cRNA, were recorded [259].

Statistical and functional annotation analysis

Array data from all PRAVO patient samples at each time point were pooled, irrespective of the vorinostat dose administered to the patients, to increase the statistical power of analysis of differential gene expression between the time points. Following quality control and preprocessing, the data was $\log_2$-transformed to stabilize the variance and normalize distribution of signals [260]. Differential gene expression between the sample groups T0, T2, and T24 was determined by first applying a Benjamin and Hochberg false discovery rate-adjusted p-value

cutoff of 0.05, and secondly a p-value of 0.01 and a $\log_2$-fold change cutoff of 1.0 was used. The false discovery rate is a statistical method of controlling for multiple testing [261]. Analysis was performed using Bioconductor version Release 2.11.1 and the Bioconductor packages lumi 1.14.0, linear models for microarray data (limma) 3.4.4, and illuminaHumanv3BeadID.db 1.6.0 (www.bioconductor.org).

The probes that were identified as differentially expressed among sample groups T0, T2 and T24 were analyzed using the Database for Annotation, Visualization and Integrated Discovery (DAVID v6.7), which is a bioinformatic resource that can extract biological meaning associated with large gene lists [262]. Annotation analysis can map genes by their biological processes (*e.g.*, gene ontology terms) or biological pathways, and statistically highlight the most overrepresented (enriched) biological annotation. In our study enriched biological processes and pathways were identified using the GOTERM_BP_FAT and KEGG_PATHWAY algorithm, applying a p-value cutoff of 0.01.

Data validation

RT-qPCR is often used to validate microarray results (RNA levels) for the most interesting genes [261], furthermore changes in gene expression can be validated at the protein level [261]. In our study, 38 genes with a biphasic pattern of regulation from T0, through T2 and T24 were identified by the stricter criteria used ($\log_2$-fold change cutoff 1.0, $p < 0.01$). Five genes were selected for validation by RT-qPCR.

Similarly to DNA microarrays, RT-qPCR exploits the binding of complementary nucleic acid sequences [263]. After reverse transcription of RNA to cDNA, the double-stranded DNA is denaturated at 95 C. Specific primers are used to bind to their complementary sequence on the two strands of cDNA, and the strands then are extended by a DNA polymerase. One copy of the DNA strand is made after each cycle, hence the number of copies will accumulate exponentially, and there will be a quantitative relationship between the amount of starting target sequence and the amount of PCR product accumulated at any particular cycle [264]. Fluorescent probes were used to detect the number of amplicons [265]. A fluorescence detection threshold is reached after a specific cycle depending on the initial concentration of the target DNA sequence, and relative

expression levels are calculated. The expression of house-keeping genes, constitutively expressed internal control genes, is used to normalize mRNA fraction. cDNA from a reference cell line was included on all plates to be able to pool the patients and compare baseline expression levels between patients. The data were analyzed using the GeneExpression Analysis for iCycler iQ® Real-Time PCR Detection System Software (BioRad) and expressed as gene expression relative to the level in the reference cell line. The data were subsequently $\log_2$-transformed and fold-change for T2 *versus* T0 and T24 *versus* T2 was calculated.

6.4 Statistical analyses

Except from the microarray/molecular profiling analyses, statistical analysis was performed using Predictive Analytics SoftWare Statistics version 19.0 and SigmaPlot software version 12. Two-sample Student's t-test was used for comparisons of normally distributed continuous variables between groups. The non-parametric Mann-Whitney rank-sum was used when the distribution of data did not resemble the normal distribution, determined by Q-Q plots or the Shapiro-Wilk normality test. Categorical variables were analyzed using Pearson's chi-square or Fisher exact tests. All statistical tests were 2-sided, and $p<0.05$ was considered statistically significant. Metastasis-free, disease-free and overall survival was estimated by the Kaplan-Meier method. The log-rank test was used to determine survival differences between groups of patients.

7 Discussion

7.1 Towards a more personalized rectal cancer treatment?

Cancer is a biologically heterogeneous disease resulting from accumulation of genetic and epigenetic alterations, and the clinical outcome varies among patients [257,266]. An overarching aim in cancer therapy is to customize treatment to provide the optimum result for the individual patient: personalized cancer therapy. The term 'personalized cancer therapy' is often used to describe the administration of targeted agents based on molecular characteristics of individual tumors [207], while a broader definition refers to tailoring of cancer treatment on the basis of individual patient characteristics. Based on tumor or patient characteristics, individuals may be classified into subpopulations with different predicted outcome and response to treatment.

The clinical management of rectal cancer is an excellent example of how multimodal treatment regimens may be individualized, *i.e.* tailored to subgroups of patients [208]. Clinicopathological factors, such as TNM staging, tumor histology and tumor resection margin (MRF) are utilized to divide rectal cancer patients into risk groups, stratified to receive different treatment [267]. Patients with LARC are treated with neoadjuvant fluoropyrimidine-based CRT, a treatment regimen that has proven to improve local control. Although most LARC tumors respond well to this treatment, some experience minimal or no treatment effect and may benefit from intensified treatment. As with any cancer therapy, the goal in rectal cancer treatment is to optimize outcome while minimizing treatment toxicity, and an increased treatment efficacy must be balanced towards potentially increased normal tissue effects. The standard preoperative treatment confers considerable early and late toxicity and some LARC patients may benefit from a less intensive preoperative treatment. To optimize survival and minimize treatment toxicity, rectal cancer treatment should be increasingly individualized.

To allow improved staging and stratification of rectal cancer patients for more differentiated treatment, biomarkers that predict the response of an individual patient's tumor to multimodal treatment and indicate treatment-associated toxicities prior to treatment are needed[208]. The biology of tumor heterogeneity is only partially depicted by the existing diagnostic staging

approaches in rectal cancer, and additional biological biomarkers are warranted to allow more advanced stratification of patients. Over the past years, tumor heterogeneity at the molecular level has been increasingly explored and our understanding of the molecular biology of cancer has increased enormously. New technologies that characterize cancers on the molecular level have emerged, *e.g.* genome, transcriptome, proteome and kinome profiling [268]. In addition to the identification of potential biomarkers, these technologies withhold potential to explore the tumor biology and identify novel molecular targets of therapy [208]. High-throughput microarray-based molecular profiling has been utilized both to identify prognostic and predictive signatures as well as to explore the molecular aspects of rectal cancer [267].

Tumor heterogeneity is also depicted by differences in the tumor microenvironment [269]. Tumor hypoxia is an important element of the microenvironment known to be a mediator of resistance to cytotoxic therapy (radiation and chemotherapy) and metastatic disease progression. While the problem of hypoxia has been addressed for many years, increased knowledge of the adaptive responses to hypoxia on a molecular level, together with and focus on personalized therapy, has reemphasized the importance of tumor hypoxia in cancer therapy.

7.2 Hypoxic signaling and metastatic development

Tumor hypoxia is one of the major forces driving the metastatic process [88]. On the molecular level, adaptive cellular responses to hypoxia involve activation of a range of signaling pathways that interfere with regulatory mechanisms, collectively contributing to a malignant phenotype. Hypoxic signaling interferes with almost every step of the metastatic processes. Molecular profiling is a potential strategy to explore the biological complexity in hypoxic tumors. Tyrosine kinases are key mediators in signaling cascades activated by hypoxia and regulating central biological processes of malignancy, such as proliferation and angiogenesis. Studying the functional tumor kinome in early metastatic progression of rectal cancer could improve our understanding of the hypoxic response in metastasis, and potentially enable identification of actionable targets in hypoxic metastatic signaling.

The recently completed prospective phase II trial, the LARC-RRP study, offers a unique opportunity to explore the concept of tumor hypoxia as a determinant of metastatic behavior in a defined clinical context. Tyrosine kinase activity profiling of biopsies from primary tumors from which tumor cells had disseminated to the patients' red bone marrow compartment at the time of diagnosis, interpreted as a biomarker of early systemic dissemination, allowed us to study molecular profiles of tumors with high metastatic recurrence risk. In **paper I**, we compared tumor kinase activity in LARC-patients with and without DTC in the bone marrow. Using peptide arrays with tyrosine kinase substrates, several kinases involved in angiogenic signaling were found to be differentially inhibited by the kinase-inhibitor sunitinib in tumor samples from patients with and without early tumor dissemination, implying different levels of tumor kinase activity in these patients. Interestingly, the *ex vivo* sunitinib inhibition of phosphorylation of PDGFRB array substrates by tumor samples from patients with DTC was significantly lower than for patients without DTC. Low sunitinib inhibition of PDGFRB phosphorylation may reflect a low level of PDGF-mediated signaling in these tumors. PDGF binds to its receptor expressed on pericytes, stimulating their proliferation and attachment to the endothelial layer [115]. Pericytes within the primary tumor microenvironment probably serve as gatekeepers in tumor cell metastasis. Pericyte depletion, or a poor pericyte coverage of the tumor endothelium, may result from tumor hypoxia [88] and therefore be associated with poor patient prognosis. The role of pericytes in the process of tumor metastasis and the relationship to tumor hypoxia should be further explored.

7.3 Hypoxic tumor radiosensitization by histone deacetylase inhibitors

New insight into molecular radiobiology has provided an opportunity for the rational integration of molecularly targeted therapeutics in radiotherapy for biological optimization of radiation effect. An array of novel actionable molecular targets, which may be exploited to enhance tumor response to radiotherapy, have been uncovered; including targets in pathways involved in tumor proliferation, angiogenesis and hypoxia [38]. Tumor hypoxia is recognized as a main contributor to clinical radiation resistance. Since the first description of the phenomena of hypoxic radioresistance more than 100 years ago, not long after the discovery of ionizing radiation, targeting of tumor hypoxia as a strategy to improve radiation response has been explored. With

the recent developments in molecular oncology, new strategies have emerged. An appealing strategy for improving radiation efficacy may be to counteract hypoxia-induced tumor signaling activity.

The HDAC inhibitors were originally designed as epigenetic therapeutics for modification of the chromatin structure, but have been found to modify several non-histone proteins. HDAC inhibition influences several processes involved in cellular radiation response *e.g.* angiogenesis, DNA damage signaling, cell cycle progression and apoptosis, and are shown to exert radiosensitizing effect in experimental and clinical studies. Recently, results from experimental models have indicated that HDAC inhibitors suppress hypoxic signaling by repressing the HIF-1α transcription factor, and this could be the mechanistic rationale for the observed radiosenstitizing properties of HDAC inhibitors [270].

Preclinical evaluation of vorinostat

Vorinostat, one of the most studied HDAC inhibitors and the first to be approved for clinical use, has been evaluated by our group in the preclinical and early clinical setting. Initially, tumor cell radiosensitization and associated cell cycle responses in human CRC cell lines incubated with HDAC inhibitors were assessed [203,271]. In human CRC xenograft models, significant delay of tumor growth was observed following fractionated radiation combined with daily injections of the mice with vorinostat, compared to radiation treatment alone [203].

In **paper II** the preclinical investigation of vorinostat was expanded by studying radiosensitizing effects by vorinostat under hypoxic conditions and in combination with capecitabine *in vitro* and *in vivo*. It has been suggested that all radiosensitizers should be evaluated under hypoxia in preclinical models, at least *in vitro*, as the oxygenation level is highly relevant for the radioresponse [131]. Vorinostat enhanced radiosensitivity of cell lines exposed to hypoxia during radiation, counterbalancing hypoxia-induced radioresistance. The tumor growth delay (relative to untreated tumors) of irradiated hypoxic xenografts in mice given vorinostat was similar to the growth delay of xenograft irradiated under normoxic conditions, suggesting that the drug contributed to abolish the radioresistant hypoxic phenotype.

Potential antagonistic effects of the combination of a new drug with an established standard treatment should be evaluated in the preclinical setting. Hence, in rectal cancer, potential radiosensitizers should be evaluated in combination with the standard 5-FU-based regimen. In our experiments, the combination of capecitabine and vorinostat increased radiosensitivity in terms of reduced clonogenic survival of cell cultures and delayed tumor growth of xenografts.

Biomarkers of vorinostat activity in a clinical setting

Following the initial preclinical evaluation of vorinostat, a phase I clinical trial, the PRAVO study was conducted. This trial, undertaken in patients treated with vorinostat combined with pelvic fractionated radiotherapy in advanced gastrointestinal malignancies, was the first to report on the use of an HDAC inhibitor in clinical radiotherapy, and demonstrated that vorinostat was well tolerated in combination with pelvic radiotherapy [182]. In addition to evaluation of treatment tolerability and response, the trial was designed to identify potential pharmacodynamic biomarker or indicators of vorinostat action in clinical radiotherapy.

In the setting of fractionated radiotherapy, a novel drug should elicit a radiosensitizing molecular event at each radiation fraction; hence a pharmacodynamic biomarker should reflect the timing of drug administration with regard to radiation exposure in a transient and periodic manner [149]. Tumor histone hyperacetylation has been suggested as a pharmacodynamic biomarker of HDAC inhibitor activity. However, there are several limitations of tumor histone acetylation as a biomarker of vorinostat activity in combination with fractionated radiation. With the exception of the verification that vorinostat has reached its target, tumor acetylation does not seem to be a permissive requirement for radiosensitization by vorinostat [203]. Additionally, biomarkers established for single-agent therapy will require reevaluation in clinical trials combining the agent with radiotherapy. The most direct method to study pharmacodynamic markers is by assessing tumor tissue, but the non-irradiated peripheral lymphocytes are suggested as a surrogate tissue in radiation trials if the objective is to determine mechanisms of a presumed radiosensitizing drug, as the radiation itself confers molecular perturbations in the tumor tissue. However, this method does not account for inherent tumor resistance mechanisms, such as drug efflux pumps or the inability of the drug to reach hypoxic tumors [169].

In **paper III**, we aimed to identify biomarkers of vorinostat activity, reflecting the appropriate timing of drug administration in fractionated radiotherapy applying gene expression array analysis of PRAVO study patients' PBMC sampled at baseline (T0), and on-treatment two and 24 hours (T2 and T24) after the patient had received vorinostat. 1600 array probes exhibited increased or decreased expression at T2, but returned to baseline level at T24, and were therefore identified as potential biomarkers reflecting timing of vorinostat administration in the fractionated radiotherapy protocol. Applying more stringent statistical criteria, the list of potential biomarkers was reduced to 38 candidates. Of these, we selected five genes for validation based on both the relevance in the DNA damage response, which is recognized as a mechanism contributing to radiosensitivity, and previous indication of regulation by HDAC inhibitors. The biphasic pattern of gene expression was confirmed for these genes by RT-qPCR. For the same five genes, expression levels in two CRC xenograft models 3 and 12 hours after vorinostat administration were assessed, but only the MYC regulation was validated in the xenograft models.

It has been suggested that the myc protein acts synergistically with the transcription factor HIF1α under hypoxic conditions thereby increasing radiation resistance [272 273]. As recent evidence indicates that HDAC inhibitors suppress HIF-1α activity, the radiosensitizing effect of HDAC inhibitors may potentially be mediated through suppression of the myc/HIF-1α synergy in hypoxic tumors.

7.4 Neoadjuvant chemotherapy and tumor radiation response

Most rectal cancer deaths are from systemic disease, and the administration of a chemotherapeutic agent in systemic doses to target micrometastatic disease is a potential strategy to reduce development of metastases. Adjuvant treatment has not been shown to improve survival [70]; possibly because the systemic chemotherapy is administered too late to kill early disseminated cells before metastasis are established. Also, a substantial number of patients are not fit to receive chemotherapy postoperatively [40]. Neoadjuvant chemotherapy prior to CRT (induction therapy) is an alternative strategy to deliver systemic chemotherapy. Other

neoadjuvant strategies are chemotherapy after CRT (consolidation therapy) or chemotherapy alone without CRT [143]. Applied in a neoadjuvant setting, a chemotherapeutic agent will target the primary tumor in addition to micrometastases. In this setting, the chemotherapeutic agent can be given at full systemic doses, but still with potentially acceptable toxicity. Reports from non-randomized and randomized phase II trials evaluating the addition of NACT to CRT in LARC are encouraging, with high local control rates and promising long-term outcomes [71-75]. A phase III trial is recruiting patients to be randomized to receive CRT alone or NACT followed by CRT (ClinicalTrials NCT01804790) [14,212,274].

Administered as NACT prior to CRT, a chemotherapeutic agent could potentially kill non-hypoxic cells, and by selecting for radioresistant hypoxic tumor cells reduce the efficacy of subsequent CRT. In the clinical setting, NACT might impact CRT efficacy if the added toxicity would necessitate dose reductions and interruptions in CRT treatment[275] as well as increase the risk of surgical complications. Tumor radiation response following exposure to a potential neoadjuvant chemotherapeutic agent should therefore be evaluated in experimental and clinical settings. In **Paper IV** we evaluated tumor response to NACT and CRT by MR volumetry in the phase II LARC-RRP study of patients receiving OXA-based NACT prior to CRT. A substantial downsizing of the primary tumor was observed after NACT (median tumor volume reduction 63%). An additional volume reduction of similar magnitude was observed after CRT (median tumor volume reduction 68%) and was not influenced by the response to NACT. The additional tumor volume reduction seemed to be larger in the group with poor NACT response (69 versus 60%), but the difference was not significant.

To study the influence of OXA-treatment prior to radiation in a preclinical setting, we assessed radiosensitivity by the *in vitro* clonogenic assay in OXA-resistant variants of two CRC cell lines. Interestingly, the experimental radiosensitivity of OXA-resistant cell lines was increased, rather than decreased, compared to the parental cell line. A possible mechanism for the (OXA-induced) enhanced radiosensitivity, is specific targeting of radioresistant hypoxic cells by OXA.

Only 11% of the LARC-RRP patients required NACT dose adjustment because of acute toxicity. Radiation-induced acute toxicities may cause interruption in treatment delivery and

delay definitive surgical treatment, whereas surgical complications and long-term functional impairment may strongly impede patients' quality of life [43,46]. As responses to OXA-based NACT in terms of tumor volume reduction was unexpectedly large in most patients in our study, the administration of NACT might be an alternative to CRT for selected patients, with the benefit of less normal tissue toxicity. Preliminary results from ongoing phase II trials evaluating NACT without CRT in moderate risk LARC patients, indicate encouraging efficacy [276, 277]. If applied as induction therapy, early evaluation of response to NACT would allow stratification of patients into prognostic groups scheduled to receive different treatment, *i.e.* intensified CRT or no CRT. A planned phase III study (PROSPECT) will evaluate the impact of selective use of radiation. In this study intermediate-risk patients will be randomized to receive NACT and responders will proceed directly to rectal cancer surgery [278].

An alternative approach to the standard CRT is NACT and short-course radiation before delayed surgery, assessed in the RAPIDO phase II trial [279]. Outcome and toxicity rates for the two preoperative radiotherapy regimens are similar [280,281]. In less advanced rectal tumors where downsizing is not necessary, the convenient short-course radiotherapy is equivalent to CRT [9]. Studies indicate that downsizing after short-course radiotherapy can be achieved if surgery is delayed [282, 283].

8 Conclusions

In this work, recognizing that rectal cancer is a heterogeneous disease in terms of response to treatment and the ability to metastasize, we have shown that:

1. Angiogenesis-related tumor signaling, particularly kinase activity mediated by PDGFR, was inhibited by sunitinib in LARC patients without detectable tumor cells in bone marrow at the time of diagnosis.

   If intact tumor angiogenic signaling of pericytes reflects a low likelihood of early systemic disease dissemination, deregulated PDGFR signaling may correspondingly manifest dysfunctional tumor vasculature and increased risk of tumor cell dissemination. Even with the complexity of recent study data on the use of anti-angiogenic therapeutics in CRC, the concept of tumor vasculature normalization withholds the potential to prevent development of metastasis and also to improve responses to radiation and chemotherapy [284,285].

2. The HDAC inhibitor vorinostat exhibited radiosensitizing effects under hypoxic conditions and in combination with capecitabine in experimental CRC models.

   These results support the hypothesis that vorinostat targets hypoxic radioresistant cells and encourage the introduction of vorinostat in CRT trials in high-risk LARC. Intensification of CRT in rectal cancer by the addition of vorinostat may improve treatment responses in a subgroup of poor-responding patients with treatment failure ascribed to tumor hypoxia.

3. Several potential biomarkers of HDAC inhibitor activity, *e.g.* transient MYC repression, were identified by PBMC gene expression profiling of patients in a phase I study receiving vorinostat and fractionated pelvic radiotherapy.

The strategy of gene expression array analysis of non-irradiated surrogate tissue identified genes with transient induction or repression following vorinostat administration, fulfilling the requirement of being pharmacodynamic biomarkers for HDAC inhibitor activity in fractionated radiotherapy. In studying systemic agents with presumed radiosensitizing activity, trial design to allow identification of biomarker endpoints both of drug action and of treatment tolerability and response needs particular attention, and we believe the present study design may function as a template set-up for future LARC trials.

4. In a phase II study of LARC patients, OXA-containing NACT led to substantial tumor volume reduction with particularly good responses in T3 cases, without compromising subsequent CRT response. Experimental CRC models that were made OXA-resistant showed enhanced radiosensitivity compared to the respective OXA-sensitive counterparts.

   These results suggest that OXA-containing NACT might be an alternative to CRT in low-risk T3 rectal cancer, offering a more favorable toxicity profile, and that OXA-containing chemotherapy might even contribute to enhancement of tumor radiation sensitivity.

9 Perspectives

As a common determinant of resistance to radiotherapy and development of metastasis, tumor hypoxia is recognized as a central aspect of tumor heterogeneity in rectal cancer. To improve treatment strategies for hypoxic tumors, further exploration of the complex network of the hypoxic cellular response is necessary, to elucidate mechanisms on how hypoxia drives the metastatic process and to characterize regulatory mechanisms of hypoxic radiation resistance.

The identification of reliable biomarkers of tumor hypoxia is warranted for use in clinical trials and ultimately in clinical practice. In this respect, functional MRI represents a promising technology for non-invasive assessment of the degree of tumor hypoxia. The combination of functional imaging with molecular tumor profiling may represent a novel approach to the detection of biomarkers as well as actionable targets of hypoxia. The ongoing OxyTarget clinical study at Akershus University Hospital (ClinicalTrials NCT01816607) is evaluating this approach in rectal cancer patients.

High-risk rectal cancer patients, identified by predictive or prognostic markers (*e.g.* markers of tumor hypoxia), could benefit from an intensified CRT with targeted radiosensitizers. A potential strategy to target tumor hypoxia in radiation response is to combine radiotherapy with HDAC inhibitors. There are currently a number of clinical trials investigating the combination of HDAC inhibitors and radiotherapy in various cancer forms. Our group has demonstrated encouraging results of the HDAC inhibitor vorinostat as radiosensitizer in experimental CRC models and with acceptable safety in the clinical phase I setting, and the next step should be a phase I/II trial evaluating vorinostat as additional component of preoperative CRT in LARC.

The potential role of NACT in rectal cancer is currently being explored in clinical trials. Metastatic disease is the main cause of treatment failure in rectal cancer, and administration of a systemic therapeutic agent may reduce the risk of metastatic development. While high-risk rectal cancer patients may benefit of NACT in addition to CRT, the concept of replacing CRT with

NACT in patients at low risk of local recurrences might spare patients from radiotherapy-related toxicity.

Taken together, treatment of rectal cancer in the near future will certainly apply increasingly personalized approaches by tailoring multimodal treatment to the specific requirements of each patient.

10 References

1. Ferlay, J.*, et al.* Cancer incidence and mortality patterns in Europe: estimates for 40 countries in 2012. *Eur J Cancer* **49**, 1374-1403 (2012).
2. Valentini, V.*, et al.* Evidence and research in rectal cancer. *Radiother Oncol* **87**, 449-474 (2008).
3. Weber, G.F., Rosenberg, R., Murphy, J.E., Meyer zum Buschenfelde, C. & Friess, H. Multimodal treatment strategies for locally advanced rectal cancer. *Expert Rev Anticancer Ther* **12**, 481-494 (2012).
4. Cancer-Registry-of-Norway. Cancer in Norway 2011 - Cancer incidence, mortality, survival and prevalence in Norway. (Oslo, 2013).
5. Bray, F., Wibe, A., Dorum, L.M. & Moller, B. [Epidemiology of colorectal cancer in Norway]. *Tidsskr Nor Laegeforen* **127**, 2682-2687 (2007).
6. Ferlay, J.*, et al.* Estimates of worldwide burden of cancer in 2008: GLOBOCAN 2008. *Int J Cancer* **127**, 2893-2917 (2010).
7. Verdecchia, A.*, et al.* Recent cancer survival in Europe: a 2000-02 period analysis of EUROCARE-4 data. *Lancet Oncol* **8**, 784-796 (2007).
8. Coleman, M.P.*, et al.* Cancer survival in Australia, Canada, Denmark, Norway, Sweden, and the UK, 1995-2007 (the International Cancer Benchmarking Partnership): an analysis of population-based cancer registry data. *Lancet* **377**, 127-138 (2011).
9. Schmoll, H.J.*, et al.* ESMO Consensus Guidelines for management of patients with colon and rectal cancer. a personalized approach to clinical decision making. *Ann Oncol* **23**, 2479-2516 (2012).
10. Wang, A.Y. & Ahmad, N.A. Rectal carcinoids. *Curr Opin Gastroenterol* **22**, 529-535 (2006).
11. Shin, U.S.*, et al.* Mucinous rectal cancer: effectiveness of preoperative chemoradiotherapy and prognosis. *Ann Surg Oncol* **18**, 2232-2239 (2011).
12. Oberholzer, K.*, et al.* Rectal cancer: mucinous carcinoma on magnetic resonance imaging indicates poor response to neoadjuvant chemoradiation. *Int J Radiat Oncol Biol Phys* **82**, 842-848 (2012).
13. American-Joint-Comittee-on-Cancer (ed.) *Cancer staging handbook*, (American-Joint-Committee-on-Cancer, 2010).
14. Dewdney, A., Cunningham, D. & Chau, I. Selecting patients with locally advanced rectal cancer for neoadjuvant treatment strategies. *Oncologist* **18**, 833-842 (2013).
15. Pahlman, L. & Torkzad, M.R. Rectal cancer staging: is there an optimal method? *Future Oncol* **7**, 93-100 (2011).
16. Yeung, J.M., Ferris, N.J., Lynch, A.C. & Heriot, A.G. Preoperative staging of rectal cancer. *Future Oncol* **5**, 1295-1306 (2009).
17. Norwegian-Gastrointestinal-Cancer-Group. National Programme for preoperative radiotherapy in rectal cancer. (2012).
18. Nagtegaal, I.D. & Quirke, P. What is the role for the circumferential margin in the modern treatment of rectal cancer? *J Clin Oncol* **26**, 303-312 (2008).
19. Glimelius, B.*, et al.* Mesorectal fascia instead of circumferential resection margin in preoperative staging of rectal cancer. *J Clin Oncol* **29**, 2142-2143 (2011).
20. Wibe, A.*, et al.* Prognostic significance of the circumferential resection margin following total mesorectal excision for rectal cancer. *Br J Surg* **89**, 327-334 (2002).
21. Quirke, P., Durdey, P., Dixon, M.F. & Williams, N.S. Local recurrence of rectal adenocarcinoma due to inadequate surgical resection. Histopathological study of lateral tumour spread and surgical excision. *Lancet* **2**, 996-999 (1986).
22. Smith, N. & Brown, G. Preoperative staging of rectal cancer. *Acta Oncol* **47**, 20-31 (2008).
23. MERCURY-Study-Group. Extramural depth of tumor invasion at thin-section MR in patients with rectal cancer: results of the MERCURY study. *Radiology* **243**, 132-139 (2007).

24. Taylor, F.G.*, et al.* One millimetre is the safe cut-off for magnetic resonance imaging prediction of surgical margin status in rectal cancer. *Br J Surg* **98**, 872-879 (2011).
25. Shihab, O.C.*, et al.* Relevance of magnetic resonance imaging-detected pelvic sidewall lymph node involvement in rectal cancer. *Br J Surg* **98**, 1798-1804 (2011).
26. van de Velde, C.J.*, et al.* EURECCA colorectal: Multidisciplinary management: European consensus conference colon & rectum. *Eur J Cancer* (2013).
27. Steel, G. (ed.) *Basic Clinical Radiobiology*, (Arnold, 2002).
28. Rodel, C., Hofheinz, R. & Liersch, T. Rectal cancer: state of the art in 2012. *Curr Opin Oncol* **24**, 441-447 (2012).
29. Aklilu, M. & Eng, C. The current landscape of locally advanced rectal cancer. *Nat Rev Clin Oncol* **8**, 649-659.
30. Wibe, A.*, et al.* A national strategic change in treatment policy for rectal cancer--implementation of total mesorectal excision as routine treatment in Norway. A national audit. *Dis Colon Rectum* **45**, 857-866 (2002).
31. Swedish-rectal-cancer-trial. Improved survival with preoperative radiotherapy in resectable rectal cancer. Swedish Rectal Cancer Trial. *N Engl J Med* **336**, 980-987 (1997).
32. Kapiteijn, E.*, et al.* Preoperative radiotherapy combined with total mesorectal excision for resectable rectal cancer. *N Engl J Med* **345**, 638-646 (2001).
33. Sauer, R.*, et al.* Preoperative versus postoperative chemoradiotherapy for rectal cancer. *N Engl J Med* **351**, 1731-1740 (2004).
34. Patel, P.A. Evolution of 5-fluorouracil-based chemoradiation in the management of rectal cancer. *Anticancer Drugs* **22**, 311-316 (2011).
35. Marijnen, C.A.*, et al.* No downstaging after short-term preoperative radiotherapy in rectal cancer patients. *J Clin Oncol* **19**, 1976-1984 (2001).
36. Rodel, C., Trojan, J., Bechstein, W.O. & Woeste, G. Neoadjuvant short- or long-term radio(chemo)therapy for rectal cancer: how and who should be treated? *Dig Dis* **30 Suppl 2**, 102-108 (2012).
37. Bischoff, P., Altmeyer, A. & Dumont, F. Radiosensitising agents for the radiotherapy of cancer: advances in traditional and hypoxia targeted radiosensitisers. *Expert Opin Ther Pat* **19**, 643-662 (2009).
38. Dumont, F., Altmeyer, A. & Bischoff, P. Radiosensitising agents for the radiotherapy of cancer: novel molecularly targeted approaches. *Expert Opin Ther Pat* **19**, 775-799 (2009).
39. Gerard, J.P.*, et al.* Preoperative radiotherapy with or without concurrent fluorouracil and leucovorin in T3-4 rectal cancers: results of FFCD 9203. *J Clin Oncol* **24**, 4620-4625 (2006).
40. Bosset, J.F.*, et al.* Chemotherapy with preoperative radiotherapy in rectal cancer. *N Engl J Med* **355**, 1114-1123 (2006).
41. Hofheinz, R.D.*, et al.* Chemoradiotherapy with capecitabine versus fluorouracil for locally advanced rectal cancer: a randomised, multicentre, non-inferiority, phase 3 trial. *Lancet Oncol* **13**, 579-588 (2012).
42. Roh, M.S., Yothers G. A., O'Connell M. J. The impact of capecitabine and oxaliplatin in the preoperative multilmodality treatment in patients with carcinoma of the rectum: NSABP R-04. *Journal of Clinical Oncology* **29**(2011).
43. Braendengen, M.*, et al.* Late patient-reported toxicity after preoperative radiotherapy or chemoradiotherapy in nonresectable rectal cancer: results from a randomized Phase III study. *Int J Radiat Oncol Biol Phys* **81**, 1017-1024 (2011).
44. Glimelius, B., Holm, T. & Blomqvist, L. Chemotherapy in addition to preoperative radiotherapy in locally advanced rectal cancer - a systematic overview. *Rev Recent Clin Trials* **3**, 204-211 (2008).
45. Wolff, H.A.*, et al.* Gender affects acute organ toxicity during radiochemotherapy for rectal cancer: long-term results of the German CAO/ARO/AIO-94 phase III trial. *Radiother Oncol* **108**, 48-54 (2013).

46. Bruheim, K.*, et al.* Late side effects and quality of life after radiotherapy for rectal cancer. *Int J Radiat Oncol Biol Phys* **76**, 1005-1011 (2010).
47. Compton, C., Fenoglio-Preiser, C.M., Pettigrew, N. & Fielding, L.P. American Joint Committee on Cancer Prognostic Factors Consensus Conference: Colorectal Working Group. *Cancer* **88**, 1739-1757 (2000).
48. Maas, M.*, et al.* Long-term outcome in patients with a pathological complete response after chemoradiation for rectal cancer: a pooled analysis of individual patient data. *Lancet Oncol* **11**, 835-844 (2010).
49. Rodel, C.*, et al.* Prognostic significance of tumor regression after preoperative chemoradiotherapy for rectal cancer. *J Clin Oncol* **23**, 8688-8696 (2005).
50. Bouzourene, H., Bosman, F.T., Seelentag, W., Matter, M. & Coucke, P. Importance of tumor regression assessment in predicting the outcome in patients with locally advanced rectal carcinoma who are treated with preoperative radiotherapy. *Cancer* **94**, 1121-1130 (2002).
51. Glynne-Jones, R., Mawdsley, S., Pearce, T. & Buyse, M. Alternative clinical end points in rectal cancer--are we getting closer? *Ann Oncol* **17**, 1239-1248 (2006).
52. Evans, J., Patel, U. & Brown, G. Rectal cancer: primary staging and assessment after chemoradiotherapy. *Semin Radiat Oncol* **21**, 169-177 (2011).
53. Barbaro, B.*, et al.* Locally advanced rectal cancer: MR imaging in prediction of response after preoperative chemotherapy and radiation therapy. *Radiology* **250**, 730-739 (2009).
54. Hole, K.H., Larsen, S.G., Groholt, K.K., Giercksky, K.E. & Ree, A.H. Magnetic resonance-guided histopathology for improved accuracy of tumor response evaluation of neoadjuvant treatment in organ-infiltrating rectal cancer. *Radiother Oncol* **107**, 178-183 (2013).
55. Patel, U.B.*, et al.* Magnetic resonance imaging-detected tumor response for locally advanced rectal cancer predicts survival outcomes: MERCURY experience. *J Clin Oncol* **29**, 3753-3760 (2011).
56. Yeo, S.G.*, et al.* Tumor volume reduction rate after preoperative chemoradiotherapy as a prognostic factor in locally advanced rectal cancer. *Int J Radiat Oncol Biol Phys* **82**, e193-199 (2012).
57. Yeo, W.*, et al.* Epigenetic therapy using belinostat for patients with unresectable hepatocellular carcinoma: a multicenter phase I/II study with biomarker and pharmacokinetic analysis of tumors from patients in the Mayo Phase II Consortium and the Cancer Therapeutics Research Group. *J Clin Oncol* **30**, 3361-3367 (2012).
58. Nougaret, S.*, et al.* MR volumetric measurement of low rectal cancer helps predict tumor response and outcome after combined chemotherapy and radiation therapy. *Radiology* **263**, 409-418 (2012).
59. Lambrecht, M.*, et al.* Value of diffusion-weighted magnetic resonance imaging for prediction and early assessment of response to neoadjuvant radiochemotherapy in rectal cancer: preliminary results. *Int J Radiat Oncol Biol Phys* **82**, 863-870 (2012).
60. Mathoulin-Pelissier, S., Gourgou-Bourgade, S., Bonnetain, F. & Kramar, A. Survival end point reporting in randomized cancer clinical trials: a review of major journals. *J Clin Oncol* **26**, 3721-3726 (2008).
61. Aschele, C.*, et al.* Primary tumor response to preoperative chemoradiation with or without oxaliplatin in locally advanced rectal cancer: pathologic results of the STAR-01 randomized phase III trial. *J Clin Oncol* **29**, 2773-2780 (2010).
62. Gerard, J.P.*, et al.* Comparison of two neoadjuvant chemoradiotherapy regimens for locally advanced rectal cancer: results of the phase III trial ACCORD 12/0405-Prodige 2. *J Clin Oncol* **28**, 1638-1644 (2010).
63. Gerard, J.P.*, et al.* Clinical outcome of the ACCORD 12/0405 PRODIGE 2 randomized trial in rectal cancer. *J Clin Oncol* **30**, 4558-4565 (2012).

64. Rodel, C.*, et al.* Preoperative chemoradiotherapy and postoperative chemotherapy with fluorouracil and oxaliplatin versus fluorouracil alone in locally advanced rectal cancer: initial results of the German CAO/ARO/AIO-04 randomised phase 3 trial. *Lancet Oncol* **13**, 679-687 (2012).
65. PETACC6-trial-NCT00766155. *clinical.trials.gov*.
66. Glynne-Jones, R. & Kronfli, M. Locally advanced rectal cancer: a comparison of management strategies. *Drugs* **71**, 1153-1177 (2011).
67. Glimelius, B.*, et al.* Adjuvant chemotherapy in colorectal cancer: a joint analysis of randomised trials by the Nordic Gastrointestinal Tumour Adjuvant Therapy Group. *Acta Oncol* **44**, 904-912 (2005).
68. Bujko, K., Glynne-Jones, R. & Bujko, M. Adjuvant chemotherapy for rectal cancer. *Ann Oncol* **21**, 2443 (2010).
69. Glimelius, B. Adjuvant chemotherapy in rectal cancers: why a standard in the US and not in Europe? *Nat Clin Pract Oncol* **1**, 58-59 (2004).
70. Bosset, J.F.*, et al.* Fluorouracil-based adjuvant chemotherapy after preoperative chemoradiotherapy in rectal cancer: long-term results of the EORTC 22921 randomised study. *Lancet Oncol* (2014).
71. Calvo, F.A.*, et al.* Improved incidence of pT0 downstaged surgical specimens in locally advanced rectal cancer (LARC) treated with induction oxaliplatin plus 5-fluorouracil and preoperative chemoradiation. *Ann Oncol* **17**, 1103-1110 (2006).
72. Chua, Y.J.*, et al.* Neoadjuvant capecitabine and oxaliplatin before chemoradiotherapy and total mesorectal excision in MRI-defined poor-risk rectal cancer: a phase 2 trial. *Lancet Oncol* **11**, 241-248 (2010).
73. Chau, I.*, et al.* Neoadjuvant capecitabine and oxaliplatin followed by synchronous chemoradiation and total mesorectal excision in magnetic resonance imaging-defined poor-risk rectal cancer. *J Clin Oncol* **24**, 668-674 (2006).
74. Koeberle, D.*, et al.* Phase II study of capecitabine and oxaliplatin given prior to and concurrently with preoperative pelvic radiotherapy in patients with locally advanced rectal cancer. *Br J Cancer* **98**, 1204-1209 (2008).
75. Gunnlaugsson, A.*, et al.* Multicentre phase II trial of capecitabine and oxaliplatin in combination with radiotherapy for unresectable colorectal cancer: the CORGI-L Study. *Eur J Cancer* **45**, 807-813 (2009).
76. Overgaard, J. Hypoxic radiosensitization: adored and ignored. *J Clin Oncol* **25**, 4066-4074 (2007).
77. Vaupel, P. & Mayer, A. Hypoxia in cancer: significance and impact on clinical outcome. *Cancer Metastasis Rev* **26**, 225-239 (2007).
78. Chan, D.A. & Giaccia, A.J. Hypoxia, gene expression, and metastasis. *Cancer Metastasis Rev* **26**, 333-339 (2007).
79. Ebbesen, P.*, et al.* Taking advantage of tumor cell adaptations to hypoxia for developing new tumor markers and treatment strategies. *J Enzyme Inhib Med Chem* **24 Suppl 1**, 1-39 (2009).
80. Brown, J.M. & Wilson, W.R. Exploiting tumour hypoxia in cancer treatment. *Nat Rev Cancer* **4**, 437-447 (2004).
81. Vaupel, P. The role of hypoxia-induced factors in tumor progression. *Oncologist* **9 Suppl 5**, 10-17 (2004).
82. Harris, A.L. Hypoxia--a key regulatory factor in tumour growth. *Nat Rev Cancer* **2**, 38-47 (2002).
83. Rademakers, S.E.*, et al.* Molecular aspects of tumour hypoxia. *Mol Oncol* **2**, 41-53 (2008).
84. Vaupel, P., Mayer, A. & Hockel, M. Tumor hypoxia and malignant progression. *Methods Enzymol* **381**, 335-354 (2004).
85. Harada, H. How can we overcome tumor hypoxia in radiation therapy? *J Radiat Res* **52**, 545-556 (2011).

86. Li, S.P., Padhani, A.R. & Makris, A. Dynamic contrast-enhanced magnetic resonance imaging and blood oxygenation level-dependent magnetic resonance imaging for the assessment of changes in tumor biology with treatment. *J Natl Cancer Inst Monogr*, 103-107 (2011).
87. Bristow, R.G. & Hill, R.P. Hypoxia and metabolism. Hypoxia, DNA repair and genetic instability. *Nat Rev Cancer* **8**, 180-192 (2008).
88. De Bock, K., Mazzone, M. & Carmeliet, P. Antiangiogenic therapy, hypoxia, and metastasis: risky liaisons, or not? *Nat Rev Clin Oncol* **8**, 393-404 (2011).
89. Yoo, Y.G., Christensen, J. & Huang, L.E. HIF-1alpha confers aggressive malignant traits on human tumor cells independent of its canonical transcriptional function. *Cancer Res* **71**, 1244-1252 (2011).
90. Lendahl, U., Lee, K.L., Yang, H. & Poellinger, L. Generating specificity and diversity in the transcriptional response to hypoxia. *Nat Rev Genet* **10**, 821-832 (2009).
91. Bernier, J., Hall, E.J. & Giaccia, A. Radiation oncology: a century of achievements. *Nat Rev Cancer* **4**, 737-747 (2004).
92. Gray, L.H., Conger, A.D., Ebert, M., Hornsey, S. & Scott, O.C. The concentration of oxygen dissolved in tissues at the time of irradiation as a factor in radiotherapy. *Br J Radiol* **26**, 638-648 (1953).
93. Thomlinson, R.H. & Gray, L.H. The histological structure of some human lung cancers and the possible implications for radiotherapy. *Br J Cancer* **9**, 539-549 (1955).
94. Hall, E.G., AJ. Radiobiology for the Radiologist. (Lippincott Williams & Wilkins, 2006).
95. Bertout, J.A., Patel, S.A. & Simon, M.C. The impact of O2 availability on human cancer. *Nat Rev Cancer* **8**, 967-975 (2008).
96. Meijer, T.W., Kaanders, J.H., Span, P.N. & Bussink, J. Targeting hypoxia, HIF-1, and tumor glucose metabolism to improve radiotherapy efficacy. *Clin Cancer Res* **18**, 5585-5594 (2012).
97. Shannon, A.M. & Williams, K.J. Antiangiogenics and radiotherapy. *J Pharm Pharmacol* **60**, 1029-1036 (2008).
98. Williams, K.J.*, et al.* Enhanced response to radiotherapy in tumours deficient in the function of hypoxia-inducible factor-1. *Radiother Oncol* **75**, 89-98 (2005).
99. Moeller, B.J. & Dewhirst, M.W. HIF-1 and tumour radiosensitivity. *Br J Cancer* **95**, 1-5 (2006).
100. Garcia-Barros, M.*, et al.* Tumor response to radiotherapy regulated by endothelial cell apoptosis. *Science* **300**, 1155-1159 (2003).
101. Raza, A., Franklin, M.J. & Dudek, A.Z. Pericytes and vessel maturation during tumor angiogenesis and metastasis. *Am J Hematol* **85**, 593-598 (2010).
102. Yonenaga, Y.*, et al.* Absence of smooth muscle actin-positive pericyte coverage of tumor vessels correlates with hematogenous metastasis and prognosis of colorectal cancer patients. *Oncology* **69**, 159-166 (2005).
103. Cooke, V.G.*, et al.* Pericyte depletion results in hypoxia-associated epithelial-to-mesenchymal transition and metastasis mediated by met signaling pathway. *Cancer Cell* **21**, 66-81 (2012).
104. Wilson, W.R. & Hay, M.P. Targeting hypoxia in cancer therapy. *Nat Rev Cancer* **11**, 393-410 (2011).
105. Begg, A.C., Stewart, F.A. & Vens, C. Strategies to improve radiotherapy with targeted drugs. *Nat Rev Cancer* **11**, 239-253 (2011).
106. Palayoor, S.T.*, et al.* PX-478, an inhibitor of hypoxia-inducible factor-1alpha, enhances radiosensitivity of prostate carcinoma cells. *Int J Cancer* **123**, 2430-2437 (2008).
107. Chen, S. & Sang, N. Histone deacetylase inhibitors: the epigenetic therapeutics that repress hypoxia-inducible factors. *J Biomed Biotechnol* **2011**, 197946 (2011).
108. Ali, M.A.*, et al.* SNS-032 prevents hypoxia-mediated glioblastoma cell invasion by inhibiting hypoxia inducible factor-1alpha expression. *Int J Oncol* **34**, 1051-1060 (2009).
109. Gieling, R.G. & Williams, K.J. Carbonic anhydrase IX as a target for metastatic disease. *Bioorg Med Chem* **21**, 1470-1476 (2012).

110. Valastyan, S. & Weinberg, R.A. Tumor metastasis: molecular insights and evolving paradigms. *Cell* **147**, 275-292 (2011).
111. Fidler, I.J. The pathogenesis of cancer metastasis: the 'seed and soil' hypothesis revisited. *Nat Rev Cancer* **3**, 453-458 (2003).
112. Weis, S.M. & Cheresh, D.A. Tumor angiogenesis: molecular pathways and therapeutic targets. *Nat Med* **17**, 1359-1370 (2011).
113. Carmeliet, P. & Jain, R.K. Molecular mechanisms and clinical applications of angiogenesis. *Nature* **473**, 298-307 (2011).
114. Hanahan, D. & Weinberg, R.A. Hallmarks of cancer: the next generation. *Cell* **144**, 646-674 (2011).
115. Gerhardt, H. & Semb, H. Pericytes: gatekeepers in tumour cell metastasis? *J Mol Med (Berl)* **86**, 135-144 (2008).
116. Bogenrieder, T. & Herlyn, M. Axis of evil: molecular mechanisms of cancer metastasis. *Oncogene* **22**, 6524-6536 (2003).
117. De Bock, K., Mazzone, M. & Carmeliet, P. Antiangiogenic therapy, hypoxia, and metastasis: risky liaisons, or not? *Nat Rev Clin Oncol* **8**, 393-404.
118. Pantel, K., Alix-Panabieres, C. & Riethdorf, S. Cancer micrometastases. *Nat Rev Clin Oncol* **6**, 339-351 (2009).
119. Paget. The distribution of secondary growths in cancer of the breast. *The Lancet* **1**, 571-573 (1880).
120. DeVita, V.T., Jr. & Chu, E. A history of cancer chemotherapy. *Cancer Res* **68**, 8643-8653 (2008).
121. Heald, R.J., Husband, E.M. & Ryall, R.D. The mesorectum in rectal cancer surgery--the clue to pelvic recurrence? *Br J Surg* **69**, 613-616 (1982).
122. Caley, A.K.A.T.J. Adjuvant therapy. *Medicine* **40**, 1-4 (2011).
123. Connell, P.P. & Hellman, S. Advances in radiotherapy and implications for the next century: a historical perspective. *Cancer Res* **69**, 383-392 (2009).
124. Skliarenko, J.W.P. Radiotherapy: practical applications and clinical aspects. *Medicine* **39**, 705-710 (2011).
125. Vordermark, D. Ten years of progress in radiation oncology. *BMC Cancer* **11**, 503 (2011).
126. Formenti, S.C. & Demaria, S. Systemic effects of local radiotherapy. *Lancet Oncol* **10**, 718-726 (2009).
127. Withers, H.R. Biological basis of radiation therapy for cancer. *Lancet* **339**, 156-159 (1992).
128. Steel, G.G., McMillan, T.J. & Peacock, J.H. The 5Rs of radiobiology. *Int J Radiat Biol* **56**, 1045-1048 (1989).
129. Harrington, K., Jankowska, P. & Hingorani, M. Molecular biology for the radiation oncologist: the 5Rs of radiobiology meet the hallmarks of cancer. *Clin Oncol (R Coll Radiol)* **19**, 561-571 (2007).
130. Selzer, E. & Hebar, A. Basic principles of molecular effects of irradiation. *Wien Med Wochenschr* **162**, 47-54 (2012).
131. Harrington, K.J.*, et al.* Guidelines for preclinical and early phase clinical assessment of novel radiosensitisers. *Br J Cancer* **105**, 628-639 (2011).
132. Seiwert, T.Y., Salama, J.K. & Vokes, E.E. The concurrent chemoradiation paradigm--general principles. *Nat Clin Pract Oncol* **4**, 86-100 (2007).
133. Mohiuddin, M. & Mohiuddin, M.M. Neoadjuvant chemoradiation in rectal cancer: time to start in a new direction. *J Clin Oncol* **29**, e350-351; author reply e352-353 (2011).
134. Martin, L.K. & Bekaii-Saab, T. Optimizing neoadjuvant therapy for rectal cancer with oxaliplatin. *J Natl Compr Canc Netw* **11**, 298-307; quiz 307 (2013).
135. Shewach, D.S. & Lawrence, T.S. Antimetabolite radiosensitizers. *J Clin Oncol* **25**, 4043-4050 (2007).

136. O'Connell, M.J*., et al.* Improving adjuvant therapy for rectal cancer by combining protracted-infusion fluorouracil with radiation therapy after curative surgery. *N Engl J Med* **331**, 502-507 (1994).
137. Stein, A. & Arnold, D. Oxaliplatin: a review of approved uses. *Expert Opin Pharmacother* **13**, 125-137 (2012).
138. Andre, T*., et al.* Improved overall survival with oxaliplatin, fluorouracil, and leucovorin as adjuvant treatment in stage II or III colon cancer in the MOSAIC trial. *J Clin Oncol* **27**, 3109-3116 (2009).
139. de Gramont, A*., et al.* Leucovorin and fluorouracil with or without oxaliplatin as first-line treatment in advanced colorectal cancer. *J Clin Oncol* **18**, 2938-2947 (2000).
140. Nordlinger, B*., et al.* Perioperative chemotherapy with FOLFOX4 and surgery versus surgery alone for resectable liver metastases from colorectal cancer (EORTC Intergroup trial 40983): a randomised controlled trial. *Lancet* **371**, 1007-1016 (2008).
141. Hermann, R.M., Rave-Frank, M. & Pradier, O. Combining radiation with oxaliplatin: a review of experimental results. *Cancer Radiother* **12**, 61-67 (2008).
142. Folkvord, S*., et al.* Inhibitory effects of oxaliplatin in experimental radiation treatment of colorectal carcinoma: does oxaliplatin improve 5-fluorouracil-dependent radiosensitivity? *Radiother Oncol* **86**, 428-434 (2008).
143. Glynne-Jones, R., Anyamene, N., Moran, B. & Harrison, M. Neoadjuvant chemotherapy in MRI-staged high-risk rectal cancer in addition to or as an alternative to preoperative chemoradiation? *Ann Oncol* **23**, 2517-2526 (2012).
144. Zhukov, N.V. & Tjulandin, S.A. Targeted therapy in the treatment of solid tumors: practice contradicts theory. *Biochemistry (Mosc)* **73**, 605-618 (2008).
145. Sledge, G.W., Jr. What is targeted therapy? *J Clin Oncol* **23**, 1614-1615 (2005).
146. Adjei, A.A. & Hidalgo, M. Intracellular signal transduction pathway proteins as targets for cancer therapy. *J Clin Oncol* **23**, 5386-5403 (2005).
147. Blume-Jensen, P. & Hunter, T. Oncogenic kinase signalling. *Nature* **411**, 355-365 (2001).
148. Ma, B., Corry, J., Rischin, D., Leong, T. & Peters, L.J. Combined modality treatment for locally advanced squamous-cell carcinoma of the oropharynx in a woman with Bloom's syndrome: a case report and review of the literature. *Ann Oncol* **12**, 1015-1017 (2001).
149. Ree, A.H. & Hollywood, D. Design and conduct of early-phase radiotherapy trials with targeted therapeutics: Lessons from the PRAVO experience. *Radiother Oncol* **108**, 3-16 (2013).
150. Glynne-Jones, R., Mawdsley, S. & Harrison, M. Antiepidermal growth factor receptor radiosensitizers in rectal cancer. *Anticancer Drugs* **22**, 330-340 (2011).
151. Torino, F., Sarmiento, R. & Gasparini, G. The contribution of targeted therapy to the neoadjuvant chemoradiation of rectal cancer. *Crit Rev Oncol Hematol* **87**, 283-305 (2013).
152. Bonner, J.A*., et al.* Radiotherapy plus cetuximab for squamous-cell carcinoma of the head and neck. *N Engl J Med* **354**, 567-578 (2006).
153. Weiss, C*., et al.* Preoperative radiotherapy of advanced rectal cancer with capecitabine and oxaliplatin with or without cetuximab: A pooled analysis of three prospective phase I-II trials. *Int J Radiat Oncol Biol Phys* **78**, 472-478 (2010).
154. Grimminger, P.P*., et al.* Biomarkers for cetuximab-based neoadjuvant radiochemotherapy in locally advanced rectal cancer. *Clin Cancer Res* **17**, 3469-3477 (2011).
155. Palumbo, I*., et al.* Gefitinib enhances the effects of combined radiotherapy and 5-fluorouracil in a colorectal cancer cell line. *Int J Colorectal Dis* (2013).
156. Valentini, V*., et al.* Infusional 5-fluorouracil and ZD1839 (Gefitinib-Iressa) in combination with preoperative radiotherapy in patients with locally advanced rectal cancer: a phase I and II Trial (1839IL/0092). *Int J Radiat Oncol Biol Phys* **72**, 644-649 (2008).
157. Cao, Y. Molecular mechanisms and therapeutic development of angiogenesis inhibitors. *Adv Cancer Res* **100**, 113-131 (2008).

158. Jain, R.K. Normalization of tumor vasculature: an emerging concept in antiangiogenic therapy. *Science* **307**, 58-62 (2005).
159. Marquardt, F., Rodel, F., Capalbo, G., Weiss, C. & Rodel, C. Molecular targeted treatment and radiation therapy for rectal cancer. *Strahlenther Onkol* **185**, 371-378 (2009).
160. Hurwitz, H.*, et al.* Bevacizumab plus irinotecan, fluorouracil, and leucovorin for metastatic colorectal cancer. *N Engl J Med* **350**, 2335-2342 (2004).
161. Allegra, C.J.*, et al.* Phase III trial assessing bevacizumab in stages II and III carcinoma of the colon: results of NSABP protocol C-08. *J Clin Oncol* **29**, 11-16 (2011).
162. de Gramont, A.*, et al.* Bevacizumab plus oxaliplatin-based chemotherapy as adjuvant treatment for colon cancer (AVANT): a phase 3 randomised controlled trial. *Lancet Oncol* **13**, 1225-1233 (2012).
163. Willett, C.G.*, et al.* Combined vascular endothelial growth factor-targeted therapy and radiotherapy for rectal cancer: theory and clinical practice. *Semin Oncol* **33**, S35-40 (2006).
164. Willett, C.G.*, et al.* A safety and survival analysis of neoadjuvant bevacizumab with standard chemoradiation in a phase I/II study compared with standard chemoradiation in locally advanced rectal cancer. *Oncologist* **15**, 845-851 (2010).
165. Landry, J.C.*, et al.* Phase 2 study of preoperative radiation with concurrent capecitabine, oxaliplatin, and bevacizumab followed by surgery and postoperative 5-fluorouracil, leucovorin, oxaliplatin (FOLFOX), and bevacizumab in patients with locally advanced rectal cancer: ECOG 3204. *Cancer* **119**, 1521-1527 (2012).
166. Stratton, M.R. Exploring the genomes of cancer cells: progress and promise. *Science* **331**, 1553-1558 (2011).
167. Tang, J., Yan, H. & Zhuang, S. Histone deacetylases as targets for treatment of multiple diseases. *Clin Sci (Lond)* **124**, 651-662 (2013).
168. Inche, A.G. & La Thangue, N.B. Chromatin control and cancer-drug discovery: realizing the promise. *Drug Discov Today* **11**, 97-109 (2006).
169. Shabason, J.E., Tofilon, P.J. & Camphausen, K. Grand rounds at the National Institutes of Health: HDAC inhibitors as radiation modifiers, from bench to clinic. *J Cell Mol Med* **15**, 2735-2744 (2011).
170. Camphausen, K. & Tofilon, P.J. Inhibition of histone deacetylation: a strategy for tumor radiosensitization. *J Clin Oncol* **25**, 4051-4056 (2007).
171. Khan, O. & La Thangue, N.B. HDAC inhibitors in cancer biology: emerging mechanisms and clinical applications. *Immunol Cell Biol* **90**, 85-94 (2012).
172. Spiegel, S., Milstien, S. & Grant, S. Endogenous modulators and pharmacological inhibitors of histone deacetylases in cancer therapy. *Oncogene* **31**, 537-551 (2012).
173. Richon, V.M., Garcia-Vargas, J. & Hardwick, J.S. Development of vorinostat: current applications and future perspectives for cancer therapy. *Cancer Lett* **280**, 201-210 (2009).
174. Koprinarova, M., Botev, P. & Russev, G. Histone deacetylase inhibitor sodium butyrate enhances cellular radiosensitivity by inhibiting both DNA nonhomologous end joining and homologous recombination. *DNA Repair (Amst)* **10**, 970-977 (2011).
175. Ellis, L., Hammers, H. & Pili, R. Targeting tumor angiogenesis with histone deacetylase inhibitors. *Cancer Lett* **280**, 145-153 (2009).
176. Qian, D.Z.*, et al.* Class II histone deacetylases are associated with VHL-independent regulation of hypoxia-inducible factor 1 alpha. *Cancer Res* **66**, 8814-8821 (2006).
177. Giannini, G., Cabri, W., Fattorusso, C. & Rodriquez, M. Histone deacetylase inhibitors in the treatment of cancer: overview and perspectives. *Future Med Chem* **4**, 1439-1460 (2012).
178. Baylin, S.B. & Jones, P.A. A decade of exploring the cancer epigenome - biological and translational implications. *Nat Rev Cancer* **11**, 726-734 (2011).
179. Ramalingam, S.S.*, et al.* Carboplatin and Paclitaxel in combination with either vorinostat or placebo for first-line therapy of advanced non-small-cell lung cancer. *J Clin Oncol* **28**, 56-62 (2010).

180. Fakih, M.G., Groman, A., McMahon, J., Wilding, G. & Muindi, J.R. A randomized phase II study of two doses of vorinostat in combination with 5-FU/LV in patients with refractory colorectal cancer. *Cancer Chemother Pharmacol* **69**, 743-751 (2010).
181. Munster, P.N.*, et al.* A phase II study of the histone deacetylase inhibitor vorinostat combined with tamoxifen for the treatment of patients with hormone therapy-resistant breast cancer. *Br J Cancer* **104**, 1828-1835 (2011).
182. Ree, A.H.*, et al.* Vorinostat, a histone deacetylase inhibitor, combined with pelvic palliative radiotherapy for gastrointestinal carcinoma: the Pelvic Radiation and Vorinostat (PRAVO) phase 1 study. *Lancet Oncol* **11**, 459-464 (2010).
183. Richon, V.M. Targeting histone deacetylases: development of vorinostat for the treatment of cancer. *Epigenomics* **2**, 457-465 (2010).
184. Biomarkers-Definitions-Working-Group. Biomarkers and surrogate endpoints: preferred definitions and conceptual framework. *Clin Pharmacol Ther* **69**, 89-95 (2001).
185. Strimbu, K. & Tavel, J.A. What are biomarkers? *Curr Opin HIV AIDS* **5**, 463-466 (2010).
186. Krause, M. & Baumann, M. Clinical biomarkers of kinase activity: examples from EGFR inhibition trials. *Cancer Metastasis Rev* **27**, 387-402 (2008).
187. Yaromina, A., Krause, M. & Baumann, M. Individualization of cancer treatment from radiotherapy perspective. *Mol Oncol* **6**, 211-221 (2012).
188. Benchimol, S.*, et al.* Carcinoembryonic antigen, a human tumor marker, functions as an intercellular adhesion molecule. *Cell* **57**, 327-334 (1989).
189. Bolocan, A., Ion, D., Ciocan, D.N. & Paduraru, D.N. Prognostic and predictive factors in colorectal cancer. *Chirurgia (Bucur)* **107**, 555-563 (2012).
190. Flatmark, K.*, et al.* Disseminated tumour cells as a prognostic biomarker in colorectal cancer. *Br J Cancer* **104**, 1434-1439 (2011).
191. Rahbari, N.N.*, et al.* Meta-analysis shows that detection of circulating tumor cells indicates poor prognosis in patients with colorectal cancer. *Gastroenterology* **138**, 1714-1726 (2010).
192. Pantel, K. & Alix-Panabieres, C. Circulating tumour cells in cancer patients: challenges and perspectives. *Trends Mol Med* **16**, 398-406 (2010).
193. Martini, M., Vecchione, L., Siena, S., Tejpar, S. & Bardelli, A. Targeted therapies: how personal should we go? *Nat Rev Clin Oncol* **9**, 87-97 (2011).
194. LoRusso, P.M.*, et al.* Translating clinical trials into meaningful outcomes. *Clin Cancer Res* **16**, 5951-5955 (2010).
195. Ree, A.H.*, et al.* Tumor phosphatidylinositol-3-kinase signaling and development of metastatic disease in locally advanced rectal cancer. *PLoS One* **7**, e50806 (2012).
196. Jubb, A.M. & Harris, A.L. Biomarkers to predict the clinical efficacy of bevacizumab in cancer. *Lancet Oncol* **11**, 1172-1183 (2010).
197. Willett, C.G.*, et al.* Efficacy, safety, and biomarkers of neoadjuvant bevacizumab, radiation therapy, and fluorouracil in rectal cancer: a multidisciplinary phase II study. *J Clin Oncol* **27**, 3020-3026 (2009).
198. Folkvord, S.*, et al.* Prediction of response to preoperative chemoradiotherapy in rectal cancer by multiplex kinase activity profiling. *Int J Radiat Oncol Biol Phys* **78**, 555-562 (2010).
199. Kuremsky, J.G., Tepper, J.E. & McLeod, H.L. Biomarkers for response to neoadjuvant chemoradiation for rectal cancer. *Int J Radiat Oncol Biol Phys* **74**, 673-688 (2009).
200. Ghadimi, B.M.*, et al.* Effectiveness of gene expression profiling for response prediction of rectal adenocarcinomas to preoperative chemoradiotherapy. *J Clin Oncol* **23**, 1826-1838 (2005).
201. Giannini, G., Cabri, W., Fattorusso, C. & Rodriquez, M. Histone deacetylase inhibitors in the treatment of cancer: overview and perspectives. *Future Med Chem* **4**, 1439-1460.
202. Stimson, L. & La Thangue, N.B. Biomarkers for predicting clinical responses to HDAC inhibitors. *Cancer Lett* **280**, 177-183 (2009).

203. Folkvord, S., Ree, A.H., Furre, T., Halvorsen, T. & Flatmark, K. Radiosensitization by SAHA in experimental colorectal carcinoma models-in vivo effects and relevance of histone acetylation status. *Int J Radiat Oncol Biol Phys* **74**, 546-552 (2009).
204. Griffiths, G. Clinical trials in oncology. *Medicine* **40**, 20-23 (2011).
205. LoRusso, P.M., Boerner, S.A. & Seymour, L. An overview of the optimal planning, design, and conduct of phase I studies of new therapeutics. *Clin Cancer Res* **16**, 1710-1718 (2010).
206. Le Tourneau, C., Lee, J.J. & Siu, L.L. Dose escalation methods in phase I cancer clinical trials. *J Natl Cancer Inst* **101**, 708-720 (2009).
207. Wistuba, II, Gelovani, J.G., Jacoby, J.J., Davis, S.E. & Herbst, R.S. Methodological and practical challenges for personalized cancer therapies. *Nat Rev Clin Oncol* **8**, 135-141 (2011).
208. Grade, M., Wolff, H.A., Gaedcke, J. & Ghadimi, B.M. The molecular basis of chemoradiosensitivity in rectal cancer: implications for personalized therapies. *Langenbecks Arch Surg* **397**, 543-555 (2012).
209. Peppelenbosch, M.P. Kinome profiling. *Scientifica (Cairo)* **2012**, 306798 (2012).
210. Piersma, S.R., Labots, M., Verheul, H.M. & Jimenez, C.R. Strategies for kinome profiling in cancer and potential clinical applications: chemical proteomics and array-based methods. *Anal Bioanal Chem* **397**, 3163-3171 (2010).
211. Bratland, A., Dueland, S., Hollywood, D., Flatmark, K. & Ree, A.H. Gastrointestinal toxicity of vorinostat: reanalysis of phase 1 study results with emphasis on dose-volume effects of pelvic radiotherapy. *Radiat Oncol* **6**, 33 (2011).
212. Clinicaltrials.gov. A service of the United States National Institutes of Health.
213. McAllister, S.S. & Weinberg, R.A. Tumor-host interactions: a far-reaching relationship. *J Clin Oncol* **28**, 4022-4028 (2010).
214. Kahn, J., Tofilon, P.J. & Camphausen, K. Preclinical models in radiation oncology. *Radiat Oncol* **7**, 223 (2012).
215. Nims, R.W., Sykes, G., Cottrill, K., Ikonomi, P. & Elmore, E. Short tandem repeat profiling: part of an overall strategy for reducing the frequency of cell misidentification. *In Vitro Cell Dev Biol Anim* **46**, 811-819 (2010).
216. Lacroix, M. Persistent use of "false" cell lines. *Int J Cancer* **122**, 1-4 (2008).
217. Brattain, M.G., Fine, W.D., Khaled, F.M., Thompson, J. & Brattain, D.E. Heterogeneity of malignant cells from a human colonic carcinoma. *Cancer Res* **41**, 1751-1756 (1981).
218. Leibovitz, A.*, et al.* Classification of human colorectal adenocarcinoma cell lines. *Cancer Res* **36**, 4562-4569 (1976).
219. Chen, T.R., Drabkowski, D., Hay, R.J., Macy, M. & Peterson, W., Jr. WiDr is a derivative of another colon adenocarcinoma cell line, HT-29. *Cancer Genet Cytogenet* **27**, 125-134 (1987).
220. Morikawa, K., Walker, S.M., Jessup, J.M. & Fidler, I.J. In vivo selection of highly metastatic cells from surgical specimens of different primary human colon carcinomas implanted into nude mice. *Cancer Res* **48**, 1943-1948 (1988).
221. Morton, C.L. & Houghton, P.J. Establishment of human tumor xenografts in immunodeficient mice. *Nat Protoc* **2**, 247-250 (2007).
222. Rosenthal, N. & Brown, S. The mouse ascending: perspectives for human-disease models. *Nat Cell Biol* **9**, 993-999 (2007).
223. Wouters, A., Pauwels, B., Lardon, F. & Vermorken, J.B. Review: implications of in vitro research on the effect of radiotherapy and chemotherapy under hypoxic conditions. *Oncologist* **12**, 690-712 (2007).
224. Esteban, M.A. & Maxwell, P.H. Manipulation of oxygen tensions for in vitro cell culture using a hypoxic workstation. *Expert Rev Proteomics* **2**, 307-314 (2005).
225. Vordermark, D., Katzer, A., Baier, K., Kraft, P. & Flentje, M. Cell type-specific association of hypoxia-inducible factor-1 alpha (HIF-1 alpha) protein accumulation and radiobiologic tumor hypoxia. *Int J Radiat Oncol Biol Phys* **58**, 1242-1250 (2004).

226. Harrington, K.J., *et al.* Guidelines for preclinical and early phase clinical assessment of novel radiosensitisers. *Br J Cancer* **105**, 628-639.
227. Randers-Eichhorn, L., Bartlett, R.A., Frey, D.D. & Rao, G. Noninvasive oxygen measurements and mass transfer considerations in tissue culture flasks. *Biotechnol Bioeng* **51**, 466-478 (1996).
228. Itani, W., Geara, F., Haykal, J., Haddadin, M. & Gali-Muhtasib, H. Radiosensitization by 2-benzoyl-3-phenyl-6,7-dichloroquinoxaline 1,4-dioxide under oxia and hypoxia in human colon cancer cells. *Radiat Oncol* **2**, 1 (2007).
229. Shibamoto, Y., Tachi, Y., Tanabe, K., Hatta, H. & Nishimoto, S. In vitro and in vivo evaluation of novel antitumor prodrugs of 5-fluoro-2'-deoxyuridine activated by hypoxic irradiation. *Int J Radiat Oncol Biol Phys* **58**, 397-402 (2004).
230. Jensen, E.C. The basics of western blotting. *Anat Rec (Hoboken)* **295**, 369-371 (2012).
231. Wouters, B.G. & Brown, J.M. Cells at intermediate oxygen levels can be more important than the "hypoxic fraction" in determining tumor response to fractionated radiotherapy. *Radiat Res* **147**, 541-550 (1997).
232. Yaromina, A., *et al.* Pre-treatment number of clonogenic cells and their radiosensitivity are major determinants of local tumour control after fractionated irradiation. *Radiother Oncol* **83**, 304-310 (2007).
233. Patterson, L.H., *et al.* Enhancement of chemotherapy and radiotherapy of murine tumours by AQ4N, a bioreductively activated anti-tumour agent. *Br J Cancer* **82**, 1984-1990 (2000).
234. Marini, P., *et al.* Combined treatment with lexatumumab and irradiation leads to strongly increased long term tumour control under normoxic and hypoxic conditions. *Radiat Oncol* **4**, 49 (2009).
235. Rofstad, E.K. & Maseide, K. Radiobiological and immunohistochemical assessment of hypoxia in human melanoma xenografts: acute and chronic hypoxia in individual tumours. *Int J Radiat Biol* **75**, 1377-1393 (1999).
236. Beck-Bornholdt, H.P. Should tumors be clamped in radiobiological fractionation experiments? *Int J Radiat Oncol Biol Phys* **21**, 675-682 (1991).
237. Rofstad, E.K., Gaustad, J.V., Egeland, T.A., Mathiesen, B. & Galappathi, K. Tumors exposed to acute cyclic hypoxic stress show enhanced angiogenesis, perfusion and metastatic dissemination. *Int J Cancer* **127**, 1535-1546 (2010).
238. Goethals, L., *et al.* Hypoxia in human colorectal adenocarcinoma: comparison between extrinsic and potential intrinsic hypoxia markers. *Int J Radiat Oncol Biol Phys* **65**, 246-254 (2006).
239. Hatok, J., *et al.* In vitro assays for the evaluation of drug resistance in tumor cells. *Clin Exp Med* **9**, 1-7 (2009).
240. Franken, N.A., Rodermond, H.M., Stap, J., Haveman, J. & van Bree, C. Clonogenic assay of cells in vitro. *Nat Protoc* **1**, 2315-2319 (2006).
241. Tomayko, M.M. & Reynolds, C.P. Determination of subcutaneous tumor size in athymic (nude) mice. *Cancer Chemother Pharmacol* **24**, 148-154 (1989).
242. Lieu, C.H., Tan, A.C., Leong, S., Diamond, J.R. & Eckhardt, S.G. From bench to bedside: lessons learned in translating preclinical studies in cancer drug development. *J Natl Cancer Inst* **105**, 1441-1456 (2013).
243. Mandrekar, S.J., An, M.W. & Sargent, D.J. A review of phase II trial designs for initial marker validation. *Contemp Clin Trials* **36**, 597-604 (2013).
244. Yeo, S.G., *et al.* Tumor volume reduction rate measured by magnetic resonance volumetry correlated with pathologic tumor response of preoperative chemoradiotherapy for rectal cancer. *Int J Radiat Oncol Biol Phys* **78**, 164-171 (2010).
245. Flatmark, K., *et al.* Immunomagnetic detection of micrometastatic cells in bone marrow of colorectal cancer patients. *Clin Cancer Res* **8**, 444-449 (2002).
246. Forus, A., Hoifodt, H.K., Overli, G.E., Myklebost, O. & Fodstad, O. Sensitive fluorescent in situ hybridisation method for the characterisation of breast cancer cells in bone marrow aspirates. *Mol Pathol* **52**, 68-74 (1999).

247. Went, P.*, et al.* Frequent high-level expression of the immunotherapeutic target Ep-CAM in colon, stomach, prostate and lung cancers. *Br J Cancer* **94**, 128-135 (2006).
248. Alix-Panabieres, C., Riethdorf, S. & Pantel, K. Circulating tumor cells and bone marrow micrometastasis. *Clin Cancer Res* **14**, 5013-5021 (2008).
249. Sikkema, A.H., den Dunnen, W.F., Diks, S.H., Peppelenbosch, M.P. & de Bont, E.S. Optimizing targeted cancer therapy: towards clinical application of systems biology approaches. *Crit Rev Oncol Hematol* **82**, 171-186 (2011).
250. Manning, G., Whyte, D.B., Martinez, R., Hunter, T. & Sudarsanam, S. The protein kinase complement of the human genome. *Science* **298**, 1912-1934 (2002).
251. Krause, D.S. & Van Etten, R.A. Tyrosine kinases as targets for cancer therapy. *N Engl J Med* **353**, 172-187 (2005).
252. Sikkema, A.H.*, et al.* Kinome profiling in pediatric brain tumors as a new approach for target discovery. *Cancer Res* **69**, 5987-5995 (2009).
253. Parikh, K. & Peppelenbosch, M.P. Kinome profiling of clinical cancer specimens. *Cancer Res* **70**, 2575-2578 (2010).
254. Bratland, A.*, et al.* Osteoblast-induced EGFR/ERBB2 signaling in androgen-sensitive prostate carcinoma cells characterized by multiplex kinase activity profiling. *Clin Exp Metastasis* **26**, 485-496 (2009).
255. Roe, K.*, et al.* Hypoxic tumor kinase signaling mediated by STAT5A in development of castration-resistant prostate cancer. *PLoS One* **8**, e63723 (2013).
256. Schrage, Y.M.*, et al.* Kinome profiling of chondrosarcoma reveals SRC-pathway activity and dasatinib as option for treatment. *Cancer Res* **69**, 6216-6222 (2009).
257. Marusyk, A., Almendro, V. & Polyak, K. Intra-tumour heterogeneity: a looking glass for cancer? *Nat Rev Cancer* **12**, 323-334 (2012).
258. Sandor, V.*, et al.* Phase I trial of the histone deacetylase inhibitor, depsipeptide (FR901228, NSC 630176), in patients with refractory neoplasms. *Clin Cancer Res* **8**, 718-728 (2002).
259. Bucca, G.*, et al.* Gene expression profiling of human cancers. *Ann N Y Acad Sci* **1028**, 28-37 (2004).
260. Raspe, E., Decraene, C. & Berx, G. Gene expression profiling to dissect the complexity of cancer biology: pitfalls and promise. *Semin Cancer Biol* **22**, 250-260 (2012).
261. White, C.A. & Salamonsen, L.A. A guide to issues in microarray analysis: application to endometrial biology. *Reproduction* **130**, 1-13 (2005).
262. Huang da, W., Sherman, B.T. & Lempicki, R.A. Systematic and integrative analysis of large gene lists using DAVID bioinformatics resources. *Nat Protoc* **4**, 44-57 (2009).
263. Kendall, L.V. & Riley, L.K. Reverse transcriptase polymerase chain reaction (RT-PCR). *Contemp Top Lab Anim Sci* **39**, 42 (2000).
264. Arya, M.*, et al.* Basic principles of real-time quantitative PCR. *Expert Rev Mol Diagn* **5**, 209-219 (2005).
265. Kendall, L.V., Besselsen, D.G. & Riley, L.K. Fluorogenic 5' nuclease PCR (real time PCR). *Contemp Top Lab Anim Sci* **39**, 41 (2000).
266. Cusnir, M. & Cavalcante, L. Inter-tumor heterogeneity. *Hum Vaccin Immunother* **8**, 1143-1145 (2012).
267. Van Schaeybroeck, S., Allen, W.L., Turkington, R.C. & Johnston, P.G. Implementing prognostic and predictive biomarkers in CRC clinical trials. *Nat Rev Clin Oncol* **8**, 222-232 (2011).
268. Stricker, T., Catenacci, D.V. & Seiwert, T.Y. Molecular profiling of cancer--the future of personalized cancer medicine: a primer on cancer biology and the tools necessary to bring molecular testing to the clinic. *Semin Oncol* **38**, 173-185 (2011).
269. Cusnir, M. & Cavalcante, L. Inter-tumor heterogeneity. *Hum Vaccin Immunother* **8**, 1143-1145.
270. Yu, J., Mi, J., Wang, Y., Wang, A. & Tian, X. Regulation of radiosensitivity by HDAC inhibitor trichostatin A in the human cervical carcinoma cell line Hela. *Eur J Gynaecol Oncol* **33**, 285-290 (2012).

271. Flatmark, K.*, et al.* Radiosensitization of colorectal carcinoma cell lines by histone deacetylase inhibition. *Radiat Oncol* **1**, 25 (2006).
272. Podar, K. & Anderson, K.C. A therapeutic role for targeting c-Myc/Hif-1-dependent signaling pathways. *Cell Cycle* **9**, 1722-1728 (2010).
273. Huang, L.E. Carrot and stick: HIF-alpha engages c-Myc in hypoxic adaptation. *Cell Death Differ* **15**, 672-677 (2008).
274. Dewdney, A.*, et al.* Multicenter randomized phase II clinical trial comparing neoadjuvant oxaliplatin, capecitabine, and preoperative radiotherapy with or without cetuximab followed by total mesorectal excision in patients with high-risk rectal cancer (EXPERT-C). *J Clin Oncol* **30**, 1620-1627 (2012).
275. Glynne-Jones, R., Grainger, J., Harrison, M., Ostler, P. & Makris, A. Neoadjuvant chemotherapy prior to preoperative chemoradiation or radiation in rectal cancer: should we be more cautious? *Br J Cancer* **94**, 363-371 (2006).
276. Schrag, D.*, et al.* Neoadjuvant FOLFOX-bev, without radiation, for locally advanced rectal cancer. *Journal of Clinical Oncology* **28**, Abstract 3511 (2010).
277. Fernandez-Martos, C., Estevan, E., Salud, A., Pericay, C. & Gallen, M. Neoadjuvant capecitabine, oxaliplatin, and bevacizumab (CAPOX-B) in intermediate-risk rectal cancer (RC) patients defined by magnetic resonance (MR): GEMCAD 0801 trial. . *Journal of Clinical Oncology* **30**, Abstract 3586 (2012).
278. Schrag, D. Evolving role of neoadjuvant therapy in rectal cancer. *Curr Treat Options Oncol* **14**, 350-364 (2013).
279. Nilsson, P.J.*, et al.* Short-course radiotherapy followed by neo-adjuvant chemotherapy in locally advanced rectal cancer--the RAPIDO trial. *BMC Cancer* **13**, 279 (2013).
280. Bujko, K.*, et al.* Long-term results of a randomized trial comparing preoperative short-course radiotherapy with preoperative conventionally fractionated chemoradiation for rectal cancer. *Br J Surg* **93**, 1215-1223 (2006).
281. Ngan, S.Y.*, et al.* Randomized trial of short-course radiotherapy versus long-course chemoradiation comparing rates of local recurrence in patients with T3 rectal cancer: Trans-Tasman Radiation Oncology Group trial 01.04. *J Clin Oncol* **30**, 3827-3833 (2012).
282. Pettersson, D.*, et al.* Preoperative short-course radiotherapy with delayed surgery in primary rectal cancer. *Br J Surg* **99**, 577-583 (2011).
283. Pettersson, D.*, et al.* Interim analysis of the Stockholm III trial of preoperative radiotherapy regimens for rectal cancer. *Br J Surg* **97**, 580-587 (2010).
284. Fokas, E., McKenna, W.G. & Muschel, R.J. The impact of tumor microenvironment on cancer treatment and its modulation by direct and indirect antivascular strategies. *Cancer Metastasis Rev* **31**, 823-842 (2012).
285. Fokas, E.*, et al.* Dual inhibition of the PI3K/mTOR pathway increases tumor radiosensitivity by normalizing tumor vasculature. *Cancer Res* **72**, 239-248 (2011).

11 Paper I-IV

I

Angiogenesis (2011) 14:481–489
DOI 10.1007/s10456-011-9231-3

ORIGINAL PAPER

Tumor kinase activity in locally advanced rectal cancer: angiogenic signaling and early systemic dissemination

Marie Grøn Saelen · Kjersti Flatmark · Sigurd Folkvord · Rik de Wijn · Heidi Rasmussen · Øystein Fodstad · Anne Hansen Ree

Received: 11 May 2011 / Accepted: 30 July 2011 / Published online: 11 August 2011

Abstract Tumor hypoxia is a common determinant of resistance to cytotoxic therapies and metastatic behavior. In rectal cancer patients receiving preoperative chemoradiotherapy, tyrosine kinase activities in tumors with poor and good treatment responses were found to differ. Given that tyrosine kinase signaling mediates hypoxic tissue adaptation, the present study examined whether tumor kinase activity might also correlate with systemic dissemination of rectal cancer. Immunomagnetic selection of disseminated tumor cells (DTC) from bone marrow aspirates was undertaken in 55 patients with locally advanced rectal cancer. Using peptide arrays with 144 tyrosine kinase substrates, phosphopeptide signatures were generated from patients' baseline tumor biopsies, to study association between DTC and tumor tyrosine kinase activity regulated ex vivo by sunitinib. Disseminated tumor cells were detected in 60% of cases, and these patients had significantly poorer metastasis-free survival than patients without DTC. Phosphorylation of 31 array tyrosine kinase substrates by tumor samples was significantly more strongly inhibited by sunitinib in the DTC-negative patients, with a number of phosphosubstrates representing angiogenic factors. In this cohort of rectal cancer patients, tumor phenotypes defined by a subset of tyrosine kinase activities correlating with weak ex vivo inhibition by sunitinib, was associated with early systemic dissemination.

Keywords Rectal cancer · Tyrosine kinase signaling · Angiogenesis · Disseminated tumor cells · Metastasis

Introduction

In order to cure rectal cancer, two therapeutic challenges must be met, namely eradication of tumor within the pelvic cavity and secondly, the prevention of systemic tumor dissemination. The natural disease course of rectal cancer makes it an ideal model system to explore the possible role of tumor hypoxia in therapy resistance and development of metastasis. Tissue hypoxia is defined by reduced oxygen levels, typically 2% oxygen or less, and occurs in a wide range of pathological conditions [1, 2]. Within classical radiobiology, hypoxia is recognized as a main mechanism involved in tumor resistance to radiation [3, 4]. Moreover, recent research supports the hypothesis that tumor hypoxia is one of the major driving forces of the metastatic process [5]. Adaptive cellular responses to hypoxia allow for processes such as proliferation, migration, and in particular angiogenesis, and involve activation of a range of kinase

Electronic supplementary material The online version of this article (doi:10.1007/s10456-011-9231-3) contains supplementary material, which is available to authorized users.

M. G. Saelen · K. Flatmark · S. Folkvord · H. Rasmussen · Ø. Fodstad
Department of Tumor Biology, Oslo University Hospital – Radiumhospitalet, Oslo, Norway

M. G. Saelen · Ø. Fodstad · A. H. Ree
Institute of Clinical Medicine, University of Oslo, Oslo, Norway

K. Flatmark
Department of Surgical Oncology, Oslo University Hospital – Radiumhospitalet, Oslo, Norway

R. de Wijn
PamGene International B.V., 's-Hertogenbosch, The Netherlands

A. H. Ree (✉)
Department of Oncology, Akershus University Hospital, 1478 Lørenskog, Norway
e-mail: a.h.ree@medisin.uio.no

signaling pathways, among them signaling initiated by the receptor tyrosine kinases PDGFR, VEGFR, and EPOR [1, 5, 6].

Locally advanced rectal cancer (LARC) comprises primary tumors that grow beyond the rectal wall to an extent that precludes primary surgical removal with adequate microscopic margins. Hence, treatment of LARC is multimodal, involving preoperative chemoradiotherapy aimed at macroscopic downsizing and control of subclinical tumor extension within the pelvic cavity, to enable complete tumor removal by subsequent surgery. However, even with successful local treatment, a substantial number of patients will develop metastatic disease as result of early undetected systemic dissemination of tumor cells [7]. The phase II trial *Locally Advanced Rectal Cancer—Radiation Response Prediction (LARC-RRP),* registered with ClinicalTrials.gov number NCT00278694, was launched primarily to identify predictive biomarkers of tumor radiation sensitivity, and we have recently reported that this was feasible by kinase activity profiling of baseline tumor biopsies [8]. Using peptide arrays with tyrosine kinase substrates, we found that phosphopeptide levels generated by tumors with poor response to the preoperative chemoradiotherapy were significantly higher than substrate phosphorylation resulting from tumors with good treatment response. The elevated kinase activity in poor-responding tumors was suppressed by ex vivo addition of the tyrosine kinase inhibitor sunitinib, and represented signaling implicated in experimental radiation resistance.

Given that tyrosine kinase signaling is involved in adaptive responses to tumor hypoxia, the present study aimed to determine how tumor kinase activity might relate to systemic disease dissemination. Hence, in the investigation of the LARC-RPP study patients reported here, we endeavored to correlate the individual patient's tumor tyrosine kinase activity to negative or positive status for disseminated tumor cells (DTC) to bone marrow as the clinical endpoint, using the presence of DTC as biomarker of metastatic recurrence risk [9]. Immunomagnetic selection of DTC was performed at the time of diagnosis, and by applying previously acquired ex vivo sunitinib inhibition profiles from the baseline primary tumor biopsies [8], the association between the tumor kinome and early systemic dissemination in terms of DTC status was studied.

Patients and methods

Patients and procedures

The patient population reported here was enrolled between October 2005 and December 2007. Patient eligibility criteria and evaluation procedures have been described previously [8]. Three patients with synchronous resectable liver metastases were also included in this study. The experimental treatment protocol, intended to intensify preoperative therapy for LARC, consisted of two cycles of neoadjuvant chemotherapy (the Nordic FLOX regimen: oxaliplatin 85 mg/m^2 on day 1 and daily bolus fluorouracil 500 mg/m^2 and folinic acid 100 mg on days 1 and 2 every second week) followed by chemoradiotherapy. Radiation was delivered in daily 2-Gy fractions 5 days per week over a five-week period; the initial 23 fractions to the macroscopic tumor volume and area at risk, and the two final fractions restricted to the macroscopic tumor, as determined by computed tomography-based planning. During the radiotherapy course, concomitant chemotherapy was given as oxaliplatin 50 mg/m^2 once weekly and capecitabine 825 mg/m^2 twice daily on days of radiotherapy. Surgery was planned 6–8 weeks after completion of the preoperative treatment. In accordance with national guidelines, the patients did not receive postoperative therapy.

The resected primary tumor specimens were histologically evaluated for response to the preoperative treatment according to standard criteria (ypTN) and histomorphologic tumor regression grade (TRG), as previously detailed [8]. Briefly, tumor response was graded within one of five TRG categories, spanning from the absence of residual tumor cells in the resected specimen (pathologic complete response; TRG 1) to the lack of morphologic signs of tissue response to treatment (TRG 5) [10]. The review procedures of patient follow-up included clinical examination, blood tests, and computed tomography scanning of the chest, abdomen, and pelvis, at three- and six-month intervals for the first and second year, respectively, and twelve months thereafter. Locally recurrent or metastatic disease and death of any cause were recorded. Thus, the study endpoints were histomorphologic tumor response to neoadjuvant therapy, disease-free survival, and overall survival. Follow-up data was obtained from the clinical database and censored on April 6th, 2011. Valid observations of the presence or absence of distant metastases or local recurrence required designated radiological examination and/or bioptic verification. The three patients with resectable liver metastases at the time of diagnosis were excluded from analysis of metastasis-free survival.

Study-specific procedures

At the time of diagnosis, baseline study-specific primary tumor biopsies (snap-frozen in liquid nitrogen and stored at −80°C) and bone marrow (15–40 ml drawn from the anterior iliac crests) were obtained from 71 patients under heavy sedation. Of these, 16 patients were excluded from the present study, as six patients had bone marrow samples

that contained too few mononuclear cells for immunomagnetic selection, and ten patients had tumor biopsy specimens in which kinase activity profiling had not been performed because the patients were either ineligible after study registration ($n = 3$), had withdrawn consent ($n = 1$), had unexpectedly died during the preoperative treatment ($n = 1$), had developed metastatic disease progression during preoperative treatment that precluded definitive surgery ($n = 1$), had tumor cell content less than 20% within the biopsy specimen ($n = 2$), or had a biopsy specimen in which kinase activity analysis was missing of unknown reasons ($n = 2$). Thus, tumor kinase activity signatures based on previous array phosphosubstrate data were successfully identified for 55 patients with known DTC status, and this study population is present within the current analyses.

The tumor biopsies were sectioned using a cryostat microtome, and hematoxylin-eosin stained slides were evaluated for tumor content. The average tumor cell content in the biopsy specimens was 44%, and no difference was found between patients positive and negative for DTC ($P > 0.66$; two-sample t-test). Each biopsy specimen was aliquoted by cryostat sectioning into 10-μm slices, and total tissue volume was calculated by multiplying the surface area of the section with the number of sample sections. Protein lysates were prepared by adding 36 μl lysis buffer (M-PER Mammalian Extraction Reagent containing Halt Phosphatase Inhibitor Cocktail and EDTA-free Halt Protease Inhibitor Cocktail; Pierce Biotechnology, Inc., Rockford, IL) per mm^3 tissue, and following vortexing and centrifugation, 5 μl of the supernatant was added to the reaction mixture, which was composed of Abl Reaction Buffer (50 mmol/l Tris–HCl pH 7.5, 10 mmol/l $MgCl_2$, 1 mmol/l EGTA, 2 mmol/l dithiothreitol, 0.01% Brij 35; New England BioLabs, Inc., Ipswich, MA), 1 mg/ml bovine serum albumin, 100 μmol/l ATP, and 12.5 μg/ml of the monoclonal, FITC-conjugated anti-phosphotyrosine antibody (Exalpha Biologicals, Inc., Maynard, MA) to a total volume of 40 μl in each array. No significant variation was observed in protein concentration in the sample lysates. Four technical replicates were analyzed from each patient sample to generate basal phosphosubstrate data. On the same array plate, using three technical replicates for each condition, each sample was also incubated in the presence of 2.5 μmol/l sunitinib (Axxora, Lausen, Switzerland).

For determination of DTC status, superparamagnetic sheep-antimouse IgG particles (Dynabeads M450; Invitrogen–Life Technologies, Oslo, Norway) were conjugated with the monoclonal antibody MOC-31 (IQ Products, Groningen, The Netherlands), and for each study patient, immunomagnetic selection of tumor cells in bone marrow was undertaken as previously described [11]. Briefly, mononuclear cells were isolated from the bone marrow aspirate and incubated with magnetic immunobeads with conjugated antibody, or without antibody for negative control, and subsequently exposed to a magnet field to separate bead-rosetting cells from unbound cells. A patient sample was classified as positive for DTC if a minimum of two cells rosetted at least five beads with the MOC-31 antibody and no rosetted cells were detected in the negative control.

Data adaptation and statistical analyses

The array data is available in the ArrayExpress database [12] by accession number E-TABM-913. The curated sunitinib inhibition data set that had been calculated from the signal intensity from each array peptide after background subtraction and used previously [8] was applied as input for the current statistical analysis. The data was log-transformed after handling a small number of negative data points by subtracting the 1% percentile of the data and subsequently setting all remaining data points with value less than 1 to the value 1. For each peptide, the sunitinib-induced log-fold change was calculated by subtracting the log-transformed signal in the absence of sunitinib (control) from that in the presence of this tyrosine kinase inhibitor. Peptides with sample-averaged signal less than 2^{10} in the control condition were excluded, leaving 102 peptides above this threshold. A two-sample t-test was performed to test for different level of sunitinib inhibition in DTC-positive and DTC-negative patients (Supplementary Table 1). The sunitinib inhibition profiles were visualized as data color maps, in which clustering of peptides and samples was imposed by sorting the data according to the value of the first principal component (peptides) and the value of the scores on the first principal component (samples) of a principal component analysis, using samples as observations and spots as variables. Distribution of value of the score on the first principal component was compared to clinical parameters using correlation coefficients for continuous variables and one-way ANOVA tests for categorical data. Data processing and visualizations were performed in Matlab R2010A including the statistics toolbox (Mathworks, Natick, MA).

Disease-free and overall survival was estimated by the Kaplan–Meier method. The log-rank test was used to determine survival differences in DTC-positive and DTC-negative patients. Survival was measured from the date of bone marrow sampling to the date of recurrent disease detection or death. Distribution of parameters between different groups was compared using Pearson's Chi-square exact two-sided test for categorical data and two-sample t-test for continuous variables. The data analysis was performed using SPSS version 16.0 (SPSS Inc., Chicago, IL). P values less than 0.05 were considered statistically

significant. Pathway connectivity of peptides was determined using UniProtKB/SwissProt database [13] and literature search.

Results

Patients

Table 1 describes characteristics of the 55 patients, in whom immunomagnetic selection of tumor cells in bone marrow aspirates as well as tyrosine kinase activity profiling of tumor biopsies at the time of study enrolment were performed. In 60% of patients, a median tumor cell count of 6 (range 2–150) was detected in the bone marrow samples (DTC-positive patients). No differences were found between DTC-positive and DTC-negative patients regarding gender, age, radiological TNM stage at diagnosis, serum carcinoembryonic antigen levels or hemoglobin count at the time of diagnosis, or histological ypTN stage or histomorphologic TRG score of the surgical specimens. Median follow-up was 42 months (range 7–65). Three patients (one DTC-negative and two DTC-positive individuals) were noted to have locally recurrent disease.

Table 1 Patient characteristics

	All patients ($n = 55$)	DTC-negative patients ($n = 22$)	DTC-positive patients ($n = 33$)
TNM stage at diagnosis			
T2	3 (5.5%)	2 (9.1%)	1 (3.0%)
T3	33 (60.0%)	14 (63.6%)	19 (57.6%)
T4	19 (34.5%)	6 (27.3%)	13 (39.4%)
N0	6 (10.9%)	2 (9.1%)	4 (12.1%)
N1	8 (14.5%)	3 (13.6%)	5 (15.2%)
N2	41 (74.5%)	17 (77.3%)	24 (72.3%)
M0	52 (94.5%)	21 (95.5%)	31 (93.9%)
M1	3 (5.5%)	1 (4.5%)	2 (6.1%)
TN stage after chemoradiotherapy			
ypT0	12 (21.8%)	5 (22.7%)	7 (21.2%)
ypT1	8 (14.5%)	4 (18.2%)	4 (12.1%)
ypT2	13 (23.6%)	6 (27.3%)	7 (21.2%)
ypT3	14 (25.5%)	4 (18.2%)	10 (30.3%)
ypT4	8 (14.5%)	3 (13.6%)	5 (15.2%)
ypN0	43 (78.2%)	19 (86.4%)	24 (72.7%)
ypN1	9 (16.4%)	3 (13.6%)	6 (18.2%)
ypN2	3 (5.5%)	0 (0%)	3 (9.1%)
TRG			
1–2, good responders	40 (72.7%)	16 (72.7%)	24 (72.7%)
3, intermediate responders	9 (16.4%)	5 (22.7%)	4 (12.1%)
4, poor responders	6 (10.9%)	1 (4.5%)	5 (15.2%)
CEA			
<5 μg/l	33 (60.0%)	14 (63.6%)	19 (57.6%)
≥5 μg/l	22 (40.0%)	8 (36.4%)	14 (42.4%)
Median hemoglobin count, g/dl (range)	13.9 (10.0–16.3)	14.0 (10.0–16.3)	13.9 (10.8–15.4)
Gender			
Male	31 (56.4%)	13 (59.1%)	18 (54.5%)
Female	24 (43.6%)	9 (40.9%)	15 (45.5%)
Median age, years (range)	61 (31–73)	61 (38–73)	59 (31–73)
Follow-up results[a]			
Locally recurrent disease	3 (5.5%)	1 (4.5%)	2 (6.1%)
Metastatic disease	16 (29.1%)	2 (9.1%)	14 (42.4%)
Death	8 (14.5%)	2 (9.1%)	6 (18.2%)

TNM tumor–node–metastasis, *yp* histopathologic staging following chemoradiotherapy, *TRG* histomorphologic tumor regression grade following chemoradiotherapy, *CEA* carcinoembryonic antigen

[a] Censored at a median period of 42 months (range 7–65)

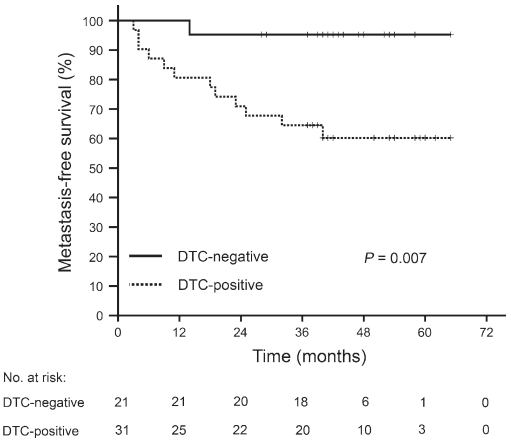

Fig. 1 Metastasis-free survival of 52 study patients with locally advanced rectal cancer as function of negative or positive status for disseminated tumor cells (DTC) to bone marrow at the time of diagnosis

Metastasis-free survival was assessed for 52 patients, as the three patients with synchronous liver metastases at the time of diagnosis were omitted from this analysis, with the DTC-positive group demonstrating significantly poorer metastasis-free survival (61%) than the DTC-negative group (95%; $P = 0.007$; Fig. 1). At the time of follow-up data censoring, eight patients were reported as deceased; the number of cases was not statistically different between the two groups of patients with negative and positive DTC status.

Tumor tyrosine kinase activities

Ex vivo sunitinib inhibition profiles were derived from 102 (of 144 on the array) peptide kinase substrates that had signal intensities above the defined threshold. In Fig. 2, patients (horizontal axis) and peptides (vertical axis) were sorted according to principal component analysis. No correlation was observed between tumor kinase activity inhibition and gender, age, diagnostic TNM stage, ypTN stage, or serum carcinoembryonic antigen levels or hemoglobin count. A borderline significant association was found between inhibition of the phosphosubstrates and tumor response to preoperative treatment in terms of TRG status ($P = 0.049$), with the poor responders exhibiting strongest inhibition (Supplementary Fig. 1).

Based on the scores of the principal component analysis, ex vivo sunitinib inhibition of tumor kinase activity in DTC-negative patients was stronger than in patients with positive DTC status ($P = 0.042$; Supplementary Fig. 2). Of the 102 peptides constituting the tyrosine kinase

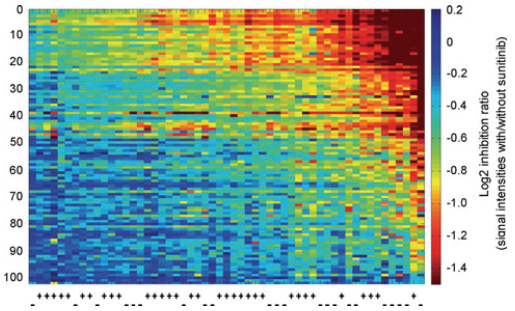

Fig. 2 Ex vivo sunitinib inhibition profiles from 102 kinase substrates. Patient tumor samples along *horizontal axis*, annotated by negative (−) or positive (+) status for disseminated tumor cells to bone marrow, and phosphosubstrates along *vertical axis*. *Red* corresponds to stronger and *blue* to weaker inhibition of substrate phosphorylation. (Color figure online)

inhibition profile, phosphorylation of 31 kinase substrates was significantly more strongly inhibited in the DTC-negative patients than in the DTC-positive individuals (Table 2). The 31 discriminating phosphopeptides represented proteins derived from signaling pathways implicated in various cellular processes, such as proliferation, angiogenesis, and invasion. Of these, 13 peptides, mainly representing PDGFR, VEGFR, and EPOR, were proteins involved in angiogenesis-related pathways. Within the entire 102-peptide panel, 23 angiogenesis-related substrates were identified (Fig. 3), and sunitinib inhibition of these phosphosubstrates was stronger in patients with negative DTC status than in DTC-positive patients ($P = 0.019$; Supplementary Fig. 3). Additionally, a significantly larger portion of angiogenesis-related substrates (13 peptides) appeared among the 31 phosphopeptides discriminating DTC status than within the remaining group of substrates (ten angiogenesis-related among a total of 71; $P = 0.002$).

Discussion

In this cohort of 55 LARC patients, tumor kinase activity signatures associated with early systemic dissemination were identified. For 31 peptides on the tyrosine kinase substrate array, ex vivo sunitinib inhibition of phosphorylation generated by tumor biopsy specimens was significantly stronger for DTC-negative patients than for patients with tumor cells identified in bone marrow, as assessed by immunomagnetic selection at the time of diagnosis. Many of the discriminating peptide substrates represented signaling pathways that are activated by tissue hypoxia, such as signaling mediated by PDGFR, VEGFR, and EPOR [1, 6]. Accordingly, tumor-generated

Table 2 Array phosphopeptides (generated by tumors from patients with and without disseminated tumor cells to bone marrow) with different levels of ex vivo sunitinib inhibition ($P < 0.05$), listed according to signaling pathway connectivity

Peptide substrate[a]	Position of peptide sequence[b]	Phosphorylation[b]	Common name[a]
Angiogenesis			
PDGFRB	1002–1014	Y1009	Beta platelet-derived growth factor receptor
PDGFRB	709–721	Y716	Beta platelet-derived growth factor receptor
PDGFRB	771–783	Y771, Y775, Y778	Beta platelet-derived growth factor receptor
PDGFRB	768–780	Y771, Y775, Y778	Beta platelet-derived growth factor receptor
PDGFRB	572–584	Y579, Y581	Beta platelet-derived growth factor receptor
FLT-1 (VEGFR1)	1326–1338	Y1327, Y1333	Vascular endothelial growth factor receptor 1
KDR (VEGFR2)	1168–1180	Y1175	Vascular endothelial growth factor receptor 2
KDR (VEGFR2)	989–1001	Y996	Vascular endothelial growth factor receptor 2
EPOR	361–373	Y368	Erythropoietin receptor
EPOR	419–431	Y426	Erythropoietin receptor
PECAM-1	706–718	Y713	Platelet endothelial cell adhesion molecule
PIK3R1	600–612	Y607	Phosphatidylinositol 3-kinase regulatory alpha subunit
EGFR	1190–1202	Y1197	Epidermal growth factor receptor
Cell adhesion, migration, and invasion			
CALM1	95–107	Y100	Calmodulin
FES	706–718	Y713	Proto-oncogene tyrosine-protein kinase Fes/Fps
FER	707–719	Y714	Proto-oncogene tyrosine-protein kinase FER
LCK	387–399	Y394	Proto-oncogene tyrosine-protein kinase LCK
PXN	111–123	Y118	Paxillin
PXN	24–36	Y31/33	Paxillin
MST1R	1353–1365	Y1353, Y1360	Macrophage-stimulating protein receptor
CTTN	476–488	Y477, Y483	Src substrate protein p85
Cell survival and proliferation			
CTNNB1	79–91	Y86	Beta-catenin
JAK1	1015–1027	Y1022, Y1023	Tyrosine-protein kinase JAK1
PDPK1	2–14	Y9	3-phosphoinositide dependent protein kinase 1
Other			
CD247	116–128	Y123	T-cell surface glycoprotein CD3 zeta chain
CDK2	8–20	Y15, Y19	Cell division protein kinase 2
EPHA7	607–619	Y608, Y614	Ephrin type-A receptor 7
EPHB1	771–783	Y778	Ephrin type-B receptor 1
FRK	380–392	Y387	Tyrosine-protein kinase FRK
KRT6E	53–65	Y62	Keratin, type II cytoskeletal 6E
RET	1022–1034	Y1029	Proto-oncogene tyrosine-protein kinase receptor ret

[a] Substrate identities and common names are retrieved from UniProtKB/SwissProt [13]

[b] For each substrate, positions of the peptide sequence and the phosphorylation sites within the protein are indicated

phosphorylation of 23 angiogenesis-related peptides was weakly inhibited in DTC-positive patients, who had significantly poorer metastasis-free survival than patients without evidence of early systemic tumor dissemination.

Various reports have demonstrated that the presence of tumor cells in bone marrow is a prognostic biomarker associated with metastatic recurrence [14], including in colorectal cancer [9]. In this study, hypothesizing that hypoxic tumor signaling mediates both radiation resistance and metastatic progression in rectal cancer, and using previously acquired data [8], we endeavored to correlate the individual patient's tumor tyrosine kinase activity to the DTC status. In two previous works applying the array technology with tyrosine kinase substrates, we were able to calculate basal kinase activity data and correlate with the biological parameters of interest [8, 15]. In the present study, however, after normalization of basal phosphosubstrate level read-outs, no difference was found among the study patients when comparing those with and without DTC (data not shown). Since a reasonable explanation

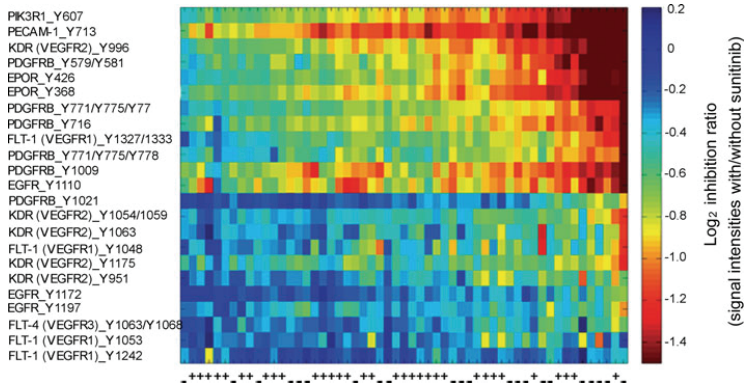

Fig. 3 Ex vivo sunitinib inhibition profiles from 23 angiogenesis-related kinase substrates. Patient tumor samples along *horizontal axis*, annotated by negative (−) or positive (+) status for disseminated tumor cells to bone marrow, and phosphosubstrates along *vertical axis*. *Red* corresponds to stronger and *blue* to weaker inhibition of substrate phosphorylation. *Left panel* Substrate identities. For each substrate, the position of phosphorylation sites within the protein is indicated. (Color figure online)

might be technical variation among 96-well array plates, the analytical strategy of including a tyrosine kinase inhibitor was attempted, to enable direct comparison of substrate phosphorylation in its presence and absence on the same array plate, and possibly diminishing plate-to-plate variation [8]. Sunitinib is thoroughly characterized in vitro and in vivo for inhibiting tyrosine kinase signaling related to tumor hypoxia [16]. Whether other tyrosine kinase inhibitors might have worked equally well for normalization of basal kinase activity data in the clinical setting of interest (primary tumor signaling and DTC status), is not known.

Using this strategy, phosphorylation of 31 kinase substrates by tumor sample lysates was found to be significantly more strongly inhibited by sunitinib in the DTC-negative patients than in patients with positive DTC status. As tumors outgrow their blood supply or are otherwise deprived of oxygen, adaptive responses to the resulting hypoxic conditions are initiated [17]. In this context, the transcription factors hypoxia-inducible factor types 1α and 2α have emerged as key regulators of a range of target genes that induce angiogenesis, including genes encoding platelet-derived growth factor, vascular endothelial growth factor, and erythropoietin [1]. In this study, components of hypoxia-driven signaling were identified in the 31-peptide panel demonstrating differential response to sunitinib inhibition in patients with negative and positive DTC status, which included receptors for these ligands; five of six PDGFR type β substrates, three of ten VEGFR substrates (one VEGFR1 and two VEGFR2), and both EPOR substrates on the array. The observed ex vivo regulation of phosphorylation of these particular substrates was not unexpected, since sunitinib has been noted to inhibit several receptor tyrosine kinases, among which members of the VEGFR and PDGFR families are predominant targets [16].

Signaling initiated by VEGFR and PDGFR is fundamental for the angiogenic response [1, 5, 6], which comprises proliferation and invasion of endothelial cells and also formation of pericyte coverage of vascular sprouts for stabilization of the newly formed vessel walls. In this process, PDGFR-dependent signaling is required for pericyte differentiation directed by the tissue stroma [18]. It is tempting to speculate that the strong ex vivo sunitinib inhibition of the PDGFR array substrate phosphorylation generated by tumor samples from DTC-negative patients in this study reflects high pericyte signaling activity of mature tumor vessel that are less permeable for metastasizing tumor cells [19].

However, it cannot be ignored that among the 23 peptides identified as angiogenesis-related in this study, ten substrates were not correlated with the patients' DTC status, including seven of ten VEGFR substrates. Regulation of tumor angiogenesis is a complex phenomenon. In colorectal cancer, this complexity has recently been highlighted by the observation that anti-angiogenic therapy (bevacizumab) that has proven efficacious in metastatic colorectal cancer, failed to meet the endpoint of prolonged disease-free survival in randomized phase III trials in the adjuvant setting [20, 21]. Interestingly, studies in experimental models have indicated that mature pericytes protect endothelial cells against VEGFR-directed therapies [22, 23]. The recent demonstration that tumor cells are able to induce pericyte maturation of the neovasculature during early formation of micrometastatic foci [24] might provide one explanation for the lack of efficacy of bevacizumab in eradicating occult metastatic disease in colorectal cancer.

The panel of 31 differentially inhibited phosphopeptides also included EPOR, the receptor for erythropoietin, which is expressed in many non-hematopoietic tissues, including endothelial cells and colorectal cancer [25], and has been associated with angiogenic responses in experimental tumor models [26]. Furthermore, this panel comprised other candidate angiogenic regulators, such as PECAM-1 (platelet endothelial cell adhesion molecule-1), PIK3R1 (the PI3 K regulatory subunit α), and EGFR [27–29], as well as the ephrin receptor types A7 and B1. Although experimental studies suggest that several types of ephrin receptors are activated in tumor vascularization [30], the function of many subgroups is incompletely understood, and in the current analyses, we therefore chose to exclude ephrin receptors from the angiogenesis-related 23-peptide panel.

The bone marrow compartment represents an important site for hematogenous micrometastatic spread in breast and prostate cancer, and clinical data has provided evidence for an association between tumor cells detected in bone marrow at the time of tumor resection and postoperative metastatic relapse in these cancer types [14]. The presence of systemically disseminated tumor cells has also been proposed as biomarker of metastatic recurrence risk in colorectal cancer [31]. In a study by Flatmark and co-workers [11], the immunomagnetic selection method was used to determine DTC status in 275 patients with primarily resectable colorectal cancer, and recent update of the clinical data shows that the presence of DTC was also associated with poor long-term outcome in this patient cohort [9]. In the present LARC-RRP study, using the same method to examine bone marrow aspirates, absence of DTC at the time of diagnosis was predictive of good short-term metastasis-free survival after radical treatment of the pelvic cavity. At the present stage of follow-up (median of 42 months), a non-significant trend towards the same association was found with overall survival. The overall frequency of DTC-positive samples was higher in the present study (60%) than in Flatmark's study (17%), which might be anticipated from the more locally advanced disease stage.

In summary, within a cohort of LARC patients, tumor phenotypes defined by tyrosine kinase activities that appeared to correlate with weak ex vivo inhibition by sunitinib, particularly related to angiogenic signaling, were associated with early systemic dissemination. These patients were also noted to have heightened risk of developing metastatic disease following the course of radical treatment of the pelvic cavity. This novel strategy for studying the functional tumor kinome in early metastatic progression of rectal cancer may be used to improve our understanding of the angiogenic response in metastasis.

Acknowledgments This work was supported by the European Union 7th Framework Programme Grant 222741 – METOXIA, the South-Eastern Norway Regional Health Authority Grant 20100014, the Norwegian Cancer Society Grant 0910106, and Astri and Birger Torsted's Legacy. M. G. Saelen is Research Fellow 2010–2012 of the South-Eastern Norway Regional Health Authority.

Ethics The LARC-RRP study protocol was approved by the Institutional Review Board and the Regional Committee for Medical and Health Research Ethics, and was in accordance with the Helsinki Declaration. The study was conducted according to national and local law and regulations. Written informed consent was required for participation.

Conflicts of interest R de Wijn is PamGene International B.V. employee. The other authors declare that they have no conflict of interest.

References

1. Bertout JA, Patel SA, Simon MC (2008) The impact of O2 availability on human cancer. Nat Rev Cancer 8:967–975. doi:10.1038/nrc2540
2. Ebbesen P, Pettersen EO, Gorr TA, Jobst G, Williams K, Kieninger J, Wenger RH, Pastorekova S, Dubois L, Lambin P, Wouters BG, Van Den Beucken T, Supuran CT, Poellinger L, Ratcliffe P, Kanopka A, Görlach A, Gasmann M, Harris AL, Maxwell P, Scozzafava A (2009) Taking advantage of tumor cell adaptations to hypoxia for developing new tumor markers and treatment strategies. J Enzyme Inhib Med Chem 24:S1–S39. doi:10.1080/14756360902784425
3. Harrington K, Jankowska P, Hingorani M (2007) Molecular biology for the radiation oncologist: the 5Rs of radiobiology meet the hallmarks of cancer. Clin Oncol (R Coll Radiol) 19:561–571. doi:10.1016/j.clon.2007.04.009
4. Bussink J, van der Kogel AJ, Kaanders JH (2008) Activation of the PI3-K/AKT pathway and implications for radioresistance mechanisms in head and neck cancer. Lancet Oncol 9:288–296. doi:10.1016/S1470-2045(08)70073-1
5. Lu X, Kang Y (2010) Hypoxia and hypoxia-inducible factors: master regulators of metastasis. Clin Cancer Res 16:5928–5935. doi:10.1158/1078-0432.CCR-10-1360
6. Harris AL (2002) Hypoxia—a key regulatory factor in tumour growth. Nat Rev Cancer 2:38–47. doi:10.1038/nrc704
7. Sauer R, Becker H, Hohenberger W, Rödel C, Wittekind C, Fietkau R, Martus P, Tschmelitsch J, Hager E, Hess CF, Karstens JH, Liersch T, Schmidberger H, Raab R (2004) Preoperative versus postoperative chemoradiotherapy for rectal cancer. N Engl J Med 351:1731–1740
8. Folkvord S, Flatmark K, Dueland S, de Wijn R, Grøholt KK, Hole KH, Nesland JM, Ruijtenbeek R, Boender PJ, Johansen M, Gierckskiy KE, Ree AH (2010) Prediction of response to preoperative chemoradiotherapy in rectal cancer by multiplex kinase activity profiling. Int J Radiat Oncol Biol Phys 78:555–562. doi:10.1016/j.ijrobp.2010.04.036

9. Flatmark K, Borgen E, Nesland JM, Rasmussen H, Johannessen HO, Bukholm I, Rosales R, Hårklau L, Jacobsen HJ, Sandstad B, Boye K, Fodstad Ø (2011) Disseminated tumour cells as a prognostic biomarker in colorectal cancer. Br J Cancer 104: 1434–1439. doi:10.1038/bjc.2011.97
10. Bouzourene H, Bosman FT, Seelentag W, Matter M, Coucke P (2002) Importance of tumor regression assessment in predicting the outcome in patients with locally advanced rectal carcinoma who are treated with preoperative radiotherapy. Cancer 94: 1121–1130. doi:10.1002/cncr.10327
11. Flatmark K, Bjornland K, Johannessen HO, Hegstad E, Rosales R, Hårklau L, Solhaug JH, Faye RS, Søreide O, Fodstad Ø (2002) Immunomagnetic detection of micrometastatic cells in bone marrow of colorectal cancer patients. Clin Cancer Res 8:444–449
12. European Bioinformatics Institute: ArrayExpress Experiments Archive. http://www.ebi.ac.uk/microarray-as/ae/. Accessed 26 February 2010
13. European Bioinformatics Institute/Swiss Institute of Bioinformatics/Protein Information Resource: Universal Protein Knowledgebase, UniProtKB/Swiss-Prot. http://au.expasy.org/sprot. Accessed 11 August 2010
14. Pantel K, Alix-Panabieres C (2010) Circulating tumour cells in cancer patients: challenges and perspectives. Trends Mol Med 16:398–406. doi:10.1016/j.molmed.2010.07.001
15. Bratland Å, Boender PJ, Høifødt HK, Østensen IHG, Ruijtenbeek R, Wang M, Berg JP, Lilleby W, Fodstad Ø, Ree AH (2009) Osteoblast-induced EGFR/ERBB2 signaling in androgen-sensitive prostate carcinoma cells characterized by multiplex kinase activity profiling. Clin Exp Metastasis 26:485–496. doi:10.1007/s10585-009-9248-9
16. Chow LQ, Eckhardt SG (2007) Sunitinib: from rational design to clinical efficacy. J Clin Oncol 25:884–896. doi:10.1200/JCO.2006.06.3602
17. Bicknell R, Harris AL (2004) Novel angiogenic signaling pathways and vascular targets. Annu Rev Pharmacol Toxicol 44: 219–238. doi:10.1146/annurev.pharmtox.44.101802.121650
18. Andrae J, Gallini R, Betsholtz C (2008) Role of platelet-derived growth factors in physiology and medicine. Genes Dev 22: 1276–1312. doi:10.1101/gad.165370
19. Ebos JM, Kerbel RS (2011) Antiangiogenic therapy: impact on invasion, disease progression, and metastasis. Nat Rev Clin Oncol 8:210–221. doi:10.1038/nrclinonc.2011.21
20. Allegra CJ, Yothers G, O'Connell MJ, Sharif S, Petrelli NJ, Colangelo LH, Atkins JN, Seay TE, Fehrenbacher L, Goldberg RM, O'Reilly S, Chu L, Azar CA, Lopa S, Wolmark N (2011) Phase III trial assessing bevacizumab in stages II and III carcinoma of the colon: results of NSABP protocol C-08. J Clin Oncol 29:1–16. doi:10.1200/JCO.2010.30.0855
21. De Gramont A, Van Cutsem E, Tabernero J, Moore MJ, Cunningham D, Rivera F, Im SA, Makrutzki M, Shang A, Hoff PM (2011) AVANT: results from a randomized, three-arm multinational phase III study to investigate Bevacizumab with either XELOX or FOLFOX4 versus FOLFOX4 alone as adjuvant treatment for colon cancer. In: Proceedings of 2011 Gastrointestinal Cancers Symposium, San Francisco, CA, January 20–22, 2011
22. Helfrich I, Scheffrahn I, Bartling S, Weis J, von Felbert V, Middleton M, Kato M, Ergün S, Schadendorf D (2010) Resistance to antiangiogenic therapy is directed by vascular phenotype, vessel stabilization, and maturation in malignant melanoma. J Exp Med 207:491–503. doi:10.1084/jem.20091846
23. Hlushchuk R, Baum O, Gruber G, Wood J, Djonov V (2007) The synergistic action of a VEGF-receptor tyrosine-kinase inhibitor and a sensitizing PDGF-receptor blocker depends upon the stage of vascular maturation. Microcirculation 14:813–825. doi:10.1080/10739680701370021
24. Zhou Z, Stewart KS, Yu L, Kleinerman ES (2011) Bone marrow cells participate in tumor vessel formation that supports the growth of Ewing's sarcoma in the lung. Angiogenesis 14: 125–133. doi:10.1007/s10456-010-9196-7
25. Chabowska AM, Sulkowska M, Chabowski A, Wincewicz A, Koda M, Sulkowski S (2008) Erythropoietin and erythropoietin receptor in colorectal cancer. Int J Surg Pathol 16:269–276. doi:10.1177/1066896908315796
26. Hardee ME, Cao Y, Fu P, Jiang X, Zhao Y, Rabbani ZN, Vujaskovic Z, Dewhirst MW, Arcasoy MO (2007) Erythropoietin blockade inhibits the induction of tumor angiogenesis and progression. PLoS One 2:e549. doi:10.1371/journal.pone.0000549
27. Cao G, Fehrenbach ML, Williams JT, Finklestein JM, Zhu JX, Delisser HM (2009) Angiogenesis in platelet endothelial cell adhesion molecule-1-null mice. Am J Pathol 175:903–915. doi:10.2353/ajpath.2009.090206
28. Wouters BG, Koritzinsky M (2008) Hypoxia signalling through mTOR and the unfolded protein response in cancer. Nat Rev Cancer 8:851–864. doi:10.1038/nrc2501
29. Winder T, Lenz HJ (2010) Vascular endothelial growth factor and epidermal growth factor signaling pathways as therapeutic targets for colorectal cancer. Gastroenterology 138:2163–2176. doi:10.1053/j.gastro.2010.02.005
30. Mosch B, Reissenweber B, Neuber C, Pietzsch J (2010) Eph receptors and ephrin ligands: important players in angiogenesis and tumor angiogenesis. J Oncol 2010:135285. doi:10.1155/2010/135285
31. Rahbari NN, Aigner M, Thorlund K, Mollberg N, Motschall E, Jensen K, Diener MK, Büchler MW, Koch M, Weitz J (2010) Meta-analysis shows that detection of circulating tumor cells indicates poor prognosis in patients with colorectal cancer. Gastroenterology 138:1714–1726. doi:10.1053/j.gastro.2010.01.008

Supplementary material

Article title: **Tumor kinase activity in locally advanced rectal cancer – angiogenic signaling and early systemic dissemination**

Journal name: **Angiogenesis**

Author names: Marie Grøn Saelen, Kjersti Flatmark, Sigurd Folkvord, Rik de Wijn, Heidi Rasmussen, Øystein Fodstad, Anne Hansen Ree

Corresponding author: A. H. Ree, Department of Oncology, Akershus University Hospital, 1478 Lørenskog, Norway. E-mail: a.h.ree@medisin.uio.no.

Table 1 The 102 array substrates included in the sunitinib inhibition profile

Peptide substrate[a]	Gene name – Common name[b]	Difference[*]	P[**]
41_Y660	EPB41 - Protein 4.1	0.103	0.239
ACHD_Y383/Y390	CHRND - Acetylcholine receptor subunit delta	0.098	0.150
AMPE_Y12	ENPEP - Glutamyl aminopeptidase	0.014	0.840
ANXA1_Y21	ANXA1 - ANXA1 protein	0.078	0.265
ANXA2_Y24	ANXA2 - Annexin A2	0.198	0.060
ART_YAAPFAKKKXC	Artificial peptide	0.197	0.062
C1R_Y204/Y210	C1R - Complement C1r subcomponent	-0.008	0.881
CALM_Y100	CALM1 - Calmodulin	0.174	0.012
CBL_Y700	CBL - CBL E3 ubiquitin protein ligase	0.064	0.321
CD3Z_Y153	CD247 - T-cell surface glycoprotein CD3 zeta chain	0.280	0.018
CDK2_Y15/Y19	CDK2 - Cell division protein kinase 2	0.282	0.025
CDK7_Y169	CDK7 - Cell division protein kinase 7	0.020	0.796
CTNB1_Y86	Beta-catenin - CTNNB1	0.193	0.011
DCX_Y112	DCX - Neuronal migration protein doublecortin	0.097	0.290
DDR1_Y513	DDR1 - Epithelial discoidin domain receptor 1	0.216	0.055
DYR1A_Y319/Y321	DYRK1A - Dual-specificity tyrosine-phosphorylation regulated kinase 1A	0.067	0.361
EGFR_Y1110	EGFR - Epidermal growth factor receptor	0.145	0.110
EGFR_Y1172	EGFR - Epidermal growth factor receptor	0.051	0.315
EGFR_Y1197	EGFR - Epidermal growth factor receptor	0.101	0.036
EPHA1_Y781	EPHA1 - Ephrin type-A receptor 1	0.222	0.051
EPHA2_Y772	EPHA2 - Ephrin type-A receptor 2	0.205	0.078

EPHA4_Y596	EPHA3 - Ephrin type-A receptor 3	0.009	0.904
EPHA7_Y608/Y614	EPHA7 - Ephrin type-A receptor 7	0.236	0.033
EPHB1_Y778	EPHB1 - Ephrin type-B receptor 1	0.250	0.015
EPHB4_Y590	EPHB4 - Ephrin type-B receptor 4	0.008	0.866
EPOR_Y368	EPOR - Erythropoietin receptor	0.259	0.008
EPOR_Y426	EPOR - Erythropoietin receptor	0.265	0.013
ERBB2_Y1248	ERBB2 - Receptor tyrosine-protein kinase erbB-2	0.131	0.053
ERBB2_Y877	ERBB2 - Receptor tyrosine-protein kinase erbB-2	0.094	0.214
ERBB4_Y1284	ERBB4 - Receptor tyrosine-protein kinase erbB-4	0.073	0.240
FAK1_Y570/Y576/Y577	PTK2 - Focal adhesion kinase 1	0.100	0.130
FAK2_Y573/Y579/Y580	PTK2B - Focal adhesion kinase 2 beta	0.115	0.151
FER_Y714	FER - Proto-oncogene tyrosine-protein kinase FER	0.215	0.031
FES_Y713	FES - Proto-oncogene tyrosine-protein kinase Fes/Fps	0.261	0.025
FGFR1_Y766	FGFR1 - Basic fibroblast growth factor receptor 1	0.054	0.324
FGFR2_Y769	FGFR2 - Fibroblast growth factor receptor 2	0.095	0.135
FGFR3_Y760	FGFR3 - Fibroblast growth factor receptor 3	0.066	0.274
FRK_Y387	FRK - Tyrosine-protein kinase FRK	0.248	0.040
INSR_Y1355	INSR - Insulin receptor	-0.059	0.298
INSR_Y992/Y999	INSR - Insulin receptor	0.050	0.304
JAK1_Y1022/Y1023	JAK1 - Tyrosine-protein kinase JAK1	0.173	0.030
JAK2_Y570	JAK2 - Tyrosine-protein kinase JAK2	0.160	0.052
K2C6E_Y62	KRT6E - Keratin, type II cytoskeletal 6E	0.173	0.042
KSYK_Y525/Y526	SYK - Tyrosine-protein kinase SYK	0.087	0.071
LAT_Y200	LAT - Linker for activation of T cells	0.075	0.143
LAT_Y255	LAT - Linker for activation of T cells	0.123	0.101
LCK_Y394	LCK - Proto-oncogene tyrosine-protein kinase LCK	0.152	0.017
MBP_Y203	MBP - Myelin basic protein	0.032	0.700
MBP_Y261/Y268	MBP - Myelin basic protein	0.020	0.705
MBP_Y268	MBP - Myelin basic protein	0.060	0.338
MET_Y1230/Y1234/Y1235	MET - Hepatocyte growth factor receptor	0.133	0.142
MK01_Y187	MAPK1 - Mitogen-activated protein kinase 1	0.051	0.460
MK07_Y220	MAPK7 - Mitogen-activated protein kinase 7	0.087	0.321
MK10_Y223	MAPK10 - Mitogen-activated protein kinase 10	0.104	0.156
MK12_Y185	MAPK12 - Mitogen-activated protein kinase 12	-0.014	0.758
NCF1_Y324	NCF1 - Neutrophil cytosol factor 1	0.008	0.921
NPT2_Y511	SLC34A1 - Renal sodium-dependent phosphate transport protein 2	0.020	0.784
NTRK1_Y496	NTRK1 - High affinity nerve growth factor receptor	-0.105	0.055
NTRK2_Y702/Y706/Y707	NTRK2 - BDNF/NT-3 growth factors receptor	0.160	0.059
ODBA_Y345	BCKDHA - 2-oxoisovalerate dehydrogenase alpha subunit, mitochondrial	0.085	0.319
P2AB_/Y307	PPP2CB - Serine/threonine protein phosphatase 2A, catalytic subunit, beta isoform	0.029	0.597
P85A_Y607	PIK3R1 - Phosphatidylinositol 3-kinase regulatory alpha subunit	0.300	0.014
PAXI_Y118	PXN - Paxillin	0.252	0.025
PAXI_Y31/Y33	PXN - Paxillin	0.260	0.020
PDGFB_Y1021	PDGFRB - Beta platelet-derived growth factor receptor	0.111	0.058
PDPK1_Y373/Y376	PDPK1 - 3-phosphoinositide dependent protein kinase 1	0.117	0.169
PDPK1_Y9	PDPK1 - 3-phosphoinositide dependent protein kinase 2	0.212	0.016

PECA1_Y713	PECAM1- Platelet endothelial cell adhesion molecule	0.272	0.021
PGFRB_Y1009	PDGFRB - Beta platelet-derived growth factor receptor	0.241	0.002
PGFRB_Y579/Y581	PDGFRB - Beta platelet-derived growth factor receptor	0.223	0.044
PGFRB_Y716	PDGFRB - Beta platelet-derived growth factor receptor	0.179	0.029
PGFRB_Y771/Y775/Y778	PDGFRB - Beta platelet-derived growth factor receptor	0.182	0.020
PGFRB_Y771/Y775/Y778	PDGFRB - Beta platelet-derived growth factor receptor	0.177	0.036
PLCG1_Y771/775	PLCG1 - 1-phosphatidylinositol-4,5-bisphosphate phosphodiesterase gamma 1	0.233	0.050
PRGR_Y795	PGR - Progesterone receptor	0.108	0.122
PRRX2_Y208/Y214	PRRX2 -Paired mesoderm homeobox protein 2	0.111	0.105
PTN11_Y546/551	PTPN11 - Tyrosine-protein phosphatase, non-receptor type 11	0.086	0.199
RAF1_Y340/Y341	RAF1 - RAF proto-oncogene serine/threonine-protein kinase	0.088	0.297
RASA1_Y460	RASA1 - Ras GTPase-activating protein 1	0.171	0.086
RB_Y805/Y813	RB1 - Retinoblastoma-associated protein	0.066	0.402
RET_Y1029	RET - Proto-oncogene tyrosine-protein kinase receptor ret	0.250	0.035
RON_Y1353	MST1R - Macrophage-stimulating protein receptor	0.133	0.177
RON_Y1353/Y1360	MST1R - Macrophage-stimulating protein receptor	0.154	0.017
SRC8_Y477	CTTN - Src substrate protein p85	0.091	0.201
SRC8_Y477/Y483	CTTN - Src substrate protein p86	0.297	0.021
SRC8_Y479/486/489	CTTN - Src substrate protein p87	0.149	0.227
TEC_Y513/519	TEC - Tyrosine-protein kinase Tec	0.132	0.078
TNNT1_Y9	TNNT1 - TNNT1 protein	0.020	0.809
TYRO3_Y681/685/686	TYRO3 - Tyrosine-protein kinase receptor TYRO3	0.049	0.430
VEGFR1_Y1048	FLT1 - Vascular endothelial growth factor receptor 1	0.106	0.164
VEGFR1_Y1053	FLT1 - Vascular endothelial growth factor receptor 1	0.055	0.445
VEGFR1_Y1242	FLT1 - Vascular endothelial growth factor receptor 1	-0.020	0.707
VEGFR1_Y1327/Y1333	FLT1 - Vascular endothelial growth factor receptor 1	0.156	0.042
VEGFR2_Y1054/Y1059	KDR - Vascular endothelial growth factor receptor 2	0.063	0.268
VEGFR2_Y1063	KDR - Vascular endothelial growth factor receptor 2	0.068	0.340
VEGFR2_Y1175	KDR - Vascular endothelial growth factor receptor 2	0.122	0.023
VEGFR2_Y951	KDR - Vascular endothelial growth factor receptor 2	0.035	0.605
VEGFR2_Y996	KDR - Vascular endothelial growth factor receptor 2	0.250	0.025
VGFR3_Y1063/Y1068	FLT4 - Vascular endothelial growth factor receptor 3	0.018	0.749
VINC_Y822	VCL - Vinculin	0.033	0.587
ZAP70_Y492/Y493	ZAP70 - Tyrosine-protein kinase ZAP-70	0.153	0.087
ZBT16_Y630	ZBTB16 - Zinc finger and BTB domain containing protein 16	0.032	0.617

[a] Substrate names from the Tyrosine Kinase PamChip96 Array (PamGene International B.V,'s-Hertogenbosch, The Netherlands). For each substrate, position of phosphorylation sites within the protein is indicated

[b] Gene names and common names, retrieved from UniProtKB/SwissProt (http://au.expasy.org/sprot)

[*] Calculated as mean $\log_2$ inhibition in patients positive for disseminated tumor cells to bone

marrow minus mean $\log_2$ inhibition in negative patients

** By two-sample *t*-test

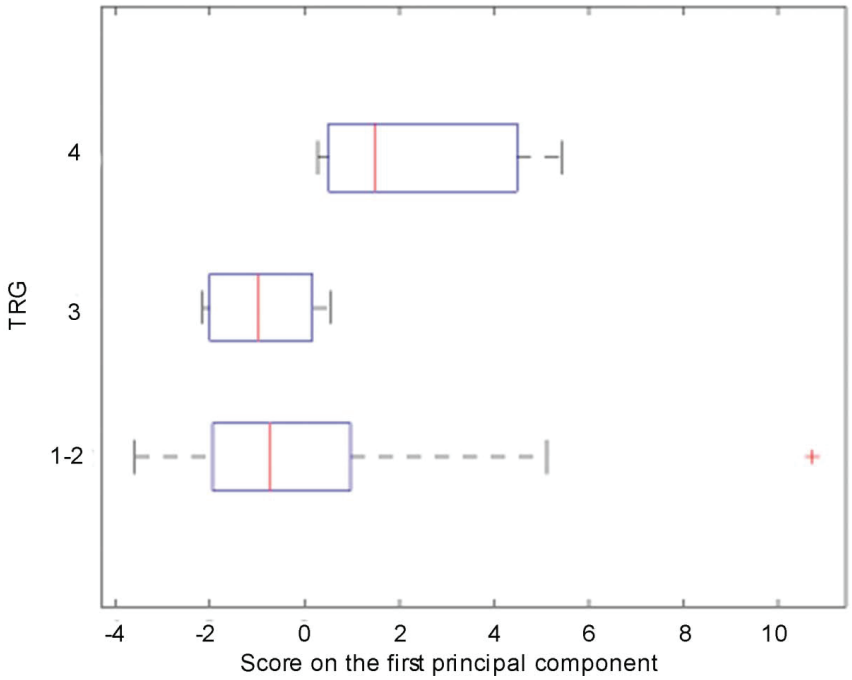

Fig. 1 Distribution of the score of the first principal component of the 102 peptide substrates among the groups of patients with different histomorphologic tumor regression grade (TRG). $P = 0.049$

TRG 1–2, good responders; TRG 3, intermediate responders; TRG 4, poor responders

Boxes, 25th, 50th, and 75th percentiles; bars, 10th and 90th percentiles; crosses, outlier values

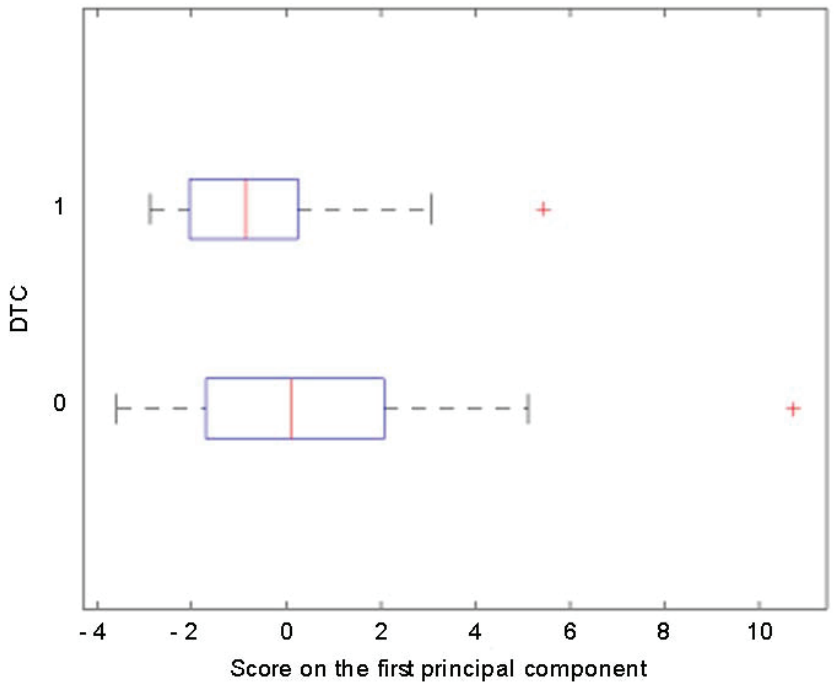

Fig. 2 Distribution of the score of the first principal component of the 102 peptide substrates among patients with positive and negative status for disseminated tumor cells (DTC) to bone marrow. $P = 0.042$

DTC 0, negative DTC status; DTC 1, positive DTC status

Boxes, 25th, 50th, and 75th percentiles; bars, 10th and 90th percentiles; crosses, outlier values

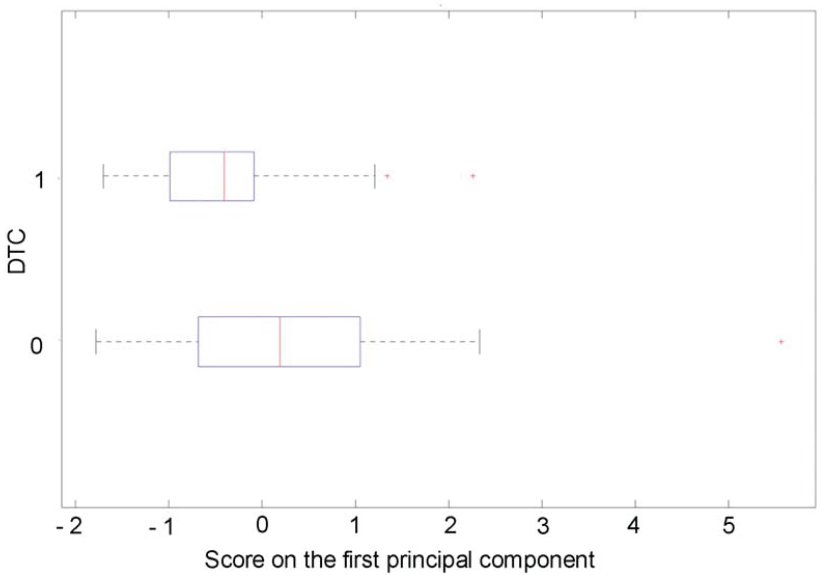

Fig. 3 Distribution of the score of the first principal component of the 23 angiogenesis-related peptide substrates among patients with positive and negative status for disseminated tumor cells (DTC) to bone marrow. $P = 0.019$

DTC 0, negative DTC status; DTC 1, positive DTC status

Boxes, 25th, 50th, and 75th percentiles; bars, 10th and 90th percentiles; crosses, outlier values

II

Saelen et al. Radiation Oncology 2012, 7:165
http://www.ro-journal.com/content/7/1/165

RADIATION ONCOLOGY

RESEARCH Open Access

Radiosensitization by the histone deacetylase inhibitor vorinostat under hypoxia and with capecitabine in experimental colorectal carcinoma

Marie Grøn Saelen[1,2], Anne Hansen Ree[2,3], Alexandr Kristian[1], Karianne Giller Fleten[1], Torbjørn Furre[4], Helga Helseth Hektoen[1,2] and Kjersti Flatmark[1*]

Abstract

Background: The histone deacetylase inhibitor vorinostat is a candidate radiosensitizer in locally advanced rectal cancer (LARC). Radiosensitivity is critically influenced by hypoxia; hence, it is important to evaluate the efficacy of potential radiosensitizers under variable tissue oxygenation. Since fluoropyrimidine-based chemoradiotherapy (CRT) is the only clinically validated regimen in LARC, efficacy in combination with this established regimen should be assessed in preclinical models before a candidate drug enters clinical trials.

Methods: Radiosensitization by vorinostat under hypoxia was studied in four colorectal carcinoma cell lines and in one colorectal carcinoma xenograft model by analysis of clonogenic survival and tumor growth delay, respectively. Radiosensitizing effects of vorinostat in combination with capecitabine were assessed by evaluation of tumor growth delay in two colorectal carcinoma xenografts models.

Results: Under hypoxia, radiosensitization by vorinostat was demonstrated *in vitro* in terms of decreased clonogenicity and *in vivo* as inhibition of tumor growth. Adding vorinostat to capecitabine-based CRT increased radiosensitivity of xenografts in terms of inhibited tumor growth.

Conclusions: Vorinostat sensitized colorectal carcinoma cells to radiation under hypoxia *in vitro* and *in vivo* and improved therapeutic efficacy in combination with capecitabine-based CRT *in vivo*. The results encourage implementation of vorinostat into CRT in LARC trials.

Keywords: Rectal cancer, Vorinostat, Fluoropyrimidine, Hypoxia, Radiation

Background

In locally advanced rectal cancer (LARC), neoadjuvant chemoradiotherapy (CRT) is given to obtain tumor downstaging to allow complete surgical removal, and single-agent fluoropyrimidine in combination with fractionated pelvic radiation remains the standard regimen [1]. Treatment responses vary considerably, and this may be particularly important in large T4 tumors that depend greatly on the effect of neoadjuvant CRT for preoperative downstaging [2]. Other potential radiosensitizing agents have been evaluated for their ability to further enhance local tumor response, but improvement has so far not been achieved, warranting the continued search for novel radiosensitizers [3-6]. Histone deacetylase (HDAC) inhibitors have emerged as a new class of drugs that has been shown to sensitize tumors to radiation in experimental models. We have previously assessed the radiosensitizing ability of the HDAC inhibitor vorinostat in experimental colorectal carcinoma models, demonstrating reduced *in vitro* clonogenicity upon radiation exposure and delayed tumor growth of xenografts exposed to fractionated radiation [7]. In a recent clinical phase I study, we reported a favorable

* Correspondence: kjersti.flatmark@rr-research.no
[1]Department of Tumor Biology, Norwegian Radium Hospital, Oslo University Hospital, P.O. Box 4953, Nydalen, 0424 Oslo, Norway
Full list of author information is available at the end of the article

toxicity profile of vorinostat in combination with pelvic palliative radiotherapy [8,9].

As recently highlighted in guidelines from the NCRI Clinical and Translational Radiotherapy Research Working Group [10], novel radiosensitizers must be adequately evaluated in relevant preclinical models in order to justify exposing patients to the risks of adding a new drug to radiotherapy or CRT. Since human solid tumors, including rectal carcinomas, often contain a substantial fraction of hypoxic cells that are intrinsically more resistant to radiotherapy, a drug's ability to radiosensitize tumor cells under hypoxia should be taken into account when investigating new CRT candidates [11]. Furthermore, since fluoropyrimidine-based CRT is the established regimen in LARC, potential interaction between a new drug and the standard treatment should be investigated to reveal possible antagonistic or synergistic effects. In the present work, radiosensitizing effects of vorinostat were assessed under hypoxic conditions in four colorectal carcinoma models *in vitro* and in one xenograft model. Moreover, radiosensitizing properties of vorinostat in combination with the fluoropyrimidine capecitabine were investigated in two colorectal carcinoma xenograft models.

Methods

Experimental treatments

Ionizing radiation (IR) was delivered to cell lines in culture at a rate of 1.0 Gy/min by Faxitron Cabinet X-ray system (model 43855 F with CP 160 Option; Faxitron Bioptics, Lincolnshire, IL). Control cells were simultaneously placed in room temperature. To tumor xenografts, IR was delivered in daily 2-Gy fractions using a 6-MV photon beam from a linear accelerator (Varian Clinac 2100 CD; Varian, San Diego, CA), at a dose rate of 2.6 Gy/min. Control mice were anaesthetized and brought to the radiation room. Vorinostat (Alexis Biochemicals, Lausen, Switzerland) and capecitabine (Roche, Basel, Switzerland) were prepared and stored as previously described [7].

In experiments involving hypoxia, the following single agent and combination treatments were given: C (control) = NO (normoxia), HO (hypoxia), IR-NO (IR under normoxia), IR-HO (IR under hypoxia), VOR-NO (vorinostat under normoxia), VOR-HO (vorinostat under hypoxia), VOR-IR-NO (vorinostat and IR under normoxia), and VOR-IR-HO (vorinostat and IR under hypoxia). For experiments involving combination of vorinostat and capecitabine, the following treatments were given: C (control), VOR (vorinostat), CAP (capecitabine), IR, VOR-IR (vorinostat and IR), CAP-IR (capecitabine and IR), and VOR-CAP-IR (vorinostat, capecitabine, and IR).

Cell lines and in vitro experiments

Human colorectal carcinoma cell lines HCT116, HT29, and SW620 (ATCC, Manassas, VA) and KM20L2 (kindly provided by Dr. M. R. Boyd, National Cancer Institute, Frederick, MD) were used. The cell lines were free from mycoplasma infection and cell line identity was validated by short tandem repeat analysis. Culturing conditions were previously described [7]. Vorinostat (1 or 2 μM) was added to the cell cultures for an incubation period of 18 h. *In vitro* hypoxia (1% O_2) was generated using an Invivo2 200 Hypoxic Workstation (Ruskinn, Bridgend, UK). Cell cultures were incubated under these conditions for 18 h before sealing the flasks using non-filter caps and transferring them to an x-ray unit. After IR exposure, culture flasks were transferred to normoxic conditions. Control cell cultures were kept under normoxic conditions at all times. Clonogenicity was performed as previously described [7] with the main modification being that cells were grown in T-25 flasks (Nunc, Roskilde, Denmark) to allow generation of hypoxia. Plating efficiencies determined from control experiments were 0.63 ± 0.07 for HCT116, 0.84 ± 0.19 for HT29, 0.61 ± 0.14 for SW620, and 0.78 ± 0.08 for KM20L2. Surviving fractions (SF) were calculated relative to the relevant control.

For analysis of HIF-1α induction, HCT116 cells were seeded in cell culture flasks and exposed to HO or NO as previously described or treated with 100 μM $CoCl_2$ for 4 h to generate a positive control for HIF-1α expression (Sigma Aldrich, St Louis, MO). Whole cells lysates were generated as previously described [12] and stored at - 80°C until analysis. Separation of 7.5 μg of protein was performed using 4-12% NuPAGE® Novex Bis-Tris Gels (Invitrogen, Carlsbad, CA) in MES buffer and transferred to Immobilon-P membranes (Millipore, Bedford, MA). Membranes were blocked for 1 h at room temperature in Tris-buffered saline with 0.1% Tween-20 (TBST) and 5% non fat dry milk and incubated over night at 4°C with mouse anti-HIF-1α antibody (# 610958; BD Transduction Laboratories, Franklin Lakes, NJ) or goat anti-actin antibody (sc-1616; Santa Cruz Biotechnology, Santa Cruz, CA). After washing, the membranes were incubated for 1 h at room temperature with appropriate horseradish peroxidase conjugated secondary antibody, and bands were visualized using Super Signal West Dura Extended Duration Substrate (Thermo Scientific, Waltham, MA).

Animal models

Locally bred female and male athymic Balb/c mice 6–8 weeks old were used. For one experiment (vorinostat, capecitabine, and IR– in vivo tumor growth, HCT116 xenografts) Balb/c nude (nu/nu) mice from Harlan Laboratories (Rossdorf, Germany) were purchased, as our

animal facility had reduced availability of inbred mice due to relocation of the department. The mice were maintained under specific pathogen-free conditions, and food and water were supplied *ad libitum*. Housing and all procedures involving animals were performed according to protocols approved by the Animal Care and Use Committee, in compliance with the National Committee for Animal Experiment's guidelines on animal welfare. Xenografts were established as previously described [7] on the thigh (hypoxia experiments) or on the rear flank (capecitabine experiments) and tumor volumes were calculated using the following formula: volume = $(\pi/6) \times a \times b^2$, in which a and b were the largest and the smallest perpendicular tumor diameters, respectively. The mice were sacrificed when tumors reached a diameter of 15 mm (thigh) or 20 mm (flank), or if the animal failed to thrive.

In vivo experiments

In vivo tumor hypoxia was achieved by placing a heavy clamp over the proximal thigh of anesthetized mice during irradiation [13]. The tumors were clamped for 3.5 min before and during IR exposure (to a total period of 5.0 min). In experiments involving hypoxia, the mice were randomized by tumor volume into groups of 5–6 animals and were treated with vorinostat concomitantly to irradiation for four consecutive days. Vorinostat (100 mg/kg) or vehicle was given daily by intraperitoneal (i.p.) injections three hours before radiation. Tumor blood supply to clamped xenografts was examined by measuring tumor radioactivity after injection of I^{125} and used as a measure of acute hypoxia. I^{125} (Hartmann Analytic, Braunschweig, Germany) in the form of an iodinated antibody and with an activity of 2.85 MBq/ml, was administered by tail vein injection (100 μL, mean activity of 10 kBq/g) to four anesthetized mice (tumor volume 91.3 ± 34.3 mm^3; mean ± standard deviation). After 5 min, the mice were sacrificed and tumors were dissected and clamped and unclamped tumors were analyzed by a gamma counter (COBRA II Auto-Gamma; Packard Canberra, Meriden, CT). The ratio of I^{125} activity (*i.e.,* activity in clamped tumor divided by activity in unclamped tumor on the same mouse) was 0.03 ± 0.01 (mean ± standard deviation), indicating a substantial reduction of blood flow to clamped tumors ($p < 0.001$).

In experiments involving capecitabine, the mice were randomized by tumor volume into treatment groups of 6–9 mice and treated with vorinostat concomitantly to irradiation for five consecutive days. Vorinostat (100 mg/kg) or vehicle was given daily by i.p. injections three hours before radiation. Capecitabine (359 mg/kg) or vehicle was given daily by oral gavage immediately after administration of vorinostat. Relative tumor volumes (RTV) were calculated relative to the tumor volume on the day of treatment initiation. For each tumor, tumor doubling time (T_{2x}) relative to the Day 1 tumor volume was determined. Tumor growth delay (TGD_{2x}) was calculated by subtracting the mean T_{2x} of the vehicle-treated tumors from the T_{2x} for each treated xenograft.

Statistical analysis

Statistical analysis was performed using SPSS 16.0 (SPSS Inc., Chicago, IL). Differences between groups were analyzed using the two-sided Student *t* test under conditions of normality and a non-parametric test (Mann–Whitney rank-sum test) under other conditions. *p* values less than 0.05 were considered statistically significant.

Results

Vorinostat, hypoxia, and IR – in vitro clonogenicity

In initial experiments on HCT116 cells, clonogenicity was not influenced by hypoxia (SF for HO cells was 0.97 ± 0.08; mean ± standard error of the mean, compared to C). Likewise, the survival of VOR-NO cells and VOR-HO cells was similar (SF were 0.35 ± 0.04 and

Table 1 *In vitro* clonogenicity - mean surviving fractions (SEM) after treatment with ionizing radiation (IR, 5 Gy), vorinostat and hypoxia

	HCT116		HT29		SW620		KM20L2	
	SF	*p*	*SF*	*p*	*SF*	*p*	*SF*	*p*
Monotherapy (relative to control)								
IR	0.029 (0.04)	<0.001	0.33 (0.02)	<0.001	0.079 (0.02)	<0.001	0.11 (0.002)	<0.001
HO	0.97 (0.08)	0.7	0.98 (0.03)	0.6	0.62 (0.28)	0.3	0.92 (0.01)	0.01
VOR	0.35 (0.04)	<0.001	0.78 (0.07)	0.05	0.84 (0.04)	0.07	0.66 (0.04)	0.04
Combination therapy								
IR-HO (relative to HO)	0.13 (0.03)	<0.001	0.51 (0.05)	0.002	0.36 (0.10)	0.02	0.20 (0.02)	<0.001
VOR-HO (relative to HO)	0.41 (0.05)	<0.001	0.88 (0.09)	0.3	0.68 (0.14)	0.1	0.68 (0.03)	0.08
VOR-IR (relative to VOR)	0.011 (0.004)	<0.001	0.18 (0.03)	<0.001	0.026 (0.02)	<0.001	0.066 (0.02)	<0.001
VOR-IR-HO (relative to VOR-HO)	0.020 (0.005)	<0.001	0.24 (0.02)	<0.001	0.052 (0.03)	<0.001	0.040 (0.006)	<0.001

SF = surviving fractions; HO = hypoxia; VOR = vorinostat; IR-HO = IR under hypoxia;
VOR-HO = vorinostat under hypoxia; VOR-IR = vorinostat and IR; VOR-IR-HO = vorinostat and IR under hypoxia.

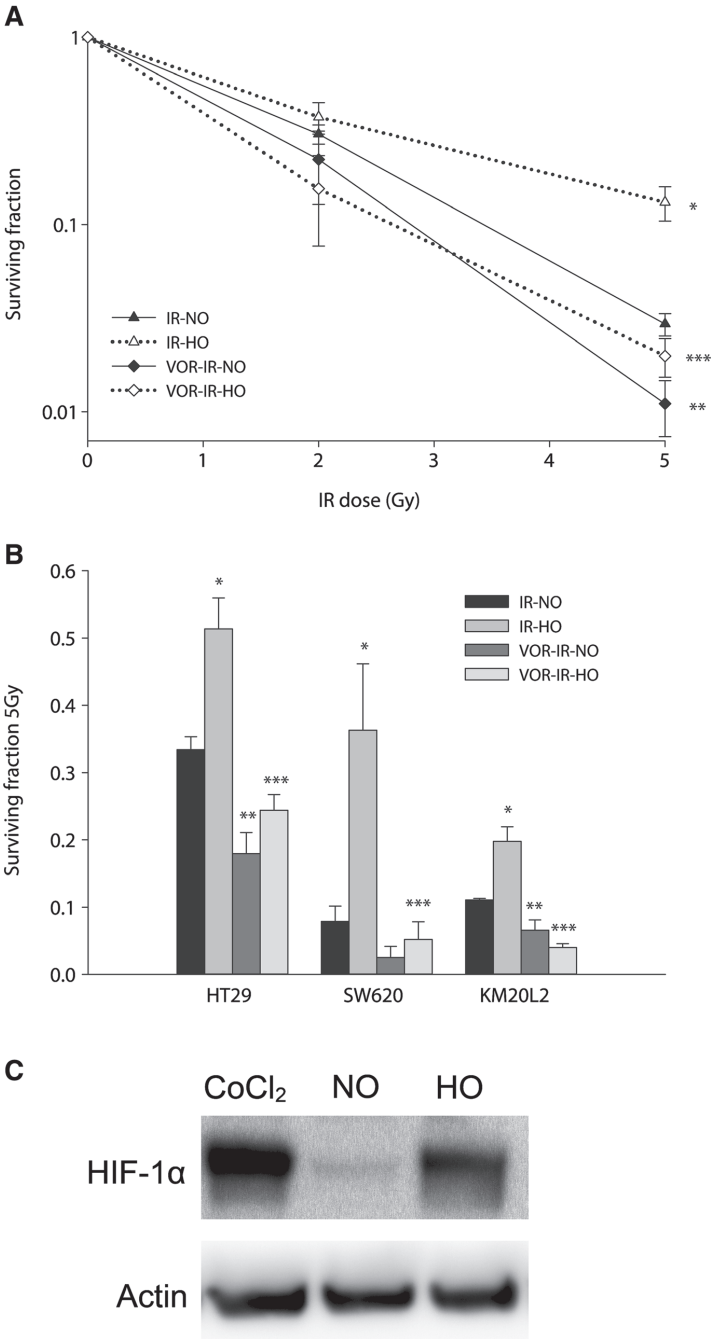

Figure 1 (See legend on next page.)

(See figure on previous page.)
Figure 1 Vorinostat, hypoxia, and ionizing radiation (IR) – *in vitro* clonogenicity and HIF-1α expression. (**A**) HCT116, (**B**) HT29, KM20L2 and SW620 cells were treated with IR under normoxia (IR-NO), IR under hypoxia (IR-HO), vorinostat and IR under normoxia (VOR-IR-NO) or vorinostat and IR under hypoxia (VOR-IR-HO). Surviving fractions are shown as mean, and bars represent SEM. * Indicates significant difference between IR-NO and IR-HO. ** Indicates significant difference between VOR-IR-NO and IR-NO. *** Indicates significant difference between VOR-IR-HO and IR-HO. (**C**) Western immunoblot analysis of HIF-1α expression in HCT116 cells exposed to normoxia (NO) or hypoxia (HO). Cells were treated with $CoCl_2$ as a positive control and actin was used as protein loading control.

0.41 ± 0.05, respectively). The presence of hypoxia was verified by western immunoblot analysis, showing induction of HIF-1α after exposure to *in vitro* hypoxia. In contrast, IR-HO cells were less sensitive to a radiation dose of 5 Gy than IR-NO cells (SF were 0.13 ± 0.03 and 0.029 ± 0.004, respectively; p = 0.002). Notably, vorinostat enhanced the 5-Gy radiation effects of both hypoxic and normoxic cells (SF for VOR-IR-HO cells was 0.020 ± 0.005; p = 0.003; SF for VOR-IR-NO cells was 0.011 ± 0.004; p = 0.006). The experiments were also performed applying 2-Gy radiation doses, and although the effects of hypoxia and vorinostat treatment exhibited the same trends as for the 5-Gy dose, the differences were not statistically significant (Table 1, Figure 1).

In subsequent experiments, a radiation dose of 5 Gy was used. Hypoxia alone did not substantially influence clonogenicity in any of the models. The cytotoxic effect of vorinostat alone varied among the cell lines (SF 0.66-0.88), but was not significantly different for VOR-HO cells compared to VOR-NO cells. Clonogenicity of IR-HO cells was higher than for the respective IR-NO counterparts (for HT29, SF 0.51 ± 0.05 *versus* 0.33 ± 0.02; p = 0.02; for SW620, SF 0.36 ± 0.10 *versus* 0.079 ± 0.02; p = 0.049; for KM20L2, SF 0.20 ± 0.02 *versus* 0.11 ± 0.002; p = 0.02). Again, in VOR-IR-HO cells compared to IR-HO cells, vorinostat caused radiosensitization (for HT29, SF 0.24 ± 0.02 *versus* 0.51 ± 0.05; p = 0.005; for SW620, SF 0.052 ± 0.03 *versus* 0.36 ± 0.10; p = 0.04; for KM20L2, SF 0.040 ± 0.006 *versus* 0.20 ± 0.02; p = 0.002). Under normoxia (VOR-IR-NO), HT29 and KM20L2 were radiosensitized by vorinostat, while the effect was not statistically significant for SW620.

Vorinostat, hypoxia, and IR – in vivo tumor growth

In a pilot experiment, radiation exposure inhibited growth of normoxic SW620 xenografts but not of hypoxic tumors. 5–6 mice were randomized to each treatment group (control, C; hypoxia, HO: ionizing radiation under normoxia, IR-NO; ionizing radiation under hypoxia, IR-HO). Experimental treatments were started 17 days after establishment of SW620 xenografts at tumor volumes of 192.7 ± 112 mm^3 (mean ± standard deviation). Of 23 mice included in the experiment, one IR-NO animal was excluded from analysis as it was sacrificed early (day 4) due to anesthesia-related complications. Untreated xenografts had a T_{2x} of 5.33 ± 2.6 days. The TGD_{2x} of HO tumors was unchanged compared to C (TGD_{2x} 0.27 ± 1.9 days; p = 0.74). The IR exposure inhibited growth of normoxic xenografts as IR-NO tumors were growth inhibited (TGD2x 5.47 ± 1.9 days; p < 0.001), while the growth rate of IR-HO tumors was not significantly different from C (TGD_{2x} 2.33 ± 3.0; p = 0.09) (Table 2, Figure 2).

A subsequent experiment was undertaken to specifically investigate the effects of vorinostat under hypoxia, involving four treatment groups: C, IR-NO, IR-HO, or VOR-IR-HO. Experimental treatments were started 13 days after establishment of SW620 xenografts at tumor volumes of 51.1 ± 35 mm^3 (mean ± standard deviation). Of 23 mice included in the experiment, four mice were excluded from analysis as they were sacrificed early (days 1–2) for the following reasons: anesthesia-related complications ($n = 3$; two VOR-IR-HO and one IR-NO) and failure to thrive ($n = 1$; VOR-IR-HO), leaving three animals for analysis in the VOR-IR-HO group. For untreated xenografts T_{2x} was 9.60 ± 7.7 days. Similarly to the pilot findings, radiation exposure inhibited growth under normoxia but not under hypoxia (for IR-NO TGD_{2x} was 7.83 ± 5.9 days; p = 0.016 compared to C); for IR-HO tumors TGD_{2x} was −1.43 ± 3.6; p = 0.40 compared to C)). Importantly, vorinostat enhanced radiosensitivity under hypoxia as growth of the VOR-IR-HO xenografts was inhibited compared to IR-HO xenografts (TGD_{2x} was 6.07 ± 2.5 versus −1.43 ± 3.6; p = 0.015).

Table 2 Vorinostat, hypoxia, and ionizing radiation - tumor growth delay

Treatment groups	TGD_{2x} (days)	Compared to (group)	p-value
SW620 Pilot			
HO	0.27 ± 1.9	C	0.7
IR-NO	5.47 ± 1.9	C	<0.001
IR-HO	2.33 ± 3.0	C	0.09
SW620 Main experiment			
IR-NO	7.83 ± 5.9	C	0.02
IR-HO	−1.43 ± 3.6	C	0.4
VOR-IR-HO	6.07 ± 2.5	IR-HO	0.02

TGD_{2x} = tumor growth delay at 2-fold increase of relative tumor volume;
C = control; HO = hypoxia; IR-NO = IR under normoxia; IR-HO = IR under hypoxia; VOR-IR-HO = vorinostat and IR under hypoxia.

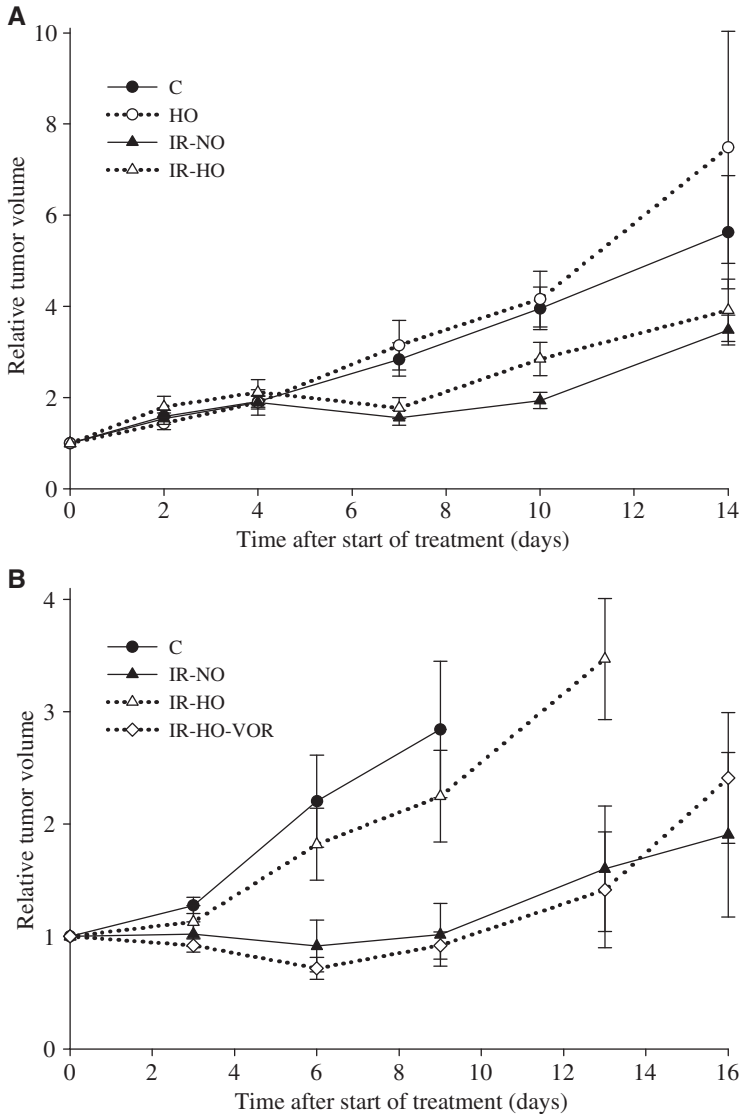

Figure 2 Vorinostat, hypoxia, and ionizing radiation (IR) – *in vivo* tumor growth. (**A**) Mice bearing SW620 xenografts were treated with vehicle (control, C), hypoxia (HO), IR under normoxia (IR-NO) and IR under hypoxia (IR-HO). (**B**) Mice bearing SW620 xenografts were treated with vehicle (control, C), IR under normoxia (IR-NO), IR under hypoxia (IR-HO), or vorinostat and IR under hypoxia (VOR-IR-HO). Relative tumor volumes (mean ± SEM) presented as function of time after start of treatments.

Vorinostat, capecitabine, and IR – in vivo tumor growth

To assess the effect of adding vorinostat to fluoropyrimidine-based CRT, two xenograft models, SW620 and HCT116, were used. The experimental setup included seven groups of mice receiving C, VOR, CAP, IR, VOR-IR, CAP-IR, or the full combination of VOR-CAP-IR. Experimental treatments were initiated 10 days (SW620) or 14 days (HCT116) after establishment of xenografts at tumor volumes of 100.8 ± 86 mm^3 and 77.0 ± 57 mm^3 (mean ± standard deviation), respectively.

Of 53 mice included in each experiment, five mice were sacrificed early (days 1–4) because of anesthesia-related complications ($n = 3$; SW620) or failure to thrive ($n = 2$; HCT116), and were excluded from analysis. Furthermore, due to ulceration of the tumors, three xenografts did not reach T_{2x} and one vehicle xenograft grew abnormally (HCT116) and were removed from the study (Table 3, Figure 3).

For untreated xenografts T_{2x} was 4.13 ± 0.9 days for HCT116 and 4.30 ± 1.3 days for SW620. While IR inhibited growth of HCT116 (TGD_{2x} was 5.68 ± 8.5 days; p = 0.025 compared to C), growth inhibition of SW620 was not statistically significant (TGD_{2x} was 1.40 ± 2.2 days, p = 0.061 compared to C). Single-agent therapy with CAP delayed tumor growth compared to C for HCT116 (TGD_{2x} was 2.68 ± 2.4 days, p = 0.001), but not for SW620 (TGD_{2x} was 0.14 ± 1.8 days, p = 0.8). Single-agent therapy with VOR did not alter tumor growth (for HCT116, TGD_{2x} was 0.24 ± 1.9 days, p = 0.7 compared to C, respectively; for SW620, TGD_{2x} was 0.88 ± 1.9 days, p = 0.2 compared to C. Tumor growth delay of VOR-IR xenografts was observed for HCT-116 (TGD_{2x} of VOR-IR was 20.06 ± 15.1 days compared to TGD_{2x} of IR which was 5.68 ± 8.5 days, p = 0.01), while for SW620 tumor growth was not significantly delayed, although a similar trend was observed (TGD_{2x} of VOR-IR was 2.78 ± 2.6 days compared to TGD_{2x} of IR which was 1.40 ± 2.2 days, p = 0.2). Only minor, non-significant changes of radiosensitivity was obtained by adding capecitabine to IR (CAP-IR) (for HCT116, TGD_{2x} of CAP-IR was 5.46 ± 6.1 days compared to TGD_{2x} of IR of 5.68 ± 8.5 days, p = 0.9; for SW620, TGD_{2x} of CAP-IR was 2.53 ± 3.1 days compared to TGD_{2x} of IR of 1.40 ± 2.2 days, p = 0.2). Notably, vorinostat in combination with capecitabine improved radiation efficacy in both models as TGD_{2x} of VOR-CAP-IR xenografts were significantly increased compared to TGD_{2x} of CAP-IR xenografts (for HCT116, TGD_{2x} of VOR-CAP-IR was 18.99 ± 7.3 days compared to TGD_{2x} of 5.46 ± 6.1 days for CAP-IR, p <0.001; for SW620, TGD_{2x} of VOR-CAP-IR was 5.78 ± 3.9 days compared to TGD_{2x} of 2.53 ± 3.1 days for CAP-IR, p = 0.03).

Table 3 Vorinostat, capecitabine, and ionizing radiation - tumor growth delay

Treatment groups	TGD_{2x} (days)	Compared to (group)	p-value
HCT116			
IR	5.68 ± 8.5	C	0.03
CAP	2.68 ± 2.4	C	0.001
VOR	0.24 ±1.9	C	0.7
CAP-IR	5.46 ± 6.1	IR	0.9
VOR-IR	20.06 ± 15.1	IR	0.01
VOR-CAP-IR	18.99 ± 7.3	CAP-IR	<0.001
SW620			
IR	1.40 ± 2.2	C	0.06
CAP	0.14 ± 1.8	C	0.8
VOR	0.88 ± 1.9	C	0.2
CAP-IR	2.53 ± 3.1	IR	0.3
VOR-IR	2.8 ± 2.6	IR	0.2
VOR-CAP-IR	5.78 ± 3.9	CAP-IR	0.03

TGD_{2x} = tumor growth delay at 2-fold increase of relative tumor volume;
IR = ionizing radiation;
C = control; CAP = capecitabine; VOR = vorinostat; CAP-IR = capecitabine and IR; VOR-IR = vorinostat and IR; VOR-CAP-IR = vorinostat, capecitabine and IR.

Discussion

Exposure to hypoxic conditions during radiation made the cells in our *in vitro* models more radioresistent, in line with theories of classical radiobiology stating that hypoxia increases the resistance of cancer cells to radiation treatment. *In vivo*, a similar effect of short-term acute hypoxia was observed, as clamped tumors were more resistant to treatment with fractionated radiation than unclamped tumors. Vorinostat enhanced radiosensitivity of cells exposed to hypoxia during radiation in all colorectal carcinoma cell lines *in vitro*, almost counterbalancing hypoxia-induced radioresistance. In line with these results, vorinostat demonstrated radiosensitizing effects in xenografts exposed to acute hypoxia, as tumor volumes of vorinostat-treated mice irradiated under hypoxia were similar to the tumor volumes of mice irradiated under normoxia, reversing the radioresistent hypoxic phenotype.

Response to cancer treatment is strongly influenced by the tumor microenvironment, and specifically, the most important determinant of radiotherapy response is tissue oxygenation. Colorectal tumors are often large, and analysis of hypoxia biomarkers in patient samples has revealed that most tumors exhibit a molecular phenotype consistent with varying hypoxia [11]. Moreover, in a recent report, expression of the hypoxia-associated protein carbonic anhydrase IX was negatively associated with CRT response in patients with rectal cancer [14]. Hence, a likely explanation for variable CRT response in rectal cancer is variable tumor oxygenation, and in this perspective, the ability to overcome hypoxia-related radioresistance would be an advantageous property of a radiosensitizing drug. In other tumor forms, a small number of drugs (such as gemcitabine, irinotecan, and the poly(ADP-ribose) polymerase-inhibitor velaparib) [15-17] have been evaluated in combination with radiotherapy under hypoxic conditions. Considering the importance of tissue oxygenation for radiotherapy efficacy, the scarcity of experimental data exploring radiosensitizers under hypoxia in LARC is remarkable. One reason for this

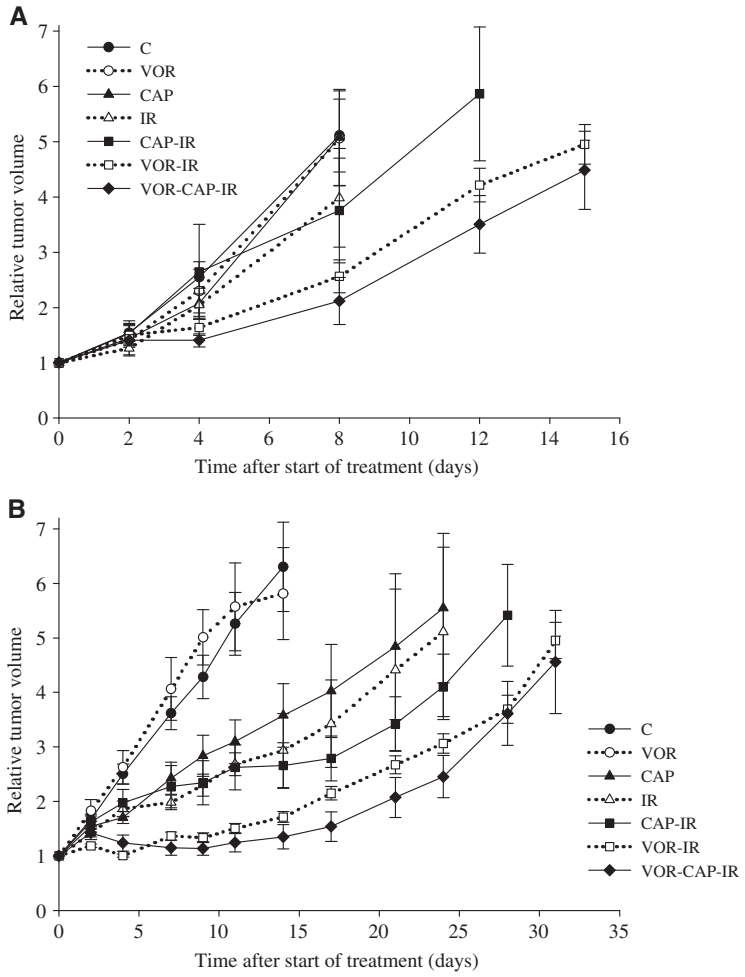

Figure 3 Vorinostat, capecitabine, and ionizing radiation (IR) – *in vivo* tumor growth. Mice bearing (**A**) SW620 and (**B**) HCT116 xenografts were treated with vehicle (control, C), vorinostat (VOR), capecitabine (CAP), IR, capecitabine and IR (CAP-IR), vorinostat and IR (VOR-IR), or vorinostat, capecitabine and IR (VOR-CAP-IR). Relative tumor volumes (mean ± SEM) presented as function of time after start of treatments.

could be related to difficulties in selecting appropriate models for mimicking clinical hypoxia when evaluating radiosensitizing drugs. This challenge was also apparent in our experiments, as the impact of hypoxia on radioresistance was less pronounced in the pilot than in the main experiment (Figure 2). This illustrates biological variation which may be partially explained by the introduction of a tighter set of hypoxia clamps in the second experimental series than in the pilot. There is also some controversy regarding how to conduct *in vivo* experiments, particularly when fractionating the radiation. Although the clamping technique has been shown to be relevant for this purpose [18], it has been questioned whether this strategy truly reflects radiosensitivity under hypoxia [19]. In this context, our approach of administering vorinostat prior to short-term hypoxia and irradiation is interesting, as our experiments represent an important attempt to evaluate a novel radiosensitizer under tumor hypoxia. However, such experiments should be repeated in larger series of animals, and with the paucity of data describing the use of conventional radiosensitizing agents in LARC

under hypoxia, the therapeutic implication of vorinostat in this clinical setting is still elusive.

In LARC, fluoropyrimidine-based neoadjuvant CRT is the established treatment regimen and any novel radiosensitizing agent must be evaluated in this context. In the present study, *in vivo* addition of vorinostat to capecitabine and fractionated radiation enhanced treatment efficacy in terms of inhibited tumor growth in two colorectal xenograft models. Vorinostat has recently been shown to synergize with fluoropyrimidine-based chemotherapy in preclinical colorectal carcinoma models [20,21], but radiosensitizing properties of the combination has to our knowledge not been evaluated. Applying radiation in combination with vorinostat or capecitabine alone, we observed trends towards enhanced radiosensitivity, although the reduction of tumor volume was not statistically significant. In our previous experiments, both these drugs were potent radiosensitizers in experimental colorectal carcinoma models [7,22]. The variable effects on radiosensitivity could be explained by the limited total treatment doses possible to administer in the experimental setting, in addition to variation associated with the biological complexity of animal models. Similar limitations were also present in the combination group and in this context, the enhanced radiosensitivity observed when combining vorinostat and capecitabine is noteworthy, and adds to the preclinical evidence supporting vorinostat as radiosensitizer in LARC [7,23].

Conclusion

Although preclinical evidence [7,23] and clinical safety data [8,9] both support the use of vorinostat as radiosensitizer in LARC, more extensive preclinical examination was necessary prior to recommending vorinostat as an additional component of CRT in LARC trials. Hence, we expanded our *in vitro* and *in vivo* models by studying radiosensitizing effects of vorinostat under hypoxic conditions and in combination with capecitabine. Importantly, the results from the present study indicate that vorinostat is a radiosensitizer under hypoxic conditions and also interacts favorably with capecitabine in experimental models of colorectal carcinoma. Recognizing the important role of hypoxia in LARC, particularly in large T4 tumors, as well as the requirement that novel drugs should be compatible with fluoropyrimidine-based standard CRT, our results encourage the implementation of vorinostat in next-generation clinical CRT trials in LARC.

Abbreviations

LARC: Locally advanced rectal cancer; CRT: Chemoradiotherapy; HDAC: Histone deacetylase; IR: Ionizing radiation; C: Control; HO: Hypoxia; IR-NO: IR under normoxia; IR-HO: IR under hypoxia; VOR: Vorinostat; VOR-IR: Vorinostat and IR; VOR-NO: Vorinostat under normoxia; VOR-HO: Vorinostat under hypoxia; VOR-IR-NO: Vorinostat and IR under normoxia; VOR-IR-HO: Vorinostat and IR under hypoxia; CAP: Capecitabine; CAP-IR: Capecitabine and IR; VOR-CAP-IR: Vorinostat, capecitabine, and IR; SF: Surviving fractions; i.p: Intraperitoneal; T_{2x}: Tumor doubling time; TGD: Tumor growth delay.

Competing interests

The authors declare that they have no competing interests.

Authors' contributions

MGS participated in study design, carried out the *in vitro* and *in vivo* radiation experiments, and drafted the manuscript. AHR and KF participated in study design, data interpretation and in writing the manuscript. TF helped with technical assistance on the *in vivo* radiation. AK and KGF assisted with the *in vivo* radiation experiments. HHH carried out the western blot analysis. All authors read and approved the final manuscript.

Acknowledgements

The authors thank Ala Yaromina and Mechthild Krause at the University of Dresden for advice on how to establish the clamping technique. We thank Randi Syljuåsen and Grete Hasvold, Department of Radiation Biology, The Norwegian Radium Hospital, for valuable discussions. Supported by the South-Eastern Norway Regional Health Authority (Grant #2010014), Norwegian Cancer Society and the European Union 7th Framework Programme (Grant #222741-METOXIA).

Author details

[1]Department of Tumor Biology, Norwegian Radium Hospital, Oslo University Hospital, P.O. Box 4953, Nydalen, 0424 Oslo, Norway. [2]Institute of Clinical Medicine, University of Oslo, Oslo, Norway. [3]Department of Oncology, Akershus University Hospital, Lørenskog, Norway. [4]Department of Medical Physics, Norwegian Radium Hospital, Oslo University Hospital, Oslo, Norway.

Received: 19 April 2012 Accepted: 21 September 2012
Published: 27 September 2012

References

1. Weiser MR: **Rectal cancer trials: no movement.** *J Clin Oncol* 2011, **29:**2746–2748.
2. Larsen SG, Wiig JN, Emblemsvaag HL, Groholt KK, Hole KH, Bentsen A, Dueland S, Vetrhus T, Giercksky KE: **Extended total mesorectal excision in locally advanced rectal cancer (T4a) and the clinical role of MRI-evaluated neo-adjuvant downstaging.** *Colorectal Dis* 2009, **11:**759–767.
3. Weiss C, Arnold D, Dellas K, Liersch T, Hipp M, Fietkau R, Sauer R, Hinke A, Rodel C: **Preoperative radiotherapy of advanced rectal cancer with capecitabine and oxaliplatin with or without cetuximab: a pooled analysis of three prospective phase I-II trials.** *Int J Radiat Oncol Biol Phys* 2010, **78:**472–478.
4. Aschele C, Cionini L, Lonardi S, Pinto C, Cordio S, Rosati G, Artale S, Tagliagambe A, Ambrosini G, Rosetti P, *et al*: **Primary tumor response to preoperative chemoradiation with or without oxaliplatin in locally advanced rectal cancer: pathologic results of the STAR-01 randomized phase III trial.** *J Clin Oncol* 2011, **29:**2773–2780.
5. Gerard JP, Azria D, Gourgou-Bourgade S, Martel-Laffay I, Hennequin C, Etienne PL, Vendrely V, Francois E, de La Roche G, Bouche O, *et al*: **Comparison of two neoadjuvant chemoradiotherapy regimens for locally advanced rectal cancer: results of the phase III trial ACCORD 12/0405-Prodige 2.** *J Clin Oncol* 2010, **28:**1638–1644.
6. Marquardt F, Rodel F, Capalbo G, Weiss C, Rodel C: **Molecular targeted treatment and radiation therapy for rectal cancer.** *Strahlenther Onkol* 2009, **185:**371–378.
7. Folkvord S, Ree AH, Furre T, Halvorsen T, Flatmark K: **Radiosensitization by SAHA in experimental colorectal carcinoma models-in vivo effects and relevance of histone acetylation status.** *Int J Radiat Oncol Biol Phys* 2009, **74:**546–552.
8. Ree AH, Dueland S, Folkvord S, Hole KH, Seierstad T, Johansen M, Abrahamsen TW, Flatmark K: **Vorinostat, a histone deacetylase inhibitor, combined with pelvic palliative radiotherapy for gastrointestinal carcinoma: the Pelvic Radiation and Vorinostat (PRAVO) phase 1 study.** *Lancet Oncol* 2010, **11:**459–464.
9. Bratland A, Dueland S, Hollywood D, Flatmark K, Ree AH: **Gastrointestinal toxicity of vorinostat: reanalysis of phase 1 study results with emphasis on dose-volume effects of pelvic radiotherapy.** *Radiat Oncol* 2011, **6:**33.

10. Harrington KJ, Billingham LJ, Brunner TB, Burnet NG, Chan CS, Hoskin P, Mackay RI, Maughan TS, Macdougall J, McKenna WG, *et al*: **Guidelines for preclinical and early phase clinical assessment of novel radiosensitisers.** *Br J Cancer* 2011, **105:**628–639.
11. Goethals L, Debucquoy A, Perneel C, Geboes K, Ectors N, De Schutter H, Penninckx F, McBride WH, Begg AC, Haustermans KM: **Hypoxia in human colorectal adenocarcinoma: comparison between extrinsic and potential intrinsic hypoxia markers.** *Int J Radiat Oncol Biol Phys* 2006, **65:**246–254.
12. Folkvord S, Flatmark K, Dueland S, de Wijn R, Groholt KK, Hole KH, Nesland JM, Ruijtenbeek R, Boender PJ, Johansen M, *et al*: **Prediction of response to preoperative chemoradiotherapy in rectal cancer by multiplex kinase activity profiling.** *Int J Radiat Oncol Biol Phys* 2010, **78:**555–562.
13. Yaromina A, Krause M, Thames H, Rosner A, Krause M, Hessel F, Grenman R, Zips D, Baumann M: **Pre-treatment number of clonogenic cells and their radiosensitivity are major determinants of local tumour control after fractionated irradiation.** *Radiother Oncol* 2007, **83:**304–310.
14. Guedj N, Bretagnol F, Rautou PE, Deschamps L, Cazals-Hatem D, Bedossa P, Panis Y, Couvelard A: **Predictors of tumor response after preoperative chemoradiotherapy for rectal adenocarcinomas.** *Hum Pathol* 2011, **42:**1702–1709.
15. Wouters A, Pauwels B, Lambrechts HA, Pattyn GG, Ides J, Baay M, Meijnders P, Peeters M, Vermorken JB, Lardon F: **Retention of the in vitro radiosensitizing potential of gemcitabine under anoxic conditions, in p53 wild-type and p53-deficient non-small-cell lung carcinoma cells.** *Int J Radiat Oncol Biol Phys* 2011, **80:**558–566.
16. Van Rensburg CE, Slabbert JP, Bohm L: **Influence of irinotecan and SN-38 on the irradiation response of WHO3 human oesophageal tumour cells under hypoxic conditions.** *Anticancer Res* 2006, **26:**389–393.
17. Liu SK, Coackley C, Krause M, Jalali F, Chan N, Bristow RG: **A novel poly (ADP-ribose) polymerase inhibitor, ABT-888, radiosensitizes malignant human cell lines under hypoxia.** *Radiother Oncol* 2008, **88:**258–268.
18. Hagtvet E, Roe K, Olsen DR: **Liposomal doxorubicin improves radiotherapy response in hypoxic prostate cancer xenografts.** *Radiat Oncol* 2011, **6:**135.
19. Beck-Bornholdt HP: **Should tumors be clamped in radiobiological fractionation experiments?** *Int J Radiat Oncol Biol Phys* 1991, **21:**675–682.
20. Di Gennaro E, Piro G, Chianese MI, Franco R, Di Cintio A, Moccia T, Luciano A, de Ruggiero I, Bruzzese F, Avallone A, *et al*: **Vorinostat synergises with capecitabine through upregulation of thymidine phosphorylase.** *Br J Cancer* 2010, **103:**1680–1691.
21. Fazzone W, Wilson PM, Labonte MJ, Lenz HJ, Ladner RD: **Histone deacetylase inhibitors suppress thymidylate synthase gene expression and synergize with the fluoropyrimidines in colon cancer cells.** *Int J Cancer* 2009, **125:**463–473.
22. Folkvord S, Flatmark K, Seierstad T, Roe K, Rasmussen H, Ree AH: **Inhibitory effects of oxaliplatin in experimental radiation treatment of colorectal carcinoma: does oxaliplatin improve 5-fluorouracil-dependent radiosensitivity?** *Radiother Oncol* 2008, **86:**428–434.
23. Flatmark K, Nome RV, Folkvord S, Bratland A, Rasmussen H, Ellefsen MS, Fodstad O, Ree AH: **Radiosensitization of colorectal carcinoma cell lines by histone deacetylase inhibition.** *Radiat Oncol* 2006, **1:**25.

doi:10.1186/1748-717X-7-165
Cite this article as: Saelen *et al.*: Radiosensitization by the histone deacetylase inhibitor vorinostat under hypoxia and with capecitabine in experimental colorectal carcinoma. *Radiation Oncology* 2012 **7**:165.

III

Biomarkers of Histone Deacetylase Inhibitor Activity in a Phase 1 Combined-modality Study with Radiotherapy

Anne Hansen Ree[1,2], Marie Grøn Saelen[3,2], Erta Kalanxhi[1], Ingrid H. G. Østensen[4], Kristina Schee[3], Kathrine Røe[1], Torveig Weum Abrahamsen[3], Svein Dueland[5] and Kjersti Flatmark[3,6]

1 Department of Oncology, Akershus University Hospital, Lørenskog, Norway, **2** Institute of Clinical Medicine, University of Oslo, Oslo, Norway, **3** Department of Tumor Biology, Oslo University Hospital—Norwegian Radium Hospital, Oslo, Norway, **4** Department of Genes and Environment, Norwegian Institute of Public Health, Oslo, Norway, **5** Department of Oncology, Oslo University Hospital—Norwegian Radium Hospital, Oslo, Norway, **6** Department of Gastroenterological Surgery, Oslo University Hospital—Norwegian Radium Hospital, Oslo, Norway.

Abstract

Background: Following the demonstration that histone deacetylase inhibitors enhanced experimental radiation-induced clonogenic suppression, the Pelvic Radiation and Vorinostat (PRAVO) phase 1 study, combining fractionated radiotherapy with daily vorinostat for pelvic carcinoma, was designed to evaluate both clinical and novel biomarker endpoints, the latter relating to pharmacodynamic indicators of vorinostat action in clinical radiotherapy.

Patients and Methods: Potential biomarkers of vorinostat radiosensitizing action, not simultaneously manifesting molecular perturbations elicited by the radiation itself, were explored by gene expression array analysis of study patients' peripheral blood mononuclear cells (PBMC), sampled at baseline (T0) and on-treatment two and 24 hours (T2 and T24) after the patients had received vorinostat.

Results: This strategy revealed 1,600 array probes that were common for the comparisons T2 *versus* T0 and T24 *versus* T2 across all of the patients, and furthermore, that no significantly differential expression was observed between the T0 and T24 groups. Functional annotation analysis of the array data showed that a significant number of identified genes were implicated in gene regulation, the cell cycle, and chromatin biology. Gene expression was validated both in patients' PBMC and in vorinostat-treated human carcinoma xenograft models, and transient repression of *MYC* was consistently observed.

Conclusion*:* Within the design of the PRAVO study, all of the identified genes showed rapid and transient induction or repression and therefore, in principle, fulfilled the requirement of being pharmacodynamic biomarkers of vorinostat action in fractionated radiotherapy, possibly underscoring the role of *MYC* in this therapeutic setting.

Introduction

Modern radiation oncology will require a synergy between high-precision radiotherapy protocols and innovative approaches for biological optimization of radiation effect. From a clinical perspective, new insights into molecular radiobiology will provide a unique opportunity for combining systemic targeted therapeutics with radiotherapy [1]. One example is the use of histone deacetylase (HDAC) inhibitors as potentially radiosensitizing drugs. Inhibition of HDAC enzymes leads to acetylation of histone and non-histone proteins, and the resultant changes in gene transcription cause alterations in key molecules that orchestrate a wide range of cellular functions, including cell cycle progression, DNA damage signaling and repair, and cell death by apoptosis and autophagy [2–5].

Following the demonstration that HDAC inhibitors enhanced radiation-induced clonogenic suppression of experimental *in vitro* and *in vivo* colorectal carcinoma models [6–9], but independently of the actual histone acetylation level at the time of radiation exposure [7,8], we conducted the Pelvic Radiation and Vorinostat (PRAVO) phase 1 study [10,11]. This trial, undertaken in sequential patient cohorts exposed to escalating dose levels of the HDAC inhibitor vorinostat combined with pelvic palliative radiotherapy for advanced gastrointestinal malignancy, was the first to report on the therapeutic use of an HDAC inhibitor in clinical radiotherapy. It was designed to demonstrate a number of key questions; whether the investigational agent reached the specific target (detection of tumor histone acetylation), the applicability of non-invasive tumor response assessment (using functional imaging), and importantly, that the combination of an HDAC inhibitor and radiation was safe and tolerable.

The ultimate goal of a first-in-human therapy trial is to conclude with a recommended treatment dose for follow-up expanded trials, and in achieving this, a phase 1 study typically is designed to determine treatment toxicity and tolerability (in terms of dose-limiting toxicity and maximum-tolerated dose (MTD), respectively) [12,13]. For molecularly targeted agents, the dose that results in a relevant level of target modulation may differ greatly from the MTD, and generally, we do not have a good understanding of the relationship between the MTD and the dose required to achieve the desired therapeutic effect [1]. An optimum biological dose may be the dose that is associated with pharmacodynamic biomarkers reflecting the mechanism of drug action. In the setting of fractionated radiotherapy, this would ideally represent a radiosensitizing molecular event occurring at each radiation fraction, or in other words, a biological indicator with a transient and periodic expression profile. Importantly, tumor specimens for this particular purpose cannot be sampled after the patient has commenced the radiation treatment. Any signaling activity in on-treatment tumor samples would reflect the combined effect of radiation and the systemic drug, and the contribution of the latter would probably be indistinguishable from the effect of the actual accumulated radiation dose. Instead, the study can be designed to collect non-irradiated surrogate tissue both before the commencement of study treatment and on-treatment at time points reflecting the timing of administration of the systemic drug with regard to the fractionated radiotherapy protocol. In addition, as a general rule, biomarkers that have been previously established for single-agent therapy will require reevaluation in a first-in-human clinical trial combining a molecularly targeted compound with radiotherapy.

Within this context, *i.e.,* that the possible mechanism of radiosensitizing action of the molecularly targeted agent should be regarded a main objective in a combined-modality study with radiotherapy, the present study reports on a correlative analytical strategy for identifying possible biomarkers of HDAC inhibitor activity, using peripheral blood mononuclear cells (PBMC) from the PRAVO phase 1 study patients receiving pelvic palliative radiotherapy as an easily accessible surrogate tissue for vorinostat exposure [14]. Gene expression array analysis identified PBMC genes that from experimental models are known to be implicated in biological processes governed by HDAC inhibitors, and might be further developed as pharmacodynamic biomarkers of vorinostat activity in the setting of fractionated radiotherapy.

Materials and Methods

Ethics Statement

Both of the protocols for the PRAVO study (ClinicalTrials ID NCT00455351) and the phase 2, non-randomized study for patients with locally advanced rectal cancer (LARC) given neoadjuvant chemoradiotherapy (ClinicalTrials ID NCT00278694) were approved by the Institutional Review Board and the Regional Committee for Medical and Health Research Ethics South-East Norway (REC South-East, Permit Number S-06289 and S-05059, respectively), and were performed in accordance with the Declaration of Helsinki. Written informed consent was required for participation. Housing and all procedures involving animals were performed according to protocols approved by the Animal Care and Use Committee at Department of Comparative Medicine, Oslo University Hospital (Permit Number 885-2616-2919-2928-3688), in compliance with the Norwegian National Committee for Animal Experiments' guidelines on animal welfare.

PRAVO Study Patients and Objectives

The patient population was enrolled between February 2007 and May 2009. The principal eligibility criterion was histologically confirmed pelvic carcinoma scheduled to receive palliative radiation to 30 Gy in 3-Gy daily fractions. Other details on eligibility are given in the initial report [10]. This phase 1 dose-escalation study adopted a standard 3+3 expansion cohort design [12], where patients with advanced gastrointestinal carcinoma were enrolled onto four sequential dose levels of vorinostat (Merck & Co., Inc., Whitehouse Station, NJ, USA), starting at 100 mg daily with dose escalation in increments of 100 mg [10]. The primary objective was to determine tolerability of vorinostat, defined by dose-limiting toxicity and MTD, when administered concomitantly with palliative radiation to pelvic target volumes. Secondary objectives were to assess the biological activity of vorinostat, including the identification of possible biomarkers of HDAC inhibitor activity, and to monitor radiological response when given with pelvic radiotherapy. The study data on patient treatment tolerability, tumor histone acetylation following vorinostat administration, and treatment-induced changes in tumor volume and apparent distribution coefficient, as assessed by magnetic resonance imaging, have been reported in detail previously [10,11].

Patient Blood Sampling and RNA Isolation

As depicted by **Figure 1**, peripheral blood, drawn on PAXgene Blood RNA Tubes (Qiagen Norge, Oslo, Norway), was collected at baseline (before commencement of study treatment; termed T0) and on-treatment the third treatment day, two and 24 hours after the patient had received the preceding daily dose of vorinostat (termed T2 and T24), respectively. A full set of three samples (T0, T2, and T24) was obtained from 14 of the 16 evaluable study patients (Table 1). The tubes were stored at –70°C until analysis. Total PBMC RNA was isolated using PAXgene Blood RNA Kit (Qiagen), following the manufacturer's protocol. RNA concentration and quality were assessed using NanoDrop 1000 and Agilent 2100 Bioanalyzer (Thermo Fisher Scientific Norway, Oslo, Norway), respectively.

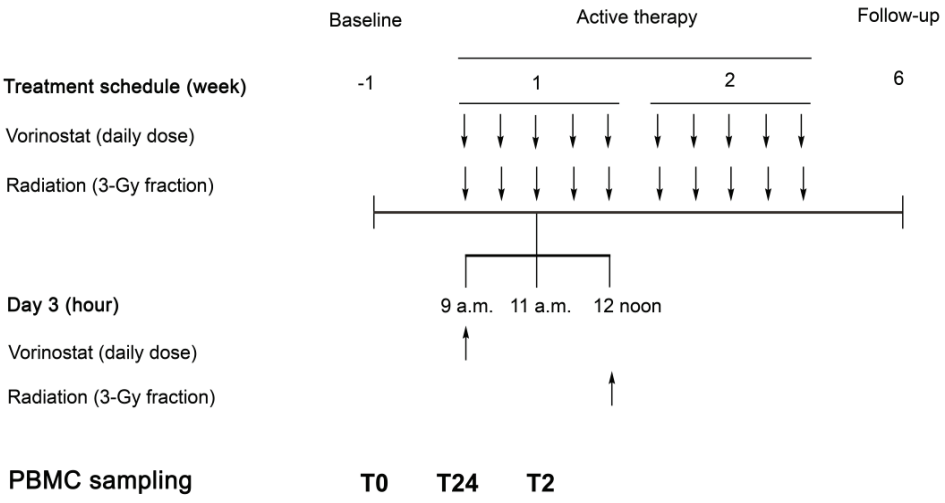

Figure 1. Treatment schedule for the Pelvic Radiation and Vorinostat phase 1 study. This study combined pelvic palliative radiotherapy (30 Gy in 3-Gy daily fractions; administered at 12 noon) with the histone deacetylase inhibitor vorinostat (given once daily at 9 a.m.) for advanced gastrointestinal malignancy. Arrows indicate administration of therapy. Study patients' peripheral blood mononuclear cells (PBMC) were sampled before commencement of treatment (T0) and on active therapy, two hours (T2; at 11 a.m. on day 3) and 24 hours (T24; at 9 a.m. on day 3) after the previous dose of vorinostat.

Gene Expression Array Analysis

This analysis was performed by the Norwegian Genomics Consortium (Oslo, Norway). Briefly, cRNA synthesis, amplification, and hybridization to Illumina Human WG-6 v3 Expression BeadChip arrays (Illumina, Inc., San Diego, CA, USA), containing 48,000 probes, were carried out as per manufacturer's instructions. Signal intensities were extracted by the BeadArray Reader Software (Illumina), and raw data were imported into the GenomeStudio v2010.1 Software, Gene Expression module v1.6.0 (Illumina). The primary array data are available in the Gene Expression Omnibus data repository (GEO accession number GSE46703).

Statistical and Functional Annotation Analyses of Array Data

Analysis was performed using Bioconductor vR2.11.1 and the Bioconductor packages lumi 1.14.0, linear models for microarray data (limma) 3.4.4, and illuminaHumanv3BeadID.db 1.6.0 (www.bioconductor.org). Following quality control and pre-processing, the data were $\log_2$-transformed, and differential gene expression between the sample groups T0, T2, and T24 was determined by applying a Benjamin and Hochberg false discovery rate-adjusted *P*-value cut-off of 0.05. The total number of probes that were identified as differentially expressed was analyzed using the Database for Annotation, Visualization and Integrated Discovery, DAVID v6.7 [15,16]. Enriched biological processes and pathways were identified using the GOTERM_BP_FAT and KEGG_PATHWAY algorithms, applying a *P*-value cut-off of 0.01. Differential expression analysis of the array data was also performed using a *P*-value of 0.01 and a $\log_2$-fold change cut-off of 1.0 in order to identify genes whose expression changes could have potentially high biological significance.

Experimental Human Colorectal Carcinoma Models

The HCT116 and SW620 colorectal carcinoma cell lines were originally purchased from American Type Culture Collection (Manassas, VA, USA), and the identities of our laboratory's versions were confirmed by short tandem repeat analysis (Table S1). The LoVo-92 colorectal carcinoma cell line was kindly provided by Dr. Paul Noordhuis (VU Medical Centre, Amsterdam, The Netherlands) [17]. The cell lines were cultured as previously described [8,17]. Xenografts were established by subcutaneous injections of HCT116 or SW620 cell suspensions (2×10^6 cells) bilaterally on the flanks of locally bred female BALB/c nude (nu/nu) or Athymic Nude-Foxn1^{nu} mice, 6–8 weeks of age. Vorinostat (Cayman Chemical, Ann Arbor, MI, USA; 100 mg/kg, dissolved in dimethyl sulfoxide to a concentration of 100 mg/ml immediately before use) or vehicle was given by intraperitoneal injection 13 days (HCT116) or 20 days (SW620) after establishment of xenografts. Three and 12 hours after administration, the tumors were extirpated, snap-frozen in liquid nitrogen, and stored at –70°C. The xenografts were sectioned using a cryostat microtome prior to RNA extraction using TRIzol® Reagent (Invitrogen Dynal AS, Oslo, Norway). RNA concentration was assessed using the RNA/DNA calculator Gene Quent II (Pharmacia Biotech, Piscataway, NJ, USA).

Tumor Samples from LARC Patients

Primary tumor biopsies were sampled at the time of diagnosis from LARC patients enrolled onto a phase 2 study on neoadjuvant chemoradiotherapy (Table S2). The biopsy samples were snap-frozen in liquid nitrogen and stored at –70°C, and sectioned on the cryostat microtome, essentially as previously reported [18], before RNA was extracted.

Reverse Transcriptase Quantitative Polymerase Chain Reaction (RT-qPCR) Analysis

cDNA was synthesized from total RNA using the qScript™ cDNA Synthesis Kit (Quanta BioSciences, Inc., Gaithersburg, MD, USA). The qPCR was run in Perfecta qPCR

Supermix (Quanta), on iCycler (Bio-Rad Laboratories Norway, Oslo, Norway) and with all reactions in parallel. Primers were designed using ProbeFinder Assay Design Software (www.roche-applied-science.com/sis/rtpcr/upl/ezhome.html), and were obtained from the Universal ProbeLibrary collection (Roche Applied Sciences, Oslo, Norway). Primer sequences are listed in Table S3. Amplified cDNA generated from the reference cell line (LoVo-92) was included on all PCR plates for relative quantification purposes (correction of plate-to-plate variation). Data were normalized to the expression levels of two reference genes; *YARS*, encoding tyrosyl-tRNA synthetase, and *TBP*, encoding the TATA box-binding protein. When tested in the patient samples, the reference genes had equal expression per ng of cDNA, independent of patient treatment (vorinostat dose and time after administration). The data were analyzed using the GeneExpression Analysis for iCycler iQ® Real-Time PCR Detection System Software (BioRad), and were calculated relative to the level in the reference cell line and subsequently $\log_2$-transformed.

Statistical Analysis of qPCR Data

Analysis was performed using Predictive Analytics SoftWare Statistics version 19.0 (SPSS Inc., Chicago, IL, USA). Q-Q plots were applied to test whether the data were normally distributed or not, before differences between groups were analyzed using two-sided Student *t*-test for the PBMC samples and Mann-Whitney *U* test for xenograft samples. *P*-values less than 0.05 were considered statistically significant.

Results

PBMC Transcriptional Response to Vorinostat – Biological Processes and Pathways

Table 1 gives study patient baseline characteristics; the full study data on treatment tolerability and response have been reported previously [10,11]. Of the 14 patients that provided a full set of PBMC samples (T0, T2, and T24), one patient was treated at vorinostat 100 mg once daily and three patients at the 200 mg dose level, whereas four and six patients received the medication at 300 or 400 mg once daily, respectively.

Importantly, as vorinostat-induced tumor histone acetylation had been observed at all dose levels [10], the array data from all patient samples at each time point (T0, T2, and T24) were pooled, irrespective of the vorinostat dose administered to the patients. This was done to increase the statistical power of the testing on analysis of differential gene expression between the individual time points. As shown by **Figure 2**, approximately 2,100 probes were differentially expressed both at two hours of vorinostat exposure (T2 *versus* T0) and on the T24 *versus* T2 comparison when applying the *P*-value cut-off of 0.05. Of these, 1,602 transcripts were found to be altered in both comparisons, and furthermore, no significantly differential expression was observed when comparing the T0 and T24 groups. Hence, all of the 1,602 mutual probes that were identified had a transient change in expression level from T0, with approximately one half found to be up-regulated and thus, the other half down-regulated at T2, followed by the opposite directional change to baseline expression at T24 (data not shown).

Table 1. Study patients.

Vorinostat dose (mg daily)	Age (years)	Gender	Comment
100	77	Female	
200	49	Female	
200	64	Female	
200	66	Female	
300	47	Female	PBMC [a] not available
300	66	Female	
300	77	Male	
300	81	Female	
300	82	Male	
300	87	Female	PBMC [a] not available
400	45	Female	
400	55	Male	
400	62	Male	
400	75	Female	
400	83	Female	
400	85	Female	

[a]Peripheral blood mononuclear cells.

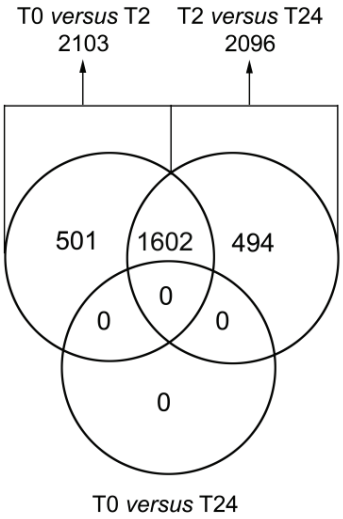

Figure 2. Venn diagram illustrating differentially expressed genes. Study patients' peripheral blood mononuclear cells were sampled at baseline (T0) and on-treatment two and 24 hours after administration of the daily dose of the study medication vorinostat (T2 and T24, respectively). Gene expression was analyzed by Illumina Human WG-6 v3 Expression BeadChip arrays. The array data from all patient samples at each time point (T0, T2, and T24) were pooled for the analysis. Probes with false discovery rate-adjusted *P*-values less than 0.05 were considered differentially expressed and subjected to Venn analysis, comparing by pairs T2 *versus* T0, T24 *versus* T2, and T24 *versus* T0. The figures represent numbers of probes in common for the various conditions.

Functional annotation analysis of the differentially expressed genes in patients' PBMC identified several enriched biological processes. Comparison of the baseline PBMC transcription profile with that obtained two hours after vorinostat administration (T2 *versus* T0) showed that 69 biological processes were over-represented, whereas the corresponding comparison of T24 *versus* T2 transcriptional profiles identified 106 processes (**Table S4**). As seen from **Table 2**, displaying the top-ten Gene Ontology terms for each of the two comparisons, seven out of the ten biological processes were present in both, with transcription being the most significant. In addition, the analysis identified enrichment of genes involved in catabolic processes, the cell cycle, RNA processing, chromatin modification, and chromosome organization. The top-three pathway networks for each of the two comparisons, in common for both, comprised signaling factors of the cell cycle, including the p53 pathway (**Table 3**).

Vorinostat Activity in PBMC – Verification of Selected Biomarkers

Next, by introducing a $\log_2$-fold change cut-off of 1.0 while decreasing the *P*-value to 0.01 in order to identify gene expression changes with presumably high biological significance, the list of differentially expressed probes, all with a biphasic pattern of regulation from T0 through T2 and T24, was reduced to 38 candidates (**Table 4**). Within this panel, two genes had duplicate array probes, whereas no reference sequence could be identified for three other probes, leaving 33 known genes as transcriptionally regulated by vorinostat following this stringent statistical analysis of the array data.

Table 2. Enriched biological processes in patients' peripheral blood mononuclear cells during 24 hours of vorinostat treatment.

Biological process [a]	*n* (%)	*P*-value	Selected transcripts [b]
T2 *versus* T0 [c]			
GO:0006350 transcription	253 (17)	5.1×10^{-14}	*MYC*, *DDIT3*
GO:0044265 cellular macromolecule catabolic process	107 (7.2)	8.2×10^{-11}	*MYC*, *BARD1*
GO:0044257 cellular protein catabolic process	93 (6.3)	1.7×10^{-10}	*BARD1*
GO:0007049 cell cycle	111 (7.5)	2.3×10^{-10}	*MYC*, *MSH6*, *BARD1*, *DDIT3*
GO:0051603 proteolysis involved in cellular protein catabolic process	92 (6.2)	2.9×10^{-10}	*BARD1*
GO:0019941 modification-dependent protein catabolic process	89 (6.0)	3.4×10^{-10}	*BARD1*
GO:0009057 macromolecule catabolic process	111 (7.5)	3.4×10^{-10}	*MYC*, *BARD1*
GO:0030163 protein catabolic process	94 (6.6)	3.9×10^{-10}	*BARD1*
GO:0006396 RNA processing	84 (5.6)	1.8×10^{-9}	
GO:0045449 regulation of transcription	276 (19)	5.0×10^{-9}	*MYC*, *DDIT3*
T24 *versus* T2 [c]			
GO:0006350 transcription	260 (17)	8.3×10^{-16}	*MYC*, *DDIT3*
GO:0007049 cell cycle	114 (7.5)	2.6×10^{-11}	*MYC*, *MSH6*, *BARD1*, *DDIT3*

GO:0045449 regulation of transcription	286 (19)	5.4×10^{-11}	*MYC*, *DDIT3*
GO:0016568 chromatin modification	55 (3.6)	1.3×10^{-10}	
GO:0006396 RNA processing	86 (5.6)	3.7×10^{-10}	
GO:0044265 cellular macromolecule catabolic process	104 (6.8)	8.8×10^{-10}	*MYC*, *BARD1*
GO:0051276 chromosome organization	78 (5.1)	9.6×10^{-10}	*MSH6*
GO:0022402 cell cycle process	85 (5.6)	4.1×10^{-9}	*MYC*, *MSH6*, *BARD1*, *DDIT3*
GO:0044257 cellular protein catabolic process	89 (5.8)	4.3×10^{-9}	*BARD1*
GO:0009057 macromolecule catabolic process	107 (7.0)	6.4×10^{-9}	*MYC*, *BARD1*

[a]Gene Ontology (GO) terms in bold: present in both comparisons.
[b]Verified by reverse transcriptase quantitative polymerase chain reaction analysis.
[c]T0 represents baseline peripheral blood mononuclear cells (PBMC) samples; T2 and T24 represent PBMC samples collected two and 24 hours, respectively, after the patients had received the daily dose of vorinostat.

Table 3. Enriched biological pathways in patients' peripheral blood mononuclear cells during 24 hours of vorinostat treatment.

Biological pathway	*n* (%)	*P*-value	Genes [a]
hsa04130 SNARE interactions in vesicular transport	10 (0.85)	1.6×10^{-4}	*STX6, STX5, STX1A, STX12, STX16, USE1, BET1, BET1L, GOSR1, VAMP1*
hsa04115 p53 signaling pathway	13 (1.1)	2.7×10^{-4}	*PMAIP1, RRM2B, SESN2, CDK4, CDK2, CCNE2, CCNE1, PPM1D, TNFRSF10B, RCHY1, APAF1,* ***GADD45B****, GADD45A*
hsa04110 cell cycle	17 (1.5)	0.0012	*CCNH, ANAPC13, CDC23, CDK7, PTTG1, CDK4, ZBTB17, TGFB1, WEE1, CDK2, CCNE2, CCNE1, YWHAG, CDKN2D,* ***GADD45B****, GADD45A,* ***MYC***

[a]Genes in bold: verified by reverse transcriptase quantitative polymerase chain reaction analysis.

Table 4. Differentially expressed genes in patients' peripheral blood mononuclear cells during 24 hours of vorinostat treatment. [a]

Accession no.	Gene [b]	Gene name	T2 *versus* T0 [c] (log_2-fold change)	T24 *versus* T2 [c] (log_2-fold change)
NM_005627	*SGK1*	serum/glucocorticoid regulated kinase 1	–1.58	1.65
NM_016478	*ZC3HC1*	zinc finger, C3HC-type containing 1	–1.43	1.39
NM_175571	*GIMAP8*	GTPase, IMAP family member 8	–1.23	1.34
NM_206938	*MS4A7*	membrane-spanning 4-domains, subfamily A, member 7	–1.21	1.06
NM_002467	***MYC***	v-myc myelocytomatosis viral oncogene homolog (avian)	–1.20	1.09
NM_001024938	*SLC2A11*	solute carrier family 2 (facilitated glucose transporter), member 11	–1.16	1.17

NM_004843	*IL27RA*	interleukin 27 receptor, alpha	–1.14	1.05
NM_000104	*CYP1B1*	cytochrome P450, family 1, subfamily B, polypeptide 1	–1.13	1.26
NM_207007	*CCL4L2*	chemokine (C-C motif) ligand 4-like 2	–1.04	1.26
NM_014167	*CCDC59*	coiled-coil domain containing 59	–1.02	1.00
NM_005346	*HSPA1B*	heat shock 70kDa protein 1B	1.82	–2.02
NM_153812	*PHF13*	PHD finger protein 13	1.80	–1.95
NM_001564	*ING2*	inhibitor of growth family, member 2	1.59	–1.71
NM_001564	*ING2*	inhibitor of growth family, member 2	1.56	–1.56
NM_001001870	none	None	1.42	–1.28
NM_016639	*TNFRSF12A*	tumor necrosis factor receptor superfamily, member 12A	1.40	–1.33
NM_152339	*SPATA2L*	spermatogenesis associated 2-like	1.38	–1.46
NM_025079	*ZC3H12A*	zinc finger CCCH-type containing 12A	1.36	–1.29
NM_015675	***GADD45B***	growth arrest and DNA-damage-inducible, beta	1.30	–1.17
NM_013368	*SERTAD3*	SERTA domain containing 3	1.24	–1.30
NM_004219	*PTTG1*	pituitary tumor-transforming 1	1.23	–1.35
NM_014711	*CP110*	CP110 protein	1.20	–1.21
NM_005341	*ZBTB48*	zinc finger and BTB domain containing 48	1.14	–1.03
NM_000179	***MSH6***	mutS homolog 6 (E. coli)	1.13	–1.23
NM_153358	*ZNF791*	zinc finger protein 791	1.13	–1.07
NM_006494	*ERF*	Ets2 repressor factor	1.12	–1.06
NR_002734	*PTTG3P*	pituitary tumor-transforming 3, pseudogene	1.11	–1.18
NM_016605	*FAM53C*	family with sequence similarity 53, member C	1.07	–1.13
NM_004219	*PTTG1*	pituitary tumor-transforming 1	1.07	–1.13
not available	none	transcribed locus Hs.559604	1.07	–1.08
NM_000024	*ADRB2*	adrenergic, beta-2-, receptor, surface	1.07	–1.07
XM_926814	none	None	1.05	–1.19
NM_006806	*BTG3*	BTG family, member 3	1.05	–1.04
NM_031212	*SLC25A28*	solute carrier family 25 (mitochondrial iron transporter), member 28	1.05	–1.00
NM_000465	***BARD1***	BRCA1 associated RING domain 1	1.02	–1.23
NM_004083	***DDIT3***	DNA-damage-inducible transcript 3	1.02	–1.08
NM_052901	*SLC25A25*	solute carrier family 25 (mitochondrial carrier; phosphate carrier), member 25	1.02	–1.06
NM_024954	*UBTD1*	ubiquitin domain containing 1	1.01	–1.01

[a]Log_2-fold change higher than 1.0; *P*-value less than 0.01.
[b]Genes in bold: chosen for validation of expression in the study patients' peripheral blood mononuclear cells (PBMC) samples and human colorectal carcinoma xenograft models.
[c]T0 represents baseline PBMC samples; T2 and T24 represent PBMC samples collected two and 24 hours, respectively, after the patients had received the daily dose of vorinostat.

Selection of genes for verification analysis by RT-qPCR was based on both the relevance in the DNA damage response, which is recognized as a significant mechanism contributing to clinical radiation sensitivity [19], and previous indication of regulation by HDAC inhibitors. Five of the 33 genes were found to fulfill both criteria: *MYC* [20,21] among the ten genes repressed at T2 and correspondingly, *GADD45B* [22], *MSH6* [23,24], *BARD1* [25,26], and *DDIT3* [27,28] among the 23 induced genes; mean PBMC expression levels at T0 relative to reference cell line expression are given in Table S5. These genes were present within the enriched biological processes and pathways identified by the functional annotation analysis of the differentially expressed genes (Table 2 and Table 3), and the biphasic pattern of regulation in PBMC through T2 and T24 was confirmed with significant time-dependent changes ($P < 0.01$) for all of the five genes (**Figure 3**).

Vorinostat Activity in Experimental Tumors – Validation of Selected Biomarkers

We have previously shown histone hyperacetylation in vorinostat-treated human colorectal carcinoma xenograft models (HCT116 and SW620), peaking three hours after vorinostat administration and with restored baseline levels of histone acetylation three to six hours later, without accumulative effect following repeat daily administration [8]. Hence, expression of the five selected genes was further assessed by RT-qPCR in HCT116 and SW620 xenografts, three and 12 hours after administering vorinostat to tumor-bearing mice; median control expression levels relative to reference cell line expression are given in Table S5. In the HCT116 model, a significant change ($P < 0.05$) in vorinostat-induced expression was found for *MYC* only. A similar transient *MYC* repression, but without statistically significant differences in expression levels through the time points, was seen in the SW620 tumors (**Figure 3**).

LARC – Primary Tumor *MYC* Expression

On identifying *MYC* repression as a possible biomarker of HDAC inhibitor activity from the strategy of analyzing, firstly, PRAVO study patients' PBMC, and secondly, vorinostat-treated colorectal carcinoma xenografts, and additionally recognizing this drug as a rational approach for biological optimization of radiation effect in pelvic gastrointestinal carcinoma [10], we investigated whether *MYC* might be expressed in the target tissue of a well-established pelvic radiotherapy protocol. In 27 LARC patients receiving neoadjuvant chemoradiotherapy [18], *MYC* expression was detected in all primary tumor samples, though at highly variable levels (median expression value was 0.47 (range 0.020–4.9) relative to reference cell line expression), but was essentially not associated with patient characteristics or treatment outcome in this small cohort (Table S2).

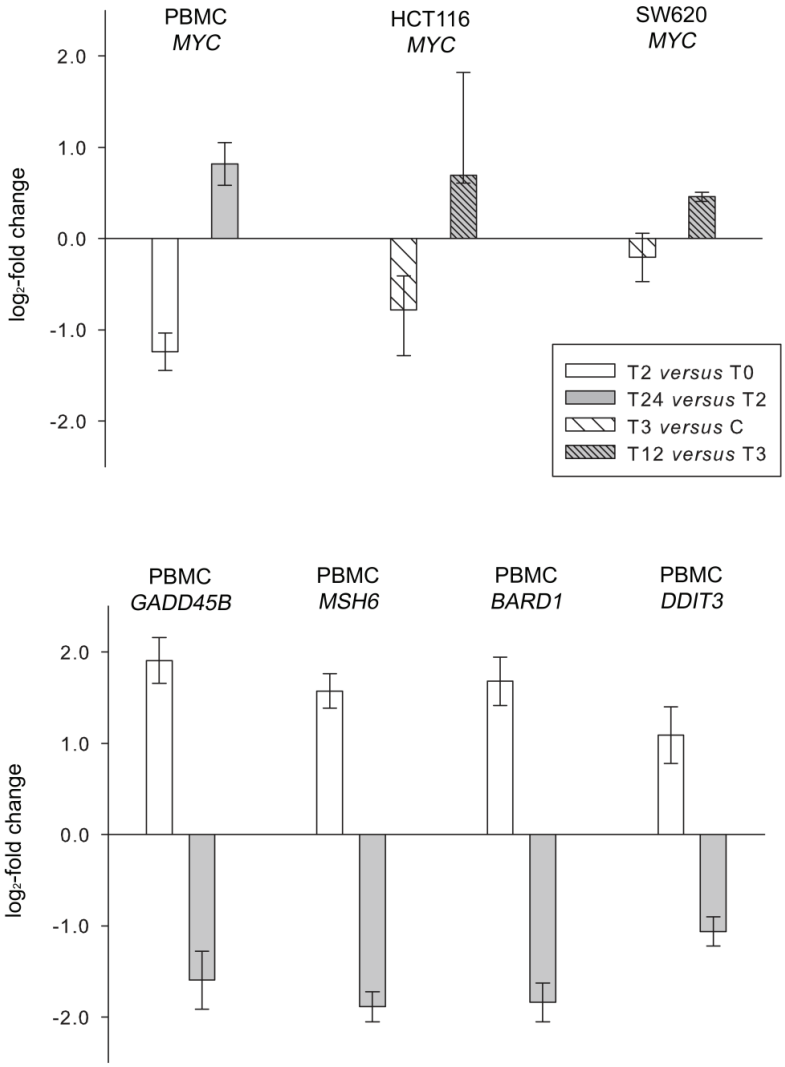

Figure 3. Validation of vorinostat-regulated expression of selected genes. Study patients' peripheral blood mononuclear cells (PBMC) were sampled at baseline (T0) and on-treatment two (T2) and 24 (T24) hours after administration of the daily dose of the study medication vorinostat, and expression of *MYC*, *GADD45B*, *MSH6*, *BARD1*, and *DDIT3* was analyzed by reverse transcriptase quantitative polymerase chain reaction (RT-qPCR). Correspondingly, mice bearing HCT116 or SW620 xenografts were injected intraperitoneally with vehicle (control, C) or vorinostat, and xenografts were harvested three (T3) and 12 (T12) hours after injection for RT-qPCR analysis of *MYC* expression. Relative gene expression (log_2-fold change) for each comparison is given as mean ± SEM of the PBMC sample values (n = 14) and as median and range of the values from control (n = 8 for HCT116; n = 4 for SW620) and vorinostat-treated (n = 4 for HCT116; n = 2 for SW620) xenografts. The compared gene expression levels were significantly different within the PBMC (P < 0.01) and HCT116 (P < 0.05) sample groups, while the differences were non-significant for the SW620 tumors.

Discussion

Within the design of the PRAVO phase 1 study (Figure 1), combining the HDAC inhibitor vorinostat with fractionated radiation to pelvic targets volumes for determination of treatment tolerability and response, gene expression array analysis was performed of study patients' PBMC, sampled at baseline (T0) and on-treatment two and 24 hours (T2 and T24) after the patient had received the daily dose of vorinostat, in order to identify possible biomarkers of HDAC inhibitor activity. This strategy revealed 1,600 array probes with biphasic pattern of expression from T0 through T2 and T24 across all of the study patients. A significant number of these genes were found implicated in processes comprising gene regulation, the cell cycle, and chromatin biology. Applying stringent criteria for array data analysis, five genes were recognized both as players in the DNA damage response and targets for regulation by HDAC inhibitors, and were therefore selected for validation of expression pattern both in study patients' PBMC and in human colorectal carcinoma xenograft models. Of these, only *MYC* consistently showed rapid and transient repression in all conditions that were tested.

In the setting of fractionated radiotherapy, a synergistic drug should preferably elicit a radiosensitizing molecular event at each radiation fraction; hence, a pharmacodynamic biomarker should reflect the timing of drug administration with regard to radiation exposure in a periodic manner [1]. Importantly, in a prior preclinical *in vivo* study combining vorinostat and fractionated radiation, we observed that tumor histone acetylation, considered a biomarker of vorinostat activity in the radiotherapy target tissue, reached a maximum three hours after intraperitoneal vorinostat injection into the experimental animals and was restored to baseline acetylation level three to six hours later, but with a repetitive, transient induction of acetylation following repeat injections. Of note, tumor growth inhibition after fractionated radiation, representing a long-term phenotypic outcome of the experimental manipulations, was significantly enhanced both when radiation was delivered at peak and restored histone acetylation levels [8]. Consequently, tumor histone hyperacetylation did not seem to be required at the time of radiation exposure, leaving the question of the optimum temporal relationship between administration of the radiosensitizing drug and radiation delivery unaddressed.

In the PRAVO study, one patient at each vorinostat dose level had both baseline (before commencement of study treatment) and repeat tumor biopsy two-and-a-half hours after administration of vorinostat (on day 3 of the treatment protocol). Histone hyperacetylation was observed in all on-treatment biopsy samples [10], confirming the presence of vorinostat in the target at the time of the daily radiation exposure. However, given that one of the objectives of the study was to determine mechanisms of the presumed radiosensitizing action of vorinostat that were not simultaneously manifesting molecular perturbations elicited by the radiation itself, non-irradiated surrogate tissue was collected for the purpose of identifying new biomarkers. Several investigators have demonstrated PBMC histone hyperacetylation on HDAC inhibitor treatment [14,29,30]. With these aspects in mind, PBMC were deemed to represent a relevant surrogate tissue for studying radiosensitizing effects of vorinostat in the context of this clinical trial.

Interestingly, using the study patients' PBMC as surrogate tissue for vorinostat exposure, all of the 1,600 probes that were found to be common for the comparisons T2 *versus* T0 and T24 *versus* T2 in principle represented pharmacodynamic biomarkers of the chosen timing of vorinostat administration in the fractionated radiotherapy protocol. The genes showed rapid and transient induction or repression, thus mirroring the kinetics of the histone acetylation response. This observation implies that the design of the PRAVO study, undertaken in patients with advanced gastrointestinal cancer, may not have provided the optimum context for detailed capture of molecular effects of vorinostat. Thus, ethical concerns may challenge the structure required within a clinical trial setting for evaluating novel biomarker endpoints. Nevertheless, in the PRAVO study, functional annotation analysis of the panel of 1,600 probes identified biological processes and pathways comprising gene regulation (transcription, RNA processing), cell cycle progression (including p53 signaling, commonly involved in the DNA damage response), and chromatin biology. These findings are consistent with well-known cellular perturbations following exposure of experimental tumor models to HDAC inhibitors [2–5].

Investigation of biomarkers of HDAC inhibitor activity has been undertaken in a number of clinical therapy trials. These include the demonstration of increased histone acetylation in patients' PBMC in the early trials [14,29,30] and the more recent confirmation of changes in tumor expression of acetylated histone and non-histone proteins [10,14,31,32], the HDAC2 enzyme [31] and HR23B protein [32,34], the latter been proposed as predictive biomarker [35], and of tumor proliferation index [36]. Plasma protein profiling has been done in glioblastoma patients receiving vorinostat in combination with an established cytotoxic regimen [37]. Furthermore, tumor gene expression array analysis has been performed in a study with the HDAC inhibitor panobinostat as single agent [38] and in one trial each of combining either vorinostat or valproate with other biologic agents (in non-small cell lung carcinoma and acute myeloid leukemia, respectively) [39,40]. To our knowledge, the present study is the first to report on gene expression array analysis as an attempt to identify pharmacodynamic biomarker(s) reflecting timing of HDAC inhibitor administration with regard to an established cytotoxic regimen.

The criteria for selecting genes for validation were both their presumed relevance in the DNA damage response and previous indications of regulation by an HDAC inhibitor [22–24,28,41], and additionally, in order to find 'tumor-specific' markers, omitting genes that typically might be associated with leukocyte biology. Four of the selected genes were induced by vorinostat in the study patients' PBMC but did not show a similar response in the experimental tumor models. *BARD1* encodes a nuclear factor with tumor suppressor activity [24], the stress response effectors encoded by *GADD45B* and *DDIT3* are implicated in cell cycle arrest, DNA repair, and apoptosis [42,43], and *MSH6* encodes a DNA mismatch repair protein [44]. To date, only three studies seem to have been published on their potential use as biomarkers of therapy response [45–47]. In contrast, the confirmation of *MYC* as the only one of the selected genes with rapid and transient change in expression in all tested conditions (*i.e.,* both in the study patients' PBMC and experimental tumor models) may point to a particular importance of myc in the therapeutic setting with fractionated radiation. Future investigations of vorinostat as possible radiosensitizing agent might be within a long-term curative radiotherapy protocol, for example as an additional component of neoadjuvant

chemoradiotherapy for LARC. The confirmed presence of *MYC* expression in the intended radiotherapy target tissue (primary rectal tumors) in LARC patients encourages future exploration of this proto-oncogene as a novel biomarker endpoint.

The myc protein acts both as transcriptional activator and repressor, regulating a myriad of genes that collectively conduct cell cycle progression, apoptosis, angiogenesis, and genetic instability [48]. Specifically, it has been suggested that myc activates DNA damage repair genes [20], and interestingly, that myc in hypoxic tumors acts synergistically with the transcription factor hypoxia-inducible factor type 1α, HIF-1α [49,50]. Recent evidence indicates that HDAC inhibition suppresses HIF-1α activity [51,52]. Consequently, mitigation of DNA damage repair capacity through suppression of myc/HIF-1α synergy in hypoxic tumors [53,54], typically being resistant to radiation, provides an appealing explanation for the radiosensitizing effect of HDAC inhibitors.

However, conflicting data have been presented as to how HDAC inhibition may influence the myc protein itself. Whereas inhibition of various HDAC enzymes has been shown to cause myc repression in a range of human cancer cell lines [21,55– 57], which corresponds well with the data in the present study, specific nuclear induction of myc to mediate HDAC inhibitor-induced apoptosis in glioblastoma cell lines has also been demonstrated [58]. Interestingly, in nasopharyngeal carcinoma cells that were resistant to radiation, myc was found to be essential through the transcriptional activation of cell cycle checkpoint kinases [59], which are signaling factors implicated in DNA damage repair, thereby facilitating tumor cell survival following radiation exposure. On the contrary, although radiosensitization was conferred by HDAC inhibition both in hypoxic and normoxic hepatocellular carcinoma cells, a lower level of myc expression was associated with the hypoxic and more radioresistant condition [60]. Of particular note, in the present study, the vorinostat-induced repression of *MYC* was found both in study patients' PBMC, clearly representing normoxic tissue, and experimental tumors that also were tested under normoxic conditions.

In conclusion, integral in the PRAVO study design was the collection of non-irradiated surrogate tissue for the identification of biomarker(s) of vorinostat activity to reflect the timing of administration and also suggest the mechanism of action of the HDAC inhibitor. This objective was achieved by gene expression array analysis of study patients' PBMC and as a consequence, the identification of genes that from experimental models are known to be implicated in biological processes and pathways governed by HDAC inhibitors. Importantly, all of the identified genes showed rapid and transient induction or repression and therefore, in principle, fulfilled the requirement of being pharmacodynamic biomarkers for this radiosensitizing drug in fractionated radiotherapy. Among the identified candidate genes, *MYC* repression was found in all patient samples and tested experimental conditions, possibly underscoring the impact of the myc proto-oncogene in this particular therapeutic setting.

Acknowledgments

The authors thank Dr. Siri Tveito and Ms. Tove Øyjord for valuable assistance with laboratory procedures and Prof. Rob G. Bristow for helpful discussion.

References

1. Ree AH, Hollywood D (2013) Design and conduct of early-phase radiotherapy trials with targeted therapeutics: Lessons from the PRAVO experience. Radiother Oncol 108: 3–16.
2. Shabason JE, Tofilon PJ, Camphausen K (2011) Grand rounds at the National Institutes of Health: HDAC inhibitors as radiation modifiers, from bench to clinic. J Cell Mol Med 15: 2735–2744.
3. Khan O, La Thangue NB (2012) HDAC inhibitors in cancer biology: emerging mechanisms and clinical applications. Immunol Cell Biol 90: 85–94.
4. Spiegel S, Milstien S, Grant S (2012) Endogenous modulators and pharmacological inhibitors of histone deacetylases in cancer therapy. Oncogene 31: 537–551.
5. Groselj B, Sharma NL, Hamdy FC, Kerr M, Kiltie AE (2013) Histone deacetylase inhibitors as radiosensitisers: effects on DNA damage signalling and repair. Br J Cancer 108: 748–754.
6. Flatmark K, Nome RV, Folkvord S, Bratland A, Rasmussen H, Ellefsen MS, Fodstad O, Ree AH (2006) Radiosensitization of colorectal carcinoma cells by histone deacetylase inhibition. Radiat Oncol 1: 25.
7. Ree AH, Folkvord S, Flatmark K (2008) HDAC2 deficiency and histone acetylation. Nat Genet 40: 812–813.
8. Folkvord S, Ree AH, Furre T, Halvorsen T, Flatmark K (2009) Radiosensitization by SAHA in experimental colorectal carcinoma models – in vivo effects and relevance of histone acetylation status. Int J Radiat Oncol Biol Phys 74: 546–552.
9. Saelen MG, Ree AH, Kristian A, Fleten KG, Furre T, Hektoen HH, Flatmark K (2012) Radiosensitization by the histone deacetylase inhibitor vorinostat under hypoxia and with capecitabine in experimental colorectal carcinoma. Radiat Oncol 7: 165.
10. Ree AH, Dueland S, Folkvord S, Hole KH, Seierstad T, Johansen M, Abrahamsen TW, Flatmark K (2010) Vorinostat, a histone deacetylase inhibitor, combined with pelvic palliative radiotherapy for gastrointestinal carcinoma: the Pelvic Radiation and Vorinostat (PRAVO) phase 1 study. Lancet Oncol 11: 459–464.
11. Bratland A, Dueland S, Hollywood D, Flatmark K, Ree AH (2011) Gastrointestinal toxicity of vorinostat: reanalysis of phase 1 study results with emphasis on dose-volume effects of pelvic radiotherapy. Radiat Oncol 6: 33.
12. Le Tourneau C, Lee JJ, Siu LL (2009) Dose escalation methods in phase I cancer clinical trials. J Natl Cancer Inst 101: 1–13.
13. LoRusso PM, Boerner SA, Seymour L (2010) An overview of the optimal planning, design, and conduct of phase I studies of new therapeutics. Clin Cancer Res 16: 1710–1718.
14. Kelly WK, Richon VM, O'Connor O, Curley T, MacGregor-Curtelli B, Tong W, Klang M, Schwartz L, Richardson S, Rosa E, Drobnjak M, Cordon-Cordo C, Chiao JH, Rifkind R, Marks PA, Scher H (2003) Phase I trial of histone deacetylase inhibitor: suberoylanilide hydroxamic acid administered intravenously. Clin Cancer Res 9: 3578–3588.
15. Huang DW, Sherman BT, Lempicki RA (2009) Systematic and integrative analysis of large gene lists using DAVID Bioinformatics Resources. Nat Protoc 4: 44–57.
16. Huang DW, Sherman BT, Lempicki RA (2009) Bioinformatics enrichment tools: paths toward the comprehensive functional analysis of large gene lists. Nucleic Acids Res 37: 1–13.
17. Noordhuis P, Laan AC, van de Born K, Losekoot N, Kathmann I, Peters GJ (2008) Oxaliplatin activity in selected and unselected human ovarian and colorectal cancer cell lines. Biochem Pharmacol 76: 53–61.
18. Folkvord S, Flatmark K, Dueland S, de Wijn R, Grøholt KK, Hole KH, Nesland JM, Ruijtenbeek R, Boender PJ, Johansen M, Giercksky KE, Ree AH (2010) Prediction of response to preoperative chemoradiotherapy in rectal cancer by multiplex kinase activity profiling. Int J Radiat Oncol Biol Phys 78: 555–562.
19. Begg AC, Stewart FA, Vens C (2011) Strategies to improve radiotherapy with targeted drugs. Nat Rev Cancer 11: 239–253.

20. Luoto KR, Meng AX, Wasylishen AR, Zhao H, Coackley CL, Penn LZ, Bristow RG (2010) Tumor cell kill by c-MYC depletion: role of MYC-regulated genes that control DNA double-strand break repair. Cancer Res 70: 8748–8759.
21. Seo SK, Jin HO, Woo SH, Kim YS, An S, Lee JH, Hong SI, Lee KH, Choe TB, Park IC (2011) Histone deacetylase inhibitors sensitize human non-small cell lung cancer cells to ionizing radiation through acetyl p53-mediated c-myc down-regulation. J Thorac Oncol 6: 1313–1319.
22. Scuto A, Kirschbaum M, Kowolik C, Kretzner L, Juhasz A, Atadja P, Pullarkat V, Bhatia R, Forman S, Yen Y, Jove R (2008) The novel histone deacetylase inhibitor, LBH589, induces expression of DNA damage response genes and apoptosis in Ph– acute lymphoblastic leukemia cells. Blood 111: 5093–5100.
23. Shahi A, Lee JH, Kang Y, Lee SH, Hyun JW, Chang IY, Jun JU, You HJ (2011) Mismatch-repair protein MSH6 is associated with Ku70 and regulates DNA double-strand break repair. Nucleic Acids Res 39: 2130–2143.
24. Rodríguez-Jiménez FJ, Moreno-Manzano V, Lucas-Dominguez R, Sánchez-Puelles JM (2008) Hypoxia causes downregulation of mismatch repair system and genomic instability in stem cells. Stem Cells 26: 2052–2062.
25. Li M, Yu X (2013) Function of BRCA1 in the DNA damage response is mediated by ADP-ribosylation. Cancer Cell 23: 693–704.
26. Zhang Y, Carr T, Dimtchev A, Zaer N, Dritschilo A, Jung M (2007) Attenuated DNA damage repair by trichostatin A through BRCA1 suppression. Radiat Res 168: 115–124.
27. Forus A, Florenes VA, Maelandsmo GM, Fodstad O, Myklebost O (1994) The protooncogene CHOP/GADD153, involved ingrowth arrest and DNA damage response, is amplified an a subset of human sarcomas. Cancer Genet Cytogenet 78: 165–171.
28. Namdar M, Perez G, Ngo L, Marks PA (2010) Selective inhibition of histone deacetylase 6 (HDAC6) induces DNA damage and sensitizes transformed cells to anticancer agents. Proc Natl Acad Sci USA 107: 20003–20008.
29. Sandor V, Bakke S, Robey RW, Kang MH, Blagosklonny MV, Bender J, Brooks R, Piekarz RL, Tucker E, Figg WD, Chan KK, Goldspiel B, Fojo AT, Balcerzak SP, Bates SE (2002) Phase I trial of the histone deacetylase inhibitor, depsipeptide (FR901228, NSC 630176), in patients with refractory neoplasms. Clin Cancer Res 8: 718–728.
30. Byrd JC, Marcucci G, Parthun MR, Xiao JJ, Klisovic RB, Moran M, Lin TS, Liu S, Sklenar AR, Davis ME, Lucas DM, Fischer B, Shank R, Tejaswi SL, Binkley P, Wright J, Chan KK, Grever MR (2005) A phase 1 and pharmacodynamics study of depsipeptide (FK228) in chronic lymphocytic leukemia and acute myeloid leukemia. Blood 105: 959–967.
31. Munster PN, Thurn KT, Thomas S, Raha P, Lacevic M, Miller A, Melisko M, Ismail-Khan R, Rugo H, Moasser M, Minton SE (2011) A phase II study of the histone deacetylase inhibitor vorinostat combined with tamoxifen for the treatment of patients with hormone therapy-resistant breast cancer. Br J Cancer 104: 1828–1835.
32. Ramaswamy B, Fiskus W, Cohen B, Pellegrino C, Hershman DL, Chuang E, Luu T, Somlo G, Goetz M, Swaby R, Shapiro CL, Stearns V, Christos P, Espinoza-Delgado I, Bhalla K, Sparano JA (2012) Phase I-II study of vorinostat plus paclitaxel and bevacizumab in metastatic breast cancer: evidence for vorinostat-induced tubulin acetylation and Hsp90 inhibition in vivo. Breast Cancer Res Treat 132: 1063–1072.
33. Khan O, Fotheringham S, Wood V, Stimson L, Zhang C, Pezzella F, Duvic M, Kerr DJ, La Thangue NB (2010) HR23B is a biomarker for tumor sensitivity to HDAC inhibitor-based therapy. Proc Natl Acad Sci USA 107: 6532–6537.
34. Yeo W, Chung HC, Chan SL, Wang LZ, Lim R, Picus J, Boyer M, Mo FK, Koh J, Rha SY, Hui EP, Jeung HC, Roh JK, Yu SC, To KF, Tao Q, Ma BB, Chan AW, Tong JH, Erlichman C, Chan AT, Goh BC (2012) Epigenetic therapy using belinostat for patients with unresectable hepatocellular carcinoma: a multicenter phase I/II study with biomarker and pharmacokinetic analysis of tumors from patients in the Mayo Phase II Consortium and the Cancer Therapeutics Research Group. J Clin Oncol 30: 3361–3367.

35. Fotheringham S, Epping MT, Stimson L, Khan O, Wood V, Pezzella F, Bernards R, La Thangue NB (2009) Genome-wide loss-of-function screen reveals an important role for the proteasome in HDAC inhibitor-induced apoptosis. Cancer Cell 15: 57–66.
36. Venugopal B, Baird R, Kristeleit R, Plummer R, Cowan R, Stewart A, Fourneau N, Hellemans P, Elsayed Y, McClue S, Smit JW, Forslund A, Phelps C, Camm J, Evans TR, de Bono JS, Banerji U (2013) A phase I study of quisinostat (JNJ-26481585), an oral hydroxamate histone deacetylase inhibitor, in patients with advanced solid tumors. Clin Cancer Res 19: 4262–4272.
37. Chinnaiyan P, Chowdhary S, Potthast L, Prabhu A, Tsai YY, Sarcar B, Kahali S, Brem S, Yu HM, Rojiani A, Murtagh R, Pan E (2012) Phase I trial of vorinostat combined with bevacizumab and CPT-11 in recurrent glioblastoma. Neuro Oncol 14: 93–100.
38. Ellis L, Pan Y, Smyth GK, George DJ, McCormack C, Williams-Truax R, Mita M, Beck J, Burris H, Ryan G, Atadja P, Butterfoss D, Dugan M, Culver K, Johnstone RW, Prince HM (2008) Histone deacetylase inhibitor panobinostat induces clinical responses with associated alterations in gene expression profiles in cutaneous T-cell lymphoma. Clin Cancer Res 14: 4500–4509.
39. Khanim FL, Bradbury CA, Arrazi J, Hayden RE, Rye A, Basu S, MacWhannell A, Sawers A, Griffiths M, Cook M, Freeman S, Nightingale KP, Grimwade D, Falciani F, Turner BM, Bunce CM, Craddock C (2009) Elevated FOSB-expression; a potential marker of valproate sensitivity in AML. Br J Haematol 144: 332–341.
40. Jones DR, Moskaluk CA, Gillenwater HH, Petroni GR, Burks SG, Philips J, Rehm PK, Olazagasti J, Kozower BD, Bao Y (2012) Phase I trial of induction histone deacetylase and proteasome inhibition followed by surgery in non-small-cell lung cancer. J Thorac Oncol 7: 1683–1690.
41. Thompson ME (2010) BRCA1 16 years later: nuclear import and export processes. FEBS J 277: 3072–3078.
42. Liebermann DA, Tront JS, Sha X, Mukherjee K, Mohamed-Hadley A, Hoffman B (2011) Gadd45 stress sensors in malignancy and leukemia. Crit Rev Oncog 16: 129–40.
43. Tabas I, Ron D (2011) Integrating the mechanisms of apoptosis induced by endoplasmic reticulum stress. Nat Cell Biol 13: 184–90.
44. Martin SA, Lord CJ, Ashworth A (2010) Therapeutic targeting of the DNA mismatch repair pathway. Clin Cancer Res 16: 5107–13.
45. Los G, Benbatoul K, Gately DP, Barton R, Christen R, Robbins KT, Vicario D, Kirmani S, Orloff LA, Weisman R, Howell SB (1999) Quantitation of the change in GADD153 messenger RNA level as a molecular marker of tumor response in head and neck cancer. Clin Cancer Res 5: 1610–8.
46. Hirohata T, Asano K, Ogawa Y, Takano S, Amano K, Isozaki O, Iwai Y, Sakata K, Fukuhara N, Nishioka H, Yamada S, Fujio S, Arita K, Takano K, Tominaga A, Hizuka N, Ikeda H, Osamura RY, Tahara S, Ishii Y, Kawamata T, Shimatsu A, Teramoto A, Matsuno A (2013) DNA mismatch repair protein (MSH6) correlated with the responses of atypical pituitary adenomas and pituitary carcinomas to temozolomide: the national cooperative study by the Japan Society for Hypothalamic and Pituitary Tumors. J Clin Endocrin Metab 98: 1130–6.
47. Ting S, Mairinger FD, Hager T, Welter S, Eberhardt WE, Wohlschlaeger J, Schmid KW, Christoph DC (2013) ERCC1, MLH1, MSH2, MSH6, and βIII-tubulin: resistance proteins associated with response and outcome to platinum-based chemotherapy in malignant pleural mesothelioma. Clin Lung Cancer 14: 558–67.
48. Meyer N, Penn LZ (2008) Reflecting on 25 years with MYC. Nat Rev Cancer 8: 976–990.
49. Dang CV, Kim JW, Gao P, Yustein J (2008) The interplay between MYC and HIF in cancer. Nat Rev Cancer 8: 51–56.
50. Podar K, Anderson KC (2010) A therapeutic role for targeting c-Myc/Hif-1-dependent signaling pathways. Cell Cycle 9: 1722–1728.

51. Ellis L, Hammers H, Pili R (2009) Targeting tumor angiogenesis with histone deacetylase inhibitors. Cancer Lett 280: 145–153.
52. Chen S, Sang N (2011) Histone deacetylase inhibitors: the epigenetic therapeutics that repress hypoxia-inducible factors. J Biomed Biotechnol 2011: 197946.
53. Huang LE (2008) Carrot and stick: HIF-α engages c-Myc in hypoxic adaptation. Cell Death Differ 15: 672–677.
54. Yoo YG, Hayashi M, Christensen J, Huang LE (2009) As essential role of the HIF-1α-c-Myc axis in malignant progression. Ann N Y Acad Sci 1177: 198–204.
55. Kretzner L, Scuto A, Dino PM, Kowolik CM, Wu J, Ventura P, Jove R, Forman SJ, Yen Y, Kirschbaum MH (2011) Combining histone deacetylase inhibitor vorinostat with aurora kinase inhibitors enhances lymphoma cell killing with repression of c-Myc, hTERT, and microRNA levels. Cancer Res 71: 3912–3920.
56. Zhu C, Chen Q, Xie Z, Ai J, Tong L, Ding J, Geng M (2011) The role of histone deacetylase 7 (HDAC7) in cancer cell proliferation: regulation on c-Myc. J Mol Med 89: 279–289.
57. Liu PY, Xu N, Malyukova A, Scarlett CJ, Sun YT, Zhang XD, Ling D, Su SP, Nelson C, Chang DK, Koach J, Tee AE, Haber M, Norris MD, Toon C, Rooman I, Xue C, Cheung BB, Kumar S, Marshall GM, Biankin AV, Liu T (2013) The histone deacetylase SIRT2 stabilizes Myc oncoproteins. Cell Death Differ 20: 503–514.
58. Bangert A, Cristofanon S, Eckhardt I, Abhari BA, Kolodziej S, Häcker S, Vellanki SH, Lausen J, Debatin KM, Fulda S (2012) Histone deacetylase inhibitors sensitize glioblastoma cells to TRAIL-induced apoptosis by c-myc-mediated downregulation of cFLIP. Oncogene 31: 4677–4688.
59. Wang WJ, Wu SP, Liu JB, Shi YS, Huang X, Zhang QB, Yao KT (2012) MYC regulation of CHK1 and CHK2 promotes radioresistance in a stem cell-like population of nasopharyngeal carcinoma cells. Cancer Res 73: 1219–1231.
60. Xie Y, Zhang J, Ye S, He M, Ren R, Yuan D, Shao C (2012) SirT1 regulates radiosensitivity of hepatoma cells differently under normoxic and hypoxic conditions. Cancer Sci 103: 1238–1244.

Supplementary Material

Supplementary Table 1. Short tandem repeat (STR) profiles of cell lines

Cell Name	STR Designation																	
	AMEL		CSF1PO		D13S317		D16S539		D5S818		D7S820		TH01		TPOX		vWA	
HCT116 ATCC	x	y	7	10	10	12	11	13	10	11	11	12	8	9	8	9	17	22
HCT116	x		7	11	10	12		13	10	11	11	12			9	10	17	
SW 620 ATCC	x		13	14		12	9	13		13	8	9	8			11	16	
SW 620	x		13	14		12	9	13		13	8	9	8			11	15	16

The cell lines were subjected to STR analysis for cell line validation using the Promega PowerPlex 16 kit (Promega, Madison, WI), and analyzed on a MegaBace1000 capillary electrophoresis system using Fragment Profiler software (GE Healthcare, Bucks, UK). The STR loci identified were compared to STR profiles published on the ATCC web site (http://www.lgcstandards-atcc.org/).

Supplementary Table 2. The Locally Advanced Rectal Cancer – Radiation response Prediction (LARC-RRP) phase 2 study (ClinicalTrials NCT00278694) – patient and treatment characteristics

	***N* (%)**
At baseline	
Median age, years (range)	56 (30–70)
Gender	
Male	15 (55.6)
Female	12 (44.4)
T-status	
T3	12 (44.4)
T4	15 (55.6)
N-status	
N0	3 (11.1)
N1	2 (7.4)
N2	22 (81.5)
M-status	
M0	23 (85.2)
M1	4 (14.8)
Radiological response	
yT-status	
yT0	0
yT1	0
yT2	1 (3.7)
yT3	13 (48.1)
yT4	13 (48.1)
yN-status	
yN0	11 (40.2)
yN1	4 (14.8)
yN2	12 (44.4)
Histological response	
ypT-status	
ypT0	3 (11.1)
ypT1	0
ypT2	3 (11.1)
ypT3	12 (44.4)
ypT4	8 (29.6)
missing	1 (3.7)
ypN-status	
ypN0	13 (48.1)
ypN1	10 (37.0)
ypN2	3 (11.1)
Tumor Regression Grade *	
TRG 1 (ypT0)	3 (11.1)
TRG 2 (sparsely remaining tumor)	13 (48.1)
TRG 3 (intermediate response)	6 (22.2)

TRG 4 (poor response)	4 (14.8)
TRG 5 (poor response)	0
missing	1 (3.7)
Clinical outcome	
Development of metastatic disease **	12 (52.2)

The LARC-RRP study was conducted in patients with locally advanced rectal cancer receiving neoadjuvant chemoradiotherapy (CRT). Data from a subgroup of 27 study patients are presented here. This population was enrolled between July 2008 and March 2010. Patient eligibility criteria, evaluation procedures, study treatment, and review procedures of follow-up have been described in detail previously ***. Patients were treated with neoadjuvant fluoropyrimidine-/oxaliplatin-based chemotherapy and CRT, followed by surgery. Follow-up data was obtained from the clinical database and censored on August 31, 2012 **. Valid observations of the presence or absence of distant metastases required designated radiologic examination. Four patients with synchronous resectable liver metastases were excluded from analysis of metastasis-free survival **. Data analysis was performed using Predictive Analytics SoftWare Statistics version 16.0 (SPSS Inc., Chicago, IL). No association of tumor *MYC* expression (median value 0.47, range 0.020–4.9; mean value 0.70 ± 0.20) and patient characteristics or treatment outcome was found.

* Histologic Tumor Regression Grading (TRG) of tumor CRT response was graded within one of five TRG categories, spanning from the absence of residual tumor cells in the surgical specimen (histologic complete response; TRG 1) to the lack of morphologic signs of tissue response to treatment (TRG 5).

** Censored at a median period of 33 months (range 5–45)

*** Folkvord S, Flatmark K, Dueland S, de Wijn R, Grøholt KK et al. Prediction of response to preoperative chemoradiotherapy in rectal cancer by multiplex kinase activity profiling. Int J Radiat Oncol Biol Phys 2010; 78, 555–62

Supplementary Table 3. Primers and probes used for reverse transcriptase quantitative PCR analysis

Target	Primers	Universal Probe	NCBI Number	Amplicon Length
YARS	F: GGATTAACAGGCAGCAAAATG R: CCTTCCGATCAAGGAGATCA	# 35	NM_003680.2	67 nt
TBP	F: GCTGGCCCATAGTGATCTTT R: CTTCACACGCCAAGAAACAGT	# 3	NM_003194.3	60 nt
MYC	F: CACCAGCAGCGACTCTGA R: GATCCAGACTCTGACCTTTGC	# 34	NM_002467.4	102 nt
GADD45B	F: AGTCGGCCAAGTTGATGAAT R: CCTCCTCCTCCTCGTCAAT	# 34	NM_015675.2	75 nt
MSH6	F: TGAATTGGCAGTTTGTGATGA R: TGTTACGTAAGTTGTGCCTACTC	# 21	NM_0000179.2	76 nt
BARD1	F: ACATTCTGAGAGAGCCTGTGTG R: TCCAATGCAGTCACTTACACAA	# 88	NM_000465.2	77 nt
DDIT3	F: AAGGCACTGAGCGTATCATGT R: TGAAGATACACTTCCTTCTTGAACAC	# 21	NM_004083.4	105 nt

Abbreviations: F, forward; R, reverse; nt, nucleotides

Supplementary Table 4. Gene Ontology (GO) enriched biological processes in patients' peripheral blood mononuclear cells during 24 hours of vorinostat treatment

Biological Process	***N***	**%**	***P*-value**
T2 versus T0			
GO:0006350 transcription	253	17	5.1×10^{-14}
GO:0044265 cellular macromolecule catabolic process	107	7.2	8.2×10^{-10}
GO:0044257 cellular protein catabolic process	93	6.3	1.7×10^{-10}
GO:0007049 cell cycle	111	7.5	2.4×10^{-10}
GO:0051603 proteolysis involved in cellular protein catabolic process	92	6.2	2.9×10^{-10}
GO:0019941 modification-dependent protein catabolic process	89	6.0	3.4×10^{-10}
GO:0043632 modification-dependent macromolecule catabolic process	89	6.0	3.4×10^{-10}
GO:0009057 macromolecule catabolic process	111	7.5	3.4×10^{-10}
GO:0030163 protein catabolic process	94	6.3	4.0×10^{-10}
GO:0006396 RNA processing	84	5.7	1.8×10^{-9}
GO:0045449 regulation of transcription	276	19	5.0×10^{-9}
GO:0022402 cell cycle process	79	5.3	3.4×10^{-7}
GO:0008380 RNA splicing	48	3.2	5.4×10^{-7}
GO:0051276 chromosome organization	70	4.7	5.4×10^{-7}
GO:0006366 transcription from RNA polymerase II promoter	42	2.8	6.2×10^{-7}
GO:0016568 chromatin modification	46	3.1	1.2×10^{-6}
GO:0006351 transcription, DNA-dependent	48	3.2	1.2×10^{-6}
GO:0032774 RNA biosynthetic process	48	3.2	1.8×10^{-6}
GO:0016071 mRNA metabolic process	56	3.8	2.0×10^{-6}
GO:0000278 mitotic cell cycle	56	3.8	2.0×10^{-6}
GO:0006259 DNA metabolic process	69	4.6	5.0×10^{-6}
GO:0006397 mRNA processing	49	3.3	7.7×10^{-6}
GO:0006325 chromatin organization	55	3.7	8.3×10^{-6}

GO:0045184 establishment of protein localization	93	6.3	1.6×10^{-5}
GO:0015031 protein transport	92	6.2	1.9×10^{-5}
GO:0006974 response to DNA damage stimulus	52	3.5	4.9×10^{-5}
GO:0006511 ubiquitin-dependent protein catabolic process	38	2.6	5.1×10^{-5}
GO:0022403 cell cycle phase	56	3.8	5.6×10^{-5}
GO:0008104 protein localization	101	6.8	6.1×10^{-5}
GO:0051726 regulation of cell cycle	47	3.2	7.6×10^{-5}
GO:0033554 cellular response to stress	69	4.6	1.8×10^{-4}
GO:0034660 ncRNA metabolic process	35	2.4	1.9×10^{-4}
GO:0034470 ncRNA processing	30	2.0	2.5×10^{-4}
GO:0010605 negative regulation of macromolecule metabolic process	84	5.7	2.8×10^{-4}
GO:0043933 macromolecular complex subunit organization	81	5.5	4.1×10^{-4}
GO:0010604 positive regulation of macromolecule metabolic process	94	6.3	5.0×10^{-4}
GO:0006281 DNA repair	39	2.6	6.7×10^{-4}
GO:0051301 cell division	40	2.7	7.1×10^{-4}
GO:0048285 organelle fission	33	2.2	8.2×10^{-4}
GO:0051252 regulation of RNA metabolic process	176	11	8.8×10^{-4}
GO:0000279 M phase	43	2.9	9.2×10^{-4}
GO:0065003 macromolecular complex assembly	75	5.1	9.5×10^{-4}
GO:0000087 M phase of mitotic cell cycle	32	2.2	0.001
GO:0007067 mitosis	31	2.1	0.002
GO:0000280 nuclear division	31	2.1	0.002
GO:0016265 death	79	5.3	0.002
GO:0006508 proteolysis	108	7.3	0.002
GO:0006355 regulation of transcription, DNA-dependent	170	11	0.002
GO:0008219 cell death	78	5.3	0.002
GO:0070727 cellular macromolecule localization	49	3.3	0.003
GO:0045941 positive regulation of transcription	63	4.2	0.003
GO:0045934 negative regulation of nucleobase, nucleoside, nucleotide and nucleic acid metabolic process	58	3.9	0.003
GO:0045935 positive regulation of nucleobase, nucleoside,	68	4.6	0.004

nucleotide and nucleic acid metabolic process			
GO:0010628 positive regulation of gene expression	64	4.3	0.004
GO:0032268 regulation of cellular protein metabolic process	54	3.6	0.004
GO:0034613 cellular protein localization	48	3.2	0.005
GO:0051186 cofactor metabolic process	27	1.8	0.005
GO:0051172 negative regulation of nitrogen compound metabolic process	58	3.9	0.005
GO:0051248 negative regulation of protein metabolic process	26	1.8	0.005
GO:0012501 programmed cell death	66	4.4	0.005
GO:0046907 intracellular transport	70	4.7	0.006
GO:0010629 negative regulation of gene expression	56	3.8	0.006
GO:0032269 negative regulation of cellular protein metabolic process	25	1.7	0.006
GO:0006461 protein complex assembly	56	3.8	0.006
GO:0070271 protein complex biogenesis	56	3.8	0.006
GO:0051173 positive regulation of nitrogen compound metabolic process	68	4.6	0.008
GO:0006915 apoptosis	64	4.3	0.009
GO:0016481 negative regulation of transcription	51	3.4	0.009
GO:0031328 positive regulation of cellular biosynthetic process	71	4.8	0.010

T24 versus T2

GO:0006350 transcription	260	17	8.3×10^{-16}
GO:0007049 cell cycle	114	7.6	2.6×10^{-11}
GO:0045449 regulation of transcription	286	19	5.4×10^{-11}
GO:0016568 chromatin modification	55	3.7	1.3×10^{-10}
GO:0006396 RNA processing	86	5.7	3.7×10^{-10}
GO:0044265 cellular macromolecule catabolic process	104	6.9	8.8×10^{-10}
GO:0051276 chromosome organization	78	5.2	9.0×10^{-9}
GO:0022402 cell cycle process	85	5.7	4.0×10^{-9}
GO:0044257 cellular protein catabolic process	89	5.9	4.3×10^{-9}

GO:0009057 macromolecule catabolic process	107	7.1	6.4×10^{-9}
GO:0051603 proteolysis involved in cellular protein catabolic process	88	5.9	7.4×10^{-9}
GO:0019941 modification-dependent protein catabolic process	85	5.7	8.8×10^{-9}
GO:0043632 modification-dependent macromolecule catabolic process	85	5.7	8.8×10^{-9}
GO:0030163 protein catabolic process	90	6.0	9.4×10^{-9}
GO:0006325 chromatin organization	62	4.1	3.0×10^{-8}
GO:0006259 DNA metabolic process	75	5.0	7.2×10^{-8}
GO:0000278 mitotic cell cycle	57	3.8	9.7×10^{-7}
GO:0006351 transcription, DNA-dependent	48	3.2	1.3×10^{-6}
GO:0006366 transcription from RNA polymerase II promoter	41	2.7	1.7×10^{-6}
GO:0032774 RNA biosynthetic process	48	3.2	1.9×10^{-6}
GO:0008380 RNA splicing	46	3.1	3.3×10^{-6}
GO:0016071 mRNA metabolic process	55	3.7	4.6×10^{-6}
GO:0006397 mRNA processing	48	3.2	1.7×10^{-6}
GO:0016570 histone modification	25	1.7	1.9×10^{-6}
GO:0016569 covalent chromatin modification	25	1.7	3.3×10^{-5}
GO:0033554 cellular response to stress	72	4.8	3.5×10^{-5}
GO:0045184 establishment of protein localization	91	6.1	4.8×10^{-5}
GO:0006974 response to DNA damage stimulus	52	3.5	5.1×10^{-5}
GO:0015031 protein transport	90	6.0	5.7×10^{-5}
GO:0006281 DNA repair	42	2.8	8.0×10^{-5}
GO:0043933 macromolecular complex subunit organization	84	5.6	9.9×10^{-5}
GO:0022403 cell cycle phase	55	3.7	1.1×10^{-4}
GO:0007050 cell cycle arrest	21	1.4	1.1×10^{-4}
GO:0006511 ubiquitin-dependent protein catabolic process	36	2.4	2.6×10^{-4}
GO:0034470 ncRNA processing	30	2.0	2.6×10^{-4}
GO:0051252 regulation of RNA metabolic process	180	12	2.8×10^{-4}
GO:0010605 negative regulation of macromolecule metabolic process	84	5.6	2.9×10^{-4}
GO:0051726 regulation of cell cycle	45	3.0	3.1×10^{-4}

GO:0051338 regulation of transferase activity	49	3.3	3.3×10^{-4}
GO:0065003 macromolecular complex assembly	77	5.1	3.8×10^{-4}
GO:0008104 protein localization	97	6.5	3.9×10^{-4}
GO:0045859 regulation of protein kinase activity	46	3.1	3.9×10^{-4}
GO:0048285 organelle fission	34	2.3	4.0×10^{-4}
GO:0034660 ncRNA metabolic process	34	2.3	4.4×10^{-4}
GO:0043549 regulation of kinase activity	47	3.1	4.6×10^{-4}
GO:0006355 regulation of transcription, DNA-dependent	175	11	4.8×10^{-4}
GO:0016265 death	82	5.5	4.8×10^{-4}
GO:0008219 cell death	81	5.4	6.3×10^{-4}
GO:0070727 cellular macromolecule localization	52	3.5	6.6×10^{-4}
GO:0042325 regulation of phosphorylation	57	3.8	6.8×10^{-4}
GO:0051301 cell division	40	2.7	7.3×10^{-4}
GO:0042981 regulation of apoptosis	88	5.9	8.7×10^{-4}
GO:0000280 nuclear division	32	2.1	8.8×10^{-4}
GO:0007067 mitosis	32	2.1	8.8×10^{-4}
GO:0034613 cellular protein localization	51	3.4	9.8×10^{-4}
GO:0051174 regulation of phosphorus metabolic process	58	3.9	0.001
GO:0019220 regulation of phosphate metabolic process	58	3.9	0.001
GO:0043067 regulation of programmed cell death	88	5.9	0.001
GO:0000087 M phase of mitotic cell cycle	32	2.1	0.001
GO:0045941 positive regulation of transcription	65	4.3	0.001
GO:0010941 regulation of cell death	88	5.9	0.001
GO:0045934 negative regulation of nucleobase, nucleoside, nucleotide and nucleic acid metabolic process	60	4.0	0.001
GO:0012501 programmed cell death	69	4.6	0.002
GO:0006461 protein complex assembly	59	3.9	0.002
GO:0070271 protein complex biogenesis	59	3.9	0.002
GO:0006352 transcription initiation	16	1.1	0.002
GO:0000279 M phase	42	2.8	0.002
GO:0010628 positive regulation of gene expression	66	4.4	0.002

GO:0010604 positive regulation of macromolecule metabolic process	91	6.1	0.002
GO:0006399 tRNA metabolic process	20	1.3	0.002
GO:0006473 protein amino acid acetylation	12	0.8	0.002
GO:0051172 negative regulation of nitrogen compound metabolic process	60	4.0	0.002
GO:0008033 tRNA processing	15	1.0	0.002
GO:0006886 intracellular protein transport	46	3.1	0.002
GO:0043065 positive regulation of apoptosis	51	3.4	0.003
GO:0034621 cellular macromolecular complex subunit organization	44	2.9	0.003
GO:0045935 positive regulation of nucleobase, nucleoside, nucleotide			
and nucleic acid metabolic process	69	4.6	0.003
GO:0006915 apoptosis	67	4.5	0.003
GO:0043068 positive regulation of programmed cell death	51	3.4	0.003
GO:0051188 cofactor biosynthetic process	17	1.1	0.003
GO:0010942 positive regulation of cell death	51	3.4	0.003
GO:0006368 RNA elongation from RNA polymerase II promoter	11	0.7	0.003
GO:0046907 intracellular transport	71	4.7	0.004
GO:0000394 RNA splicing, via endonucleolytic cleavage and ligation	4	0.3	0.004
GO:0006388 tRNA splicing, via endonucleolytic cleavage and ligation	4	0.3	0.004
GO:0031327 negative regulation of cellular biosynthetic process	62	4.1	0.004
GO:0009890 negative regulation of biosynthetic process	63	4.2	0.005
GO:0031400 negative regulation of protein modification process	19	1.3	0.005
GO:0051186 cofactor metabolic process	27	1.8	0.005
GO:0006916 anti-apoptosis	28	1.9	0.005
GO:0006354 RNA elongation	11	0.7	0.005
GO:0051173 positive regulation of nitrogen compound metabolic process	69	4.6	0.005
GO:0010557 positive regulation of macromolecule biosynthetic process	70	4.7	0.005

GO:0032259 methylation	14	0.9	0.005
GO:0006367 transcription initiation from RNA polymerase II promoter	13	0.9	0.006
GO:0016481 negative regulation of transcription	52	3.5	0.006
GO:0043543 protein amino acid acylation	12	0.8	0.006
GO:0010558 negative regulation of macromolecule biosynthetic process	60	4.0	0.006
GO:0022613 ribonucleoprotein complex biogenesis	25	1.7	0.006
GO:0006732 coenzyme metabolic process	22	1.5	0.008
GO:0042791 5S class rRNA transcription	4	0.3	0.008
GO:0042797 tRNA transcription from RNA polymerase III promoter	4	0.3	0.008
GO:0000079 regulation of cyclin-dependent protein kinase activity	11	0.7	0.008
GO:0010629 negative regulation of gene expression	55	3.7	0.009
GO:0006412 translation	39	2.6	0.010
GO:0009891 positive regulation of biosynthetic process	72	4.8	0.010

Supplementary Table 5. Baseline expression levels of genes assessed by reverse transcriptase quantitative PCR analysis

	MYC	***GADD45B***	***MSH6***	***BARD1***	***DDIT3***
Study patients' PBMC	1.50 ± 0.20	6.83 ± 1.0	0.35 ± 0.06	0.48 ± 0.07	0.20 ± 0.03
HCT116 xenograft	2.17 ± 0.26	0.83 ± 0.18	0.64 ± 0.08	0.70 ± 0.17	0.19 ± 0.03
SW620 xenograft	3.32 ± 0.57	1.62 ± 0.27	1.11 ± 0.11	0.47 ± 0.4	0.28 ± 0.05

Gene expression levels relative to corresponding expression levels in the LoVo-92 cell line are given as mean ± standard deviation. For study patients' PBMC, baseline levels (before commencement of study treatment) are given. For the human colorectal carcinoma xenografts, levels in tumors treated with vehicle (dimethyl sulfoxide) are given.
Abbreviation: PBMC, peripheral blood mononuclear cells

IV